

Neutrino Magnetic Moments in the Standard Model and Beyond

Master Thesis in Theoretical Atomic, Nuclear and Particle Physics

by

Sigurd Nese



Department of Physics and Technology

University of Bergen

June 2022

Abstract

This thesis presents the theory describing the magnetic moments of Dirac and Majorana neutrinos, including a systematic method for extracting the neutrino magnetic moments from a given model using electromagnetic form factors. In the standard electroweak interactions, neutrino magnetic moments are suppressed by the small neutrino masses. Theories beyond the Standard Model which overcome this suppression lead to unacceptably large loop corrections to the neutrino masses, necessitating fine-tuning of model parameters. This model building issue, and a mechanism for avoiding it using a global symmetry, are discussed.

The excess in electron recoil events reported by the XENON1T collaboration may be interpreted as a neutrino magnetic moment many orders of magnitude above the Standard Model prediction. Adopting the interpretation of this excess as a transition magnetic moment from an active neutrino to a sub-MeV sterile neutrino, leptoquark models with couplings to right-chiral neutrinos are explored. A recently proposed scalar leptoquark model, which generates large magnetic moments without fine-tuning, is investigated. A vector leptoquark model is proposed to simultaneously explain a large neutrino magnetic moment and recent data on lepton flavor universality violating observables. If fine-tuning of the neutrino mass is accepted, the model can accommodate the desired observables simultaneously.

Acknowledgements

I would like to thank my supervisor Jörn Kersten, for his patient guidance and support during the writing of this thesis, and for everything I have learned from him these last two years. Without Jörn, this thesis would not have been possible. I would also like to thank my parents, Gurid and Steinar, for always encouraging my curiosity about the world. I am grateful to my fellow master students, who have made the last few years very enjoyable. Special thanks to my office mates Kristoffer and Mathias, for interesting discussions and good company. Last but not least, I would like to thank Thale, for always being by my side.

Contents

1	Introduction	5
2	The Standard Model and Neutrino Physics	7
2.1	Fermions, Chirality and Charge Conjugation	7
2.2	Gauge Interactions	10
2.3	The Standard Electroweak Theory	13
2.3.1	Gauge Invariant Electroweak Interactions	13
2.3.2	Spontaneous Electroweak Symmetry Breaking	15
2.3.3	Weak Interactions of Quarks	18
2.4	Neutrino Masses	20
2.5	The See-Saw Mechanism	24
2.6	Neutrino Oscillations	25
3	Magnetic Moments	28
3.1	The Classical Description	28
3.2	The Quantum Mechanical Description	29
3.3	Anomalous Magnetic Moment of a Charged Lepton	32
3.4	Effective Lagrangian for the Magnetic Moment	37
3.4.1	Chirality Flip	37
3.4.2	Effective Lagrangian in the Non-Relativistic Limit	38
3.4.3	Magnetic Moment of Majorana Neutrinos	39
4	Electromagnetic Form Factors	41
4.1	Dirac Neutrinos	41
4.2	Majorana Neutrinos	46
4.3	Effective Neutrino Magnetic Moment	47
4.4	The Experimental Situation	49
5	Neutrino Magnetic Moment in the Standard Model	52
5.1	Dirac Neutrinos	52
5.2	Majorana Neutrinos	54
6	Fine-Tuning and the Voloshin Mechanism	57
6.1	Neutrino Magnetic Moment and Mass	57
6.2	The Role of Majorana Mass Terms	59
6.3	Voloshin's Solution to the Tuning Issue	60

7	Scalar Leptoquark Model	63
7.1	The Model	63
7.2	Prediction for the Neutrino Magnetic Moment	65
7.3	More Neutrino Flavors	68
7.4	Neutrino Mass Scenarios	70
7.4.1	Double See-Saw	71
7.4.2	Inverse See-Saw	71
8	Vector Leptoquark Model	73
8.1	The Model	73
8.2	Prediction for the Neutrino Magnetic Moment	74
8.3	Flavor Physics Anomalies	76
9	Conclusions and Outlook	84
A	Feynman Rules	87
A.1	The Standard Electroweak Theory	87
A.2	Leptoquarks	88
A.3	Additional Feynman Rules for Majorana Fermions	91
B	Dirac Matrices	93
C	Translating the Voloshin Lagrangian to 4-spinor Notation	95
D	Rewriting the Numerator N^μ	97
	Bibliography	100

Chapter 1

Introduction

The Standard Model of particle physics is our best model for describing elementary particles and their interactions. It explains how fermions, the building blocks of matter, interact by exchanging gauge bosons, and how the masses of particles arise through the Higgs mechanism. With the discovery of the Higgs boson in 2012 [1, 2], all the particles predicted by the Standard Model have been observed. However, we know the Standard Model cannot be the final story, as several questions are left unanswered. Thus, we are motivated to search for new physics not explained in the Standard Model, so-called beyond the Standard Model (BSM) physics, hoping to be guided toward a better theory of nature.

An interesting probe for BSM physics is the neutrino sector. Neutrinos are the most elusive constituents of the Standard Model; they are extremely light particles which only interact weakly with other matter. Since neutrinos are electrically neutral, they do not interact directly with the electromagnetic field. In the language of quantum field theory, this means the neutrinos do not couple to the photon. Nevertheless, neutrinos may interact indirectly with the electromagnetic field through quantum loop effects. In particular, a magnetic moment may be defined and predicted for subatomic particles, including neutrinos. The concept of magnetic moments carries over from classical electrodynamics, where it characterizes the interaction between a system and an external magnetic field. The magnetic moment of neutrinos is predicted to be extremely small by the Standard Model, on the order of $10^{-19}\mu_B$, with the Bohr magneton μ_B being the scale of magnetic moments for electrons and atoms. This is many orders of magnitude lower than current experimental sensitivities. However, BSM theories may predict it to be much larger. Thus, an observation of a neutrino magnetic moment in current or future experiments would be a strong hint toward new physics.

Neutrinos are abundantly produced in nuclear fusion reactions in the Sun. Around 6×10^{10} of these solar neutrinos pass through every square centimeter on earth per second [3, p. 352]. Despite this enormous flux, the neutrinos are hard to detect due to their feeble interaction with other matter. Therefore, neutrino detectors are large, to increase the probability of seeing a neutrino interaction, and often built underground in order to shield from other particles. One such detector was the Homestake chlorine solar neutrino experiment, placed almost 1500 m underground in a gold mine. Homestake operated from 1970 to 1994, and was the first experiment to observe solar neutrinos. In the 1980s, an anticorrelation between solar neutrino flux and sun spot activity, which fluctuates in an 11-year cycle, was observed in the Homestake data [4]. This

observation spurred theoretical activity to explain the apparent connection between magnetic activity in the Sun and the observed number of neutrinos on Earth. One proposed explanation was a large neutrino magnetic moment on the order of $10^{-11}\mu_B$, which would cause the neutrinos to be affected by the magnetic field inside the Sun during their propagation through its interior. In periods of high sun spot activity the magnetic field in the Sun is strong, which would cause the neutrinos to flip their helicity from left-handed to right-handed. The right-handed neutrinos would be invisible to the detector on Earth, causing a deficit in the observed flux. Conversely, when solar activity is low, the neutrinos would pass through the Sun unaffected [5].

During these theoretical developments, it was realized that models with an enhanced neutrino magnetic moment generally give an unacceptably large quantum loop correction to the neutrino mass, owing to the similar chiral structure of the relevant operators. This leads to excessive fine-tuning of parameters in the model in order to fit experimental data. It is desirable to find models which incorporate large neutrino magnetic moments and small neutrino masses simultaneously in a more elegant way.

With the advent of neutrino flavor oscillations to explain the solar neutrino problem, interest for neutrino magnetic moments faded. Recently, however, data from the XENON1T dark matter detector has shown an excess in electron recoil events in the low end of the recoil energy spectrum. These are events where incoming neutrinos scatter off electrons, transferring momentum to the electron through a mediating gauge boson. A possible explanation for the excess is that the neutrinos have a large magnetic moment, allowing them to interact electromagnetically with the electrons in the detector [6]. Thus, interest in neutrino magnetic moments is rekindled, motivating further theoretical work on the subject. This thesis is devoted to studying the magnetic moments of neutrinos in the Standard Model and beyond.

The thesis is structured as follows: We start with a brief description of the Standard Model, including the concept of gauge interactions and the spontaneous breaking of electroweak gauge symmetry. This sets the stage for exploring BSM models. We also discuss how neutrino masses can be described in extensions of the Standard Model. In Chapter 3, we review the concept of magnetic moments in classical physics, and see how it carries over to the quantum mechanical description. We rederive the famous Schwinger electron $g - 2$ result, which guides us to the definition of the neutrino magnetic moment through an effective Lagrangian. In Chapter 4, we describe the electromagnetic interactions of neutrinos through form factors, developing a methodology of extracting the magnetic moment of Dirac and Majorana neutrinos in different theories. We discuss of how neutrino magnetic moments can be measured in experiments, and in this context we briefly summarize the current experimental results and limits. The method developed in Chapter 4 is utilized in Chapter 5, where the magnetic moment of neutrinos for Standard Model interactions is rederived. Next, in Chapter 6 we explore the issue of fine-tuning which arises in BSM theories with large magnetic moments, and how this issue can be solved by a new global symmetry. In Chapter 7 a recent result from the literature is rederived, in a model which introduces scalar leptoquarks to produce a large magnetic moment and utilizes the aforementioned symmetry mechanism. We investigate possible neutrino mass scenarios in this model as well. In Chapter 8, a vector leptoquark model is proposed which gives a large neutrino magnetic moment, and in addition explains recent data on flavor physics anomalies. Finally, we conclude in Chapter 9.

Natural units, in which $c = \hbar = 1$, are used throughout the thesis unless otherwise specified.

Chapter 2

The Standard Model and Neutrino Physics

2.1 Fermions, Chirality and Charge Conjugation

Particles are classified into two types: bosons and fermions. Bosons are particles with integer spins, examples from the Standard Model including the spin-1 photon and the spin-0 Higgs boson. Fermions have half-integer spins. Electrons and quarks, which are the constituents of ordinary matter, are examples of fermions. This class of particles also includes neutrinos, the main subjects of this thesis. As such, a brief description of fermions and some useful related operators are given in this section.

The elementary fermions in the Standard Model are spin-1/2 fermions, so we restrict our discussion to spin-1/2. We describe the elementary fermions as 4-component objects $\psi(x)$ called Dirac spinors, which satisfy the Dirac equation

$$(i\cancel{\partial} - m)\psi(x) = 0, \quad (2.1)$$

where the slash implies the contraction $\cancel{\partial} = \gamma^\mu \partial_\mu$ and γ^μ are the 4×4 Dirac matrices satisfying the Clifford algebra

$$\{\gamma^\mu, \gamma^\nu\} \equiv \gamma^\mu \gamma^\nu + \gamma^\nu \gamma^\mu = 2g^{\mu\nu}. \quad (2.2)$$

The Dirac equation is an equation of motion; it describes the free propagation of spinors, such as electrons.

Massive particles of spin J have $2J + 1$ degrees of freedom [7, p. 111]. For massive spin-1/2 fermions, this gives two polarization states, commonly referred to as spin up and spin down. However, the Dirac spinors $\psi(x)$ have four components. The Dirac spinor is thus a composite object. This is seen most clearly in the Weyl basis of the gamma matrices, where

$$\gamma^0 = \begin{pmatrix} 0 & \mathbb{1} \\ \mathbb{1} & 0 \end{pmatrix}, \quad \gamma^i = \begin{pmatrix} 0 & \sigma^i \\ -\sigma^i & 0 \end{pmatrix}, \quad (2.3)$$

with $\mathbb{1}$ being the 2×2 identity matrix and σ^i the Pauli matrices.

In this basis, one can express the Dirac equation as a set of two coupled equations,

$$\begin{aligned} i\partial_t\xi_R + i\sigma^i\partial_i\xi_R - \chi_L m &= 0 \\ i\partial_t\chi_L - i\sigma^i\partial_i\chi_L - \xi_R m &= 0, \end{aligned} \tag{2.4}$$

where we have written the Dirac spinor as

$$\psi = \begin{pmatrix} \chi_L \\ \xi_R \end{pmatrix}, \tag{2.5}$$

χ_L and ξ_R being two-component objects called left- and right-chiral Weyl spinors, respectively. Of course, this decomposition can be done in any basis of the gamma matrices. The special property of the Weyl spinors can be seen by inspecting the Lorentz transformation of Dirac spinors. From the covariance of the Dirac equation one can derive the transformation

$$\psi(x) \rightarrow \psi'(x') = \exp\left(\frac{\epsilon}{8}[\gamma_\mu, \gamma_\nu]I^{\mu\nu}\right)\psi(x), \tag{2.6}$$

where the number ϵ and the matrices $I^{\mu\nu}$ characterize the Lorentz transformation in question. The important thing here is that in the Weyl basis, the commutator $[\gamma_\mu, \gamma_\nu]$ is block diagonal. Thus, χ_L and ξ_R do not mix under a Lorentz transformation. Specifically, we have

$$\begin{aligned} \chi_L &\rightarrow \chi_L + \frac{1}{2}(i\theta^k - \beta^k)\sigma_k\chi_L \\ \xi_R &\rightarrow \xi_R + \frac{1}{2}(i\theta^k + \beta^k)\sigma_k\xi_R, \end{aligned} \tag{2.7}$$

under an infinitesimal Lorentz transformation, where θ^k are the rotation angles and β^k are the boost angles. In group theory jargon, one says that Weyl spinors transform under *irreducible* representations of the Lorentz group, while the Dirac spinor transforms under a *reducible* representation. The representations of χ_L and ξ_R are related; one can transform a left-chiral Weyl spinor into a right-chiral Weyl spinor and vice versa. To that end, we define the suggestively named Weyl spinors

$$\chi_R \equiv i\sigma^2\chi_L^*, \quad \xi_L \equiv -i\sigma^2\xi_R^*. \tag{2.8}$$

Since the left- and right-chiral Weyl spinors are distinguished by how they transform under a Lorentz transformation, let us check how χ_R transforms under a boost. Eq. (2.7) gives

$$\begin{aligned} \chi_R &\rightarrow i\sigma^2\left(\chi_L - \frac{1}{2}\beta_k\sigma^k\chi_L\right)^* \\ &= \chi_R - \frac{1}{2}\beta_k\left(i\sigma^2\sigma^{k*}\sigma^2\right)\sigma^2\chi_L^* \\ &= \chi_R + \frac{1}{2}\beta_k\sigma^k\chi_R, \end{aligned} \tag{2.9}$$

where in the second line the second term was multiplied by $\sigma^2\sigma^2 = 1$, and in the third line the property $\sigma^2\sigma^{k*}\sigma^2 = -\sigma^k$ was used. The rotation part of the Lorentz transformation receives an extra sign change from the complex conjugation, and stays unchanged. Thus, χ_R indeed transforms as a right-chiral Weyl spinor. A similar calculation for ξ_L confirms that it transforms as a left-chiral Weyl spinor.

Because χ_L and ξ_R transform under irreducible representations of the Lorentz group, one can think of them as the fundamental states, mixed through the mass term according to Eq. (2.4). The propagating particle called “the electron” is thus a combination of the left- and right-chiral spinors.

Since the equation of motion mixes χ_L and ξ_R anyway, one might say this distinction is rather pointless. However, it turns out that nature does care about chirality. Specifically, the weak interaction only acts on left-chiral particles (and right-chiral antiparticles). Thus, one could make the argument that χ_L and ξ_R are the objects we should talk about, not ψ . Indeed, one can devise Feynman rules for calculating processes in perturbation theory with two-component spinors [8]. In this thesis, however, we stick to the conventional four-spinor formalism and extract the chiral parts of the field using appropriate projector operators. Using the fifth gamma matrix

$$\gamma_5 \equiv i\gamma^0\gamma^1\gamma^2\gamma^3, \quad (2.10)$$

the chirality projection operators are defined as

$$P_L = \frac{\mathbb{1} - \gamma_5}{2}, \quad P_R = \frac{\mathbb{1} + \gamma_5}{2}, \quad (2.11)$$

which obey the projector relations

$$P_{L,R}^2 = P_{L,R}, \quad P_L + P_R = \mathbb{1}, \quad P_{L,R}P_{R,L} = 0. \quad (2.12)$$

A Dirac spinor can be decomposed as

$$\psi = (P_L + P_R)\psi \equiv \psi_L + \psi_R. \quad (2.13)$$

In the Weyl basis,

$$\psi_L = P_L\psi = \begin{pmatrix} \mathbb{1} & 0 \\ 0 & 0 \end{pmatrix} \psi = \begin{pmatrix} \chi_L \\ 0 \end{pmatrix}, \quad \psi_R = P_R\psi = \begin{pmatrix} 0 & 0 \\ 0 & \mathbb{1} \end{pmatrix} \psi = \begin{pmatrix} 0 \\ \xi_R \end{pmatrix}, \quad (2.14)$$

showing that the chirality projectors extract states of pure chirality from the Dirac spinor. In the interacting theory, ψ_L and ψ_R are treated differently. Thus, we can use the Dirac spinors to calculate processes in quantum field theory, at the price of having explicit chirality projectors in the vertex factors.

An operation we will encounter frequently is *charge conjugation*. The transformation acts on a Dirac spinor according to

$$\psi \rightarrow \psi^c = C\bar{\psi}^T, \quad (2.15)$$

where $\bar{\psi} \equiv \psi^\dagger\gamma^0$ denotes the Dirac adjoint spinor, and C is the charge conjugation matrix. C depends on the choice of basis, but has the defining property

$$C\gamma_\mu^T C^{-1} = -\gamma_\mu. \quad (2.16)$$

Charge conjugation is named as such since the electric charge of the particle is flipped under the transformation, but it is important to note that all the labels of the particle are flipped, not

just the electric charge. In particular, we have

$$(\psi_L)^c = C\overline{\psi_L}^T = C\left(\overline{\psi}P_R\right)^T = CP_R\overline{\psi}^T = P_R C\overline{\psi}^T = P_R\psi^c, \quad (2.17)$$

i.e. charge conjugation flips the chirality of the spinor. In the Weyl basis, the charge conjugation matrix is

$$C = \begin{pmatrix} -i\sigma^2 & 0 \\ 0 & i\sigma^2 \end{pmatrix}. \quad (2.18)$$

Thus, the charge conjugation operator acts on the Dirac spinor as

$$\psi = \begin{pmatrix} \chi_L \\ \xi_R \end{pmatrix} \rightarrow \psi^c = \begin{pmatrix} -\sigma^2\xi_R^* \\ \sigma^2\chi_L^* \end{pmatrix} = \begin{pmatrix} \xi_L \\ \chi_R \end{pmatrix}. \quad (2.19)$$

Evidently, the components of ψ^c are the transformed Weyl spinors defined in Eq. (2.8). Therefore, $-\sigma^2\xi_R^*$ and $\sigma^2\chi_L^*$ are called the charge conjugate Weyl spinors. As already discussed, the Weyl spinors χ and ξ are in general independent quantities, and can be interpreted to describe distinct particles. However, a special case is the spinor

$$\psi^M = \begin{pmatrix} \chi_L \\ \chi_R \end{pmatrix}, \quad (2.20)$$

which is called a Majorana spinor. It has the property $\psi^c = \psi$, as can be readily checked by Eq. (2.19). The number of degrees of freedom is halved relative to a Dirac spinor due to this constraint; the components of ψ^M are related by Eq. (2.8). As charge conjugation flips the sign of all charges, Majorana spinors can only describe neutral particles. The topic of Majorana fermions will become relevant when we discuss neutrino masses in Section 2.4.

2.2 Gauge Interactions

Free fermions of mass m are described by Eq. (2.1), which is the equation of motion corresponding to the Lagrangian

$$\mathcal{L} = \overline{\psi}(i\not{\partial} - m)\psi, \quad (2.21)$$

where $\overline{\psi} \equiv \psi^\dagger\gamma^0$. This Lagrangian is invariant under the U(1) transformation

$$\psi \rightarrow \psi e^{-i\alpha}, \quad (2.22)$$

where α is an arbitrary real number. This transformation changes the phase of the spinor by the same amount at every spacetime point, and is therefore called a global phase transformation. Let us now demand invariance under the more general, local *gauge* transformation

$$\psi \rightarrow \psi e^{-igf(x)}, \quad (2.23)$$

where g is a number and $f(x)$ is a smooth function of spacetime. Under this transformation, the Lagrangian in Eq. (2.21) transforms as

$$\mathcal{L} \rightarrow \mathcal{L} + g\overline{\psi}\gamma^\mu\psi\partial_\mu f(x), \quad (2.24)$$

that is, it is not invariant. We can restore invariance by replacing the derivative by a *covariant* derivative, defined as

$$D_\mu \psi = (\partial_\mu + igA_\mu) \psi, \quad (2.25)$$

where A_μ is the *gauge field* associated with the symmetry, transforming as

$$A_\mu \rightarrow A_\mu + \partial_\mu f(x). \quad (2.26)$$

under a gauge transformation. Together, the transformations in Eq. (2.23) and Eq. (2.26) make up a U(1) gauge transformation. The Lagrangian

$$\mathcal{L} = \bar{\psi} (i\mathcal{D} - m) \psi \quad (2.27)$$

is invariant under U(1) gauge transformations, and we got the extra term

$$\mathcal{L}_{\text{int}} = -g\bar{\psi}\gamma^\mu\psi A_\mu. \quad (2.28)$$

This is a gauge interaction term between the matter field ψ and the gauge boson field A_μ . The number g determines the coupling strength, and is therefore called the “gauge coupling”. Thus, an interacting theory arose from demanding invariance under the local transformation Eq. (2.23). This is called “gauging” the symmetry.

For a theory of electromagnetic interactions, the above description is suitable; The transformation in Eq. (2.26) is a symmetry of the Lagrangian

$$\mathcal{L} = -\frac{1}{4}F_{\mu\nu}F^{\mu\nu}, \quad (2.29)$$

where $F_{\mu\nu} = \partial_\mu A_\nu - \partial_\nu A_\mu$. Eq. (2.29) is the Lagrangian for electrodynamics. The gauge symmetry ensures that the field A_μ has only two degrees of freedom, corresponding to the two polarization states of light. Thus, the gauge field A_μ is identified with the photon field. Furthermore, by Noether’s theorem the symmetry under U(1) leads to the conserved current and charge

$$j^\mu = g\bar{\psi}\gamma^\mu\psi, \quad Q = \int d^3x j^0 = g \int d^3x \psi^\dagger\psi. \quad (2.30)$$

Identifying Q as the electric charge, the gauge coupling is $g = q$, the electric charge of the fermion ψ . We arrive at the Lagrangian for QED,

$$\mathcal{L}_{\text{QED}} = \bar{\psi} (i\mathcal{D} - m) \psi - \frac{1}{4}F_{\mu\nu}F^{\mu\nu} - q\bar{\psi}\mathcal{A}\psi. \quad (2.31)$$

q can be written in terms of the elementary charge e , which we take to be positive. Making the substitution $q = -e$ in Eq. (2.31) we obtain the familiar Lagrangian describing electrons, photons, and their interaction.

We arrived at QED by demanding invariance under local phase transformations and identifying the resulting gauge field with the photon. We could have gone the other way around. The Lagrangian in Eq. (2.29), which gives the Maxwell equations, is invariant under the U(1) gauge transformation in Eq. (2.26). This invariance must remain when introducing the interaction between photons and matter, leading to the covariant derivative in Eq. (2.25) without the

rather unmotivated step of gauging the global symmetry. Thus, we use the successful classical description of electrodynamics to guide the development of QED. This is a luxury we do not have for the other fundamental interactions, so the procedure of gauging a global symmetry is useful in building the theory of the Standard Model interactions.

The gauge theory of strong interactions, called quantum chromodynamics (QCD), is obtained by this “symmetry gauging” method. QCD is the theory describing the interactions of quarks, which are the constituents of hadrons, and gluons, which are massless gauge bosons. It is an experimental fact that quarks possess a quantum number called color charge. Particles which have this charge are said to be colored, as opposed to uncolored particles such as leptons. The color charge of quarks takes one of three values r, g, b , and quark spinors are therefore organized into three-component fields

$$\Psi = \begin{pmatrix} \psi_r & \psi_g & \psi_b \end{pmatrix}^T. \quad (2.32)$$

The Lagrangian of free quarks is

$$\mathcal{L} = \bar{\Psi} (i\not{\partial} - m) \Psi, \quad (2.33)$$

which is invariant under the global SU(3) transformations

$$\Psi \rightarrow e^{i\alpha_A \lambda_A / 2} \Psi, \quad (2.34)$$

where $A = 1, 2, \dots, 8$, α_A are arbitrary real numbers, and λ_A are the Gell-Mann matrices, which are the generators of SU(3). Conservation of color charge follows from the invariance of Eq. (2.33) under the global transformation Eq. (2.34). Thus, Eq. (2.33) is an experimentally motivated Lagrangian.

Next we gauge the symmetry by replacing the local phase transformations with the local transformations

$$\Psi \rightarrow e^{ig_s \lambda_A \omega_A(x) / 2} \Psi, \quad (2.35)$$

where g_s is a coupling constant and $\omega_A(x)$ are 8 real, smooth functions of spacetime. To obtain a Lagrangian invariant under the transformations in Eq. (2.35) we replace the derivatives acting on the quark fields by

$$D^\mu \Psi = (\partial^\mu + ig_s \lambda_A G_A^\mu / 2) \Psi, \quad (2.36)$$

where we introduced the 8 gluon fields G_A^μ . The quark Lagrangian then becomes

$$\mathcal{L} = \bar{\Psi} (i\not{D} - m) \Psi. \quad (2.37)$$

For Eq. (2.37) to be invariant, the gluon fields must transform as

$$G_A^\mu \rightarrow G_A^\mu - \partial^\mu \omega_A(x) - g_s f_{ABC} \omega_B(x) G_C^\mu \quad (2.38)$$

under an infinitesimal gauge transformation. The transformations in Eq. (2.35) and Eq. (2.38) constitute an SU(3) gauge transformation.

For a complete picture, the QCD Lagrangian should contain terms which describe gluons when no quarks are present. In QED, this was achieved by the kinetic term Eq. (2.29). An analogous

term for gluons does not work, since the expression

$$-\frac{1}{4}F_{A\mu\nu}F_A^{\mu\nu}, \quad (2.39)$$

where $F_A^{\mu\nu} = \partial^\mu G_A^\nu - \partial^\nu G_A^\mu$, is not invariant under SU(3) gauge transformations. To fix this, we define the gluon field strength tensor

$$G_A^{\mu\nu} = F_A^{\mu\nu} + g_s f_{ABC} G_B^\mu G_C^\nu \quad (2.40)$$

to write the gauge invariant gluon Lagrangian

$$\mathcal{L} = -\frac{1}{4}G_{A\mu\nu}G_A^{\mu\nu}. \quad (2.41)$$

The Lagrangian of QCD is thus

$$\mathcal{L} = \bar{\Psi}(i\cancel{\partial} - m)\Psi - \frac{1}{2}g_s\bar{\Psi}G_A\lambda_A\Psi - \frac{1}{4}G_{A\mu\nu}G_A^{\mu\nu}, \quad (2.42)$$

where we pulled the quark-gluon interaction term out from Eq. (2.37). In addition, Eq. (2.42) describes the self-interactions of 8 colored gluons in the last term.

To complete the Standard Model, we need a gauge theory of the weak interactions. This is, however, not a straightforward task. Whereas the gauge bosons of QED and QCD are massless, the weak gauge bosons, Z and W^\pm , are massive. Explicit mass terms for gauge bosons break gauge invariance, so a more involved approach is required. Thus, the next section is devoted to describing the standard electroweak theory.

2.3 The Standard Electroweak Theory

2.3.1 Gauge Invariant Electroweak Interactions

A striking feature of the weak interactions is that it affects only left-chiral particles and right-chiral antiparticles; parity is violated. Thus, the chirality projectors in Eq. (2.11) come into play. For a given fermion species ψ , the chiral components $\psi_L = P_L\psi$ and $\psi_R = P_R\psi$ have different quantum numbers and transform differently under gauge transformations. From here on, to avoid overly cluttered notation, fermion field operators are named according to their species, i.e. the electron field operator is $\ell_e = \psi_{\ell_e}$ etc.

The electroweak interactions are described by the gauge group $SU(2)_L \times U(1)_Y$. The charged lepton fields ℓ_α and neutrinos ν_α interact with the gauge bosons according to the Lagrangian

$$\mathcal{L}_L = \overline{L_{\alpha L}}i\cancel{D}L_{\alpha L} + \overline{\ell_{\alpha R}}i\cancel{D}\ell_{\alpha R}, \quad (2.43)$$

where there is an implied sum over $\alpha = e, \mu, \tau$. $L_{\alpha L}$ is the left-chiral $SU(2)_L$ doublet

$$L_{\alpha L} = \begin{pmatrix} \nu_{\alpha L} \\ \ell_{\alpha L} \end{pmatrix}, \quad (2.44)$$

and the covariant derivatives are defined as

$$D_\mu L_{\alpha L} = \left(\partial_\mu + ig \frac{\sigma^j}{2} W_\mu^j - ig' \frac{1}{2} B_\mu \right) L_{\alpha L}, \quad (2.45)$$

$$D_\mu \ell_{\alpha R} = (\partial_\mu - ig' B_\mu) \ell_{\alpha R}. \quad (2.46)$$

W_μ^j and B_μ are the three gauge bosons of $SU(2)_L$, and the gauge boson of $U(1)_Y$, respectively. We see explicitly that the left- and right-chiral components of the Dirac spinor ℓ_α behave differently. Specifically, the $SU(2)_L$ gauge bosons only couple to the left-chiral doublet. The strength of the coupling to the B_μ depends on the hypercharge Y of the field, defined as

$$Y = \frac{q}{e} - I_3^W, \quad (2.47)$$

where q/e is the electric charge of the field in units of the elementary charge, and I_3^W is the third component of the weak isospin of the field. I_3^W is 1/2 for the upper component of an $SU(2)_L$ doublet, and $-1/2$ for the lower component. These are also called isospin up and down, respectively, in analogy with the spin angular momentum quantum numbers. Thus, $L_{\alpha L}$ has $Y = -1/2$ and $\ell_{\alpha R}$ has $Y = -1$. Note that right-chiral neutrinos $\nu_{\alpha R}$ are not part of an isospin doublet and has zero electric charge, and thus zero hypercharge. $\nu_{\alpha R}$ is therefore a complete singlet under the Standard Model, and is not included in the theory. However, as we shall explore in the next section, the theory can be extended to include right-chiral neutrinos in order to explain non-zero neutrino masses.

The gauge bosons have associated kinetic and self-interaction terms, which describe their behavior when no fermions are present. These are

$$\mathcal{L}_B = -\frac{1}{4} W_{i\mu\nu} W_i^{\mu\nu} - \frac{1}{4} B_{\mu\nu} B^{\mu\nu}, \quad (2.48)$$

where

$$W_i^{\mu\nu} = \partial^\mu W_i^\nu - \partial^\nu W_i^\mu - g \epsilon_{ijk} W_j^\mu W_k^\nu, \quad (2.49)$$

$$B^{\mu\nu} = \partial^\mu B^\nu - \partial^\nu B^\mu. \quad (2.50)$$

So far, we have described an $SU(2)_L \times U(1)_Y$ gauge invariant theory with massless leptons and gauge bosons. This is not what is realized in nature; we want to describe massive fermions interacting with three massive weak bosons and a massless photon. However, naively introducing mass terms would explicitly break the gauge symmetry. To see this, consider a Dirac mass term for the charged leptons,

$$-m_l \bar{\ell}_\alpha \ell_\alpha = -m_l \bar{\ell}_\alpha (P_L + P_R) \ell_\alpha = -m_l (\bar{\ell}_{\alpha R} \ell_{\alpha L} + \bar{\ell}_{\alpha L} \ell_{\alpha R}). \quad (2.51)$$

Since $\ell_{\alpha L}$ are parts of weak isodoublets and $\ell_{\alpha R}$ are singlets, this term does not respect the gauge symmetry.

Introducing masses for the particles in a gauge invariant way requires spontaneous breaking of $SU(2)_L \times U(1)_Y$ down to $U(1)_{\text{em}}$. In doing so, we will obtain massive charged leptons and weak gauge bosons, and along the way we will find the charged- and neutral current weak interactions, as well as the familiar electromagnetic interactions of QED.

2.3.2 Spontaneous Electroweak Symmetry Breaking

The spontaneous breaking of electroweak gauge symmetry and consequent acquisition of mass for the weak gauge bosons and fermions is called the Brout-Englert-Higgs (BEH) mechanism. It is facilitated by a complex scalar doublet

$$\phi = \begin{pmatrix} \phi_1 \\ \phi_2 \end{pmatrix}, \quad (2.52)$$

called the Higgs doublet, described by the Lagrangian

$$\mathcal{L}_\phi = (D_\mu \phi)^\dagger (D^\mu \phi) - \mu^2 \phi^\dagger \phi - \lambda (\phi^\dagger \phi)^2 \equiv (D_\mu \phi)^\dagger (D^\mu \phi) - V(\phi), \quad (2.53)$$

where $\mu^2 < 0$ and $\lambda > 0$. The potential $V(\phi)$ has minima at $\phi = \phi_0$, defined by

$$\begin{aligned} \phi_0^\dagger \phi_0 &= |\phi_{10}|^2 + |\phi_{20}|^2 = -\frac{\mu^2}{2\lambda} \equiv \frac{v^2}{2} \\ \implies \sqrt{|\phi_{10}|^2 + |\phi_{20}|^2} &= \frac{v}{\sqrt{2}} e^{i\theta}, \end{aligned} \quad (2.54)$$

where v is the vacuum expectation value (vev) of the Higgs field, and $0 \leq \theta < 2\pi$. Thus, there is an infinite number of minima, depending on the phase angle θ . For the ground state of the field, a particular value must be chosen, spontaneously breaking the symmetry. Without loss of generality we choose

$$\phi_0 = \begin{pmatrix} 0 \\ v/\sqrt{2} \end{pmatrix}. \quad (2.55)$$

In order to keep electromagnetic gauge invariance unbroken, we impose that ϕ_0 respects $U(1)_{\text{em}}$. The vacuum state transforms under an electromagnetic gauge transformation as

$$\phi_0 \rightarrow \phi'_0 = \exp[-iqf(x)] \phi_0 = \exp\left[-i\left(Y + I_3^W\right)ef(x)\right] \phi_0, \quad (2.56)$$

for some differentiable function of spacetime $f(x)$. To obtain $\phi'_0 = \phi_0$ the isospin down component of the Higgs doublet must be electrically neutral, i.e. we need $Y = -I_3^W$. From this, we deduce $Y = 1/2$ for the Higgs doublet, and we can write the covariant derivative explicitly as

$$D_\mu \phi = \left(\partial_\mu + ig \frac{\sigma^j}{2} W_\mu^j + ig' \frac{1}{2} B_\mu \right) \phi. \quad (2.57)$$

Thus, we have two complex scalar fields, ϕ_1 with charge +1 and the electrically neutral ϕ_2 . To facilitate interpretation of excitations of the ground state as particles upon quantization, the Higgs doublet is parameterized in terms of deviations from the ground state, as

$$\phi = \frac{1}{\sqrt{2}} \begin{pmatrix} \eta_1 + i\eta_2 \\ v + H + i\eta_3 \end{pmatrix}, \quad (2.58)$$

where η_i and H are real scalar fields. As we will see, three of these degrees of freedom will be absorbed in the weak gauge bosons when they acquire mass. Consequently, the parametrization of the Higgs doublet in Eq. (2.58) contains redundant degrees of freedom. To remove these, we

express the field in the unitary gauge, where

$$\phi = \frac{1}{\sqrt{2}} \begin{pmatrix} 0 \\ v + H \end{pmatrix}. \quad (2.59)$$

Thus the Higgs doublet is expressed in terms on one real degree of freedom H , which is the Higgs boson. Other gauges, such as the Feynman gauge, may be more practical in calculations of higher-order diagrams. Then, the fields η_i are present and give contributions to the amplitudes. The amplitudes, corresponding to physical observables, are of course independent of gauge choice. The unitary gauge is convenient for expressing the electroweak Lagrangian, since superfluous terms corresponding to unphysical degrees of freedom disappear. For the remainder of this section, we assume that all fields in the theory are expressed in the unitary gauge.

The leptons couple to the Higgs doublet through the gauge invariant Yukawa terms

$$\mathcal{L}_Y = - \sum_{\alpha=e,\mu,\tau} y_\alpha^\ell \overline{L_{\alpha L}} \phi \ell_{\alpha R} + H.c., \quad (2.60)$$

where y_α^ℓ are dimensionless coupling constants called Yukawa couplings. After spontaneous symmetry breaking, the Higgs doublet takes the form of Eq. (2.59). Substituting into Eq. (2.60), we find

$$\mathcal{L}_Y = - \sum_{\alpha=e,\mu,\tau} \frac{y_\alpha^\ell v}{\sqrt{2}} \overline{\ell_\alpha} \ell_\alpha - \sum_{\alpha=e,\mu,\tau} \frac{y_\alpha^\ell}{\sqrt{2}} \overline{\ell_\alpha} \ell_\alpha H \quad (2.61)$$

where $\ell_\alpha = \ell_{\alpha L} + \ell_{\alpha R}$. The first term is a mass term for the charged leptons, with $m_\ell = y_\alpha^\ell v / \sqrt{2}$. The second term is an interaction between the charged leptons and the Higgs boson, with the coupling m_ℓ / v . Thus, the charged leptons acquire mass in a gauge invariant way by the BEH mechanism.

To recover the known massive gauge bosons and the massless photon, we make the identifications

$$\begin{aligned} W_\mu &= \frac{1}{\sqrt{2}} (W_\mu^1 - iW_\mu^2), \\ W_\mu^3 &= \cos \theta_W Z_\mu + \sin \theta_W A_\mu, \\ B_\mu &= -\sin \theta_W Z_\mu + \cos \theta_W A_\mu, \end{aligned} \quad (2.62)$$

where W_μ is the non-Hermitian field describing the W^\pm bosons, Z_μ and A_μ are the Z^0 boson and photon fields, respectively, and θ_W is the weak mixing angle (also called the Weinberg angle). Substituting these expressions into the lepton gauge interactions in Eq. (2.43) and imposing the constraint

$$g \sin \theta_W = g' \cos \theta_W = e \quad (2.63)$$

to obtain the correct electromagnetic interaction of QED, we find

$$\begin{aligned} \mathcal{L}_L &= -j_\mu A^\mu - \frac{g}{2\sqrt{2}} \left(J_\mu^\dagger W^\mu + J_\mu W^{\mu\dagger} \right) - \frac{g}{\cos \theta_W} \left(J_\mu^3 - \sin^2 \theta_W \frac{j_\mu}{e} \right) Z^\mu \\ &\quad + \overline{\ell_\alpha} \not{\partial} \ell_\alpha + \overline{\nu_\alpha} \not{\partial} \nu_\alpha, \end{aligned} \quad (2.64)$$

where

$$\begin{aligned}
j_\mu &= -e\overline{\ell_\alpha}\gamma_\mu\ell_\alpha, \\
J_\mu &= \overline{\nu_\alpha}\gamma_\mu(1-\gamma_5)\ell_\alpha = 2\overline{\nu_{\alpha L}}\gamma_\mu\ell_{\alpha L}, \\
J_\mu^3 &= \frac{1}{2}(\overline{\nu_{\alpha L}}\gamma_\mu\nu_{\alpha L} - \overline{\ell_{\alpha L}}\gamma_\mu\ell_{\alpha L})
\end{aligned} \tag{2.65}$$

are the electromagnetic current, the charged weak current and the neutral weak current, respectively. These are linear combinations of the currents which couple directly to W_μ^j and B_μ . In particular, the weak hypercharge current coupling to B_μ is

$$J_\mu^Y = \frac{j_\mu}{e} - J_\mu^3, \tag{2.66}$$

which explains the definition of the weak hypercharge in Eq. (2.47).

The W^\pm and Z^0 bosons acquire mass through the BEH mechanism. To see this, we plug the relations in Eq. (2.62) into the term $|D_\mu\phi_0|^2$ which appears in \mathcal{L}_ϕ after spontaneous symmetry breaking to obtain

$$|D_\mu\phi_0|^2 = \frac{1}{4}(gv)^2 W_\mu^\dagger W^\mu + \frac{1}{8}\frac{(gv)^2}{\cos^2\theta_W} Z_\mu Z^\mu, \tag{2.67}$$

and we identify the masses

$$m_W = \frac{gv}{2}, \quad m_Z = \frac{gv}{2\cos\theta_W} = \frac{m_W}{\cos\theta_W}. \tag{2.68}$$

Importantly, the photon field A_μ does not appear in Eq. (2.67), so it remains massless. The weak gauge bosons now have an additional degree of freedom, since they are massive and the longitudinal mode of polarization is allowed. This explains how the fields η_i could be removed by a choice of gauge; the corresponding physical degrees of freedom remain in the theory in the form of the longitudinal polarizations of W^\pm and Z^0 .

The rest of the terms in $|D_\mu\phi|^2$ give the kinetic term for the Higgs boson, as well as the interactions between the Higgs boson and the weak gauge bosons,

$$\begin{aligned}
(D_\mu\phi)^\dagger(D^\mu\phi) &\supset \frac{1}{2}(\partial_\mu H)(\partial^\mu H) + \frac{1}{2}vg^2 W_\mu^\dagger W^\mu H + \frac{1}{4}g^2 W_\mu^\dagger W^\mu H^2 \\
&+ \frac{vg^2}{4\cos^2\theta_W} Z_\mu Z^\mu H + \frac{g^2}{8\cos^2\theta_W} Z_\mu Z^\mu H^2.
\end{aligned} \tag{2.69}$$

To obtain the Higgs mass term and self interactions, we plug Eq. (2.59) into the potential $V(\phi)$, which gives

$$-V(\phi) = -\lambda v^2 H^2 - \lambda v H^3 - \frac{1}{4}\lambda H^4. \tag{2.70}$$

From this we infer the Higgs mass $m_H = \sqrt{2\lambda v^2}$. Combining Eq. (2.67), Eq. (2.69), and Eq. (2.70) gives \mathcal{L}_ϕ in the unitary gauge after spontaneous symmetry breaking.

The remaining task is to plug Eq. (2.62) into \mathcal{L}_B to obtain the kinetic terms for the physical gauge bosons and the interactions between them. The expression is quite lengthy, and we will only summarize the types of interactions which appear. These are trilinear couplings involving

derivatives of the gauge fields, and quadrilinear couplings. Schematically, we have

$$\mathcal{L}_B = WWZ + WWA + WWZZ + WWAA + WWAZ + WWWW + \text{kinetic terms.} \quad (2.71)$$

Putting it all together, the standard electroweak Lagrangian for massless neutrinos is given by

$$\mathcal{L} = \mathcal{L}_Y + \mathcal{L}_L + \mathcal{L}_\phi + \mathcal{L}_B \quad (2.72)$$

where the terms, after symmetry breaking, are given in the unitary gauge in Eqs. (2.61), (2.64), (2.67) and (2.69) to (2.71).

2.3.3 Weak Interactions of Quarks

So far in this section, we have only considered the electroweak interactions of quarks. The theory also applies to the quark sector in a straight-forward way. Left-chiral quarks make up the weak isospin doublets

$$Q'_{iL} = \begin{pmatrix} u'_{iL} \\ d'_{iL} \end{pmatrix}, \quad (2.73)$$

where u'_{iL} are the left-chiral up-type quarks of weak isospin $+1/2$ and electric charge $+2/3$, and d'_{iL} are the left-chiral down-type quarks of weak isospin $-1/2$ and electric charge $-1/3$. There are corresponding right-chiral fields u'_{iR} and d'_{iR} with the same electric charge as their left-chiral counterparts and no weak isospin. The prime on the field operators will be explained shortly. The index $i = 1, 2, 3$ is the flavor index, referring to the three generations

$$\begin{pmatrix} u' \\ d' \end{pmatrix}, \quad \begin{pmatrix} c' \\ s' \end{pmatrix}, \quad \begin{pmatrix} t' \\ b' \end{pmatrix}, \quad (2.74)$$

written in ascending order of mass. The quarks participate in the electroweak interaction according to the Lagrangian

$$\mathcal{L}_Q = \overline{Q'_{iL}} i \not{D} Q'_{iL} + \overline{u'_{iR}} i \not{D} u'_{iR} + \overline{d'_{iR}} i \not{D} d'_{iR}, \quad (2.75)$$

where there is an implicit sum over i , and the covariant derivatives are

$$D_\mu Q'_{iL} = \left(\partial_\mu + ig \frac{\sigma^j}{2} W_\mu^j + ig' \frac{1}{6} B_\mu \right) Q'_{iL}, \quad (2.76)$$

$$D_\mu u'_{iR} = \left(\partial_\mu + ig' \frac{2}{3} B_\mu \right) u'_{iR}, \quad (2.77)$$

$$D_\mu d'_{iR} = \left(\partial_\mu - ig' \frac{1}{3} B_\mu \right) d'_{iR}. \quad (2.78)$$

Quark masses are readily explained by the BEH mechanism. The Yukawa Lagrangian is expanded with the terms

$$\mathcal{L}_Y \supset -Y_{ij}^d \overline{Q'_{iL}} \phi d'_{jR} - Y_{ij}^u \overline{Q'_{iL}} \tilde{\phi} u'_{jR} + H.c. \quad (2.79)$$

To obtain mass terms for the up-type quarks we introduced the charge conjugate Higgs doublet

$$\tilde{\phi} = i\sigma^2\phi^* = \frac{1}{\sqrt{2}} \begin{pmatrix} v + H \\ 0 \end{pmatrix}, \quad (2.80)$$

where the second equality holds in the unitary gauge. After electroweak symmetry breaking, the Lagrangian in Eq. (2.79) gives mass terms for the quarks. Y^u and Y^d are 3×3 matrices of Yukawa couplings. These matrices are in general not diagonal, so u' and d' are not states of definite mass after symmetry breaking. To obtain the mass eigenstates we must transform into a basis in which Y^u and Y^d are diagonal. To do so, we define the unitary matrices V_L^u , V_R^u , V_L^d , and V_L^u such that

$$V_L^{d\dagger} Y^d V_R^d = Y^{d,\text{diag}}, \quad (2.81)$$

$$V_L^{u\dagger} Y^u V_R^u = Y^{u,\text{diag}}, \quad (2.82)$$

where $Y_{ij}^{d,\text{diag}} = y_i^d \delta_{ij}$, $Y_{ij}^{u,\text{diag}} = y_i^u \delta_{ij}$, and y_i^d and y_i^u are Yukawa couplings. Expanding the doublets in Eq. (2.79), we can now write

$$\begin{aligned} \mathcal{L}_Y &\supset -\frac{v+H}{\sqrt{2}} Y_{ij}^d \overline{d'_{iL}} d'_{jR} - \frac{v+H}{\sqrt{2}} Y_{ij}^u \overline{u'_{iL}} u'_{jR} + H.c. \\ &= -\frac{v+H}{\sqrt{2}} \left(V_L^d Y^{d,\text{diag}} V_R^{d\dagger} \right)_{ij} \overline{d'_{iL}} d'_{jR} - \frac{v+H}{\sqrt{2}} \left(V_L^u Y^{u,\text{diag}} V_R^{u\dagger} \right)_{ij} \overline{u'_{iL}} u'_{jR} + H.c. \\ &= -\frac{y_i^d v}{\sqrt{2}} \overline{d_i} d_i - \frac{y_i^u v}{\sqrt{2}} \overline{u_i} u_i - \frac{y_i^d}{\sqrt{2}} \overline{d_i} d_i H - \frac{y_i^u}{\sqrt{2}} \overline{u_i} u_i H \end{aligned} \quad (2.83)$$

where $u_i = u_{iL} + u_{iR}$ and $d_i = d_{iL} + d_{iR}$ are quarks of definite mass, defined by

$$\begin{aligned} d_{iL} &= \left(V_L^{d\dagger} \right)_{ij} d'_{jL}, & d_{iR} &= \left(V_R^{d\dagger} \right)_{ij} d'_{jR}, \\ u_{iL} &= \left(V_L^{u\dagger} \right)_{ij} u'_{jL}, & u_{iR} &= \left(V_R^{u\dagger} \right)_{ij} u'_{jR}. \end{aligned} \quad (2.84)$$

The quark mass terms are the first two terms in Eq. (2.83), with masses $m_{u_i} = y_i^u v / \sqrt{2}$ and $m_{d_i} = y_i^d v / \sqrt{2}$. The third and fourth terms in Eq. (2.83) are the interactions between the quarks and the Higgs boson.

To understand what the observable effects of quark mixing are, we need to see its effect on the weak charged current interaction of quarks. These currents are

$$J_\mu^Q = 2\overline{u'_{iL}} \gamma_\mu d'_{iL}, \quad (2.85)$$

similar to the leptonic charged currents J^μ in Eq. (2.65). In the mass basis, the quark weak charge current takes the form

$$J_\mu^Q = 2\overline{u_{jL}} \left(V_L^{u\dagger} \right)_{ji} \gamma_\mu \left(V_L^d \right)_{ik} d_{kL} = 2\overline{u_{jL}} \gamma_\mu \left(V_L^{u\dagger} V_L^d \right)_{jk} d_{kL}. \quad (2.86)$$

Thus, the weak charged current interactions couple the weak eigenstates within each generation in Eq. (2.74) to each other, which are admixtures of the mass eigenstates. In this way, the decay of heavy quarks to lighter quarks across generations can occur. Quark mixing has no consequence for weak neutral current interactions and electromagnetic interactions, since the

mixing matrices cancel due to unitarity. Since the only observable effect of mixing is that described by Eq. (2.86), the matrix

$$V_{u_i d_j}^{\text{CKM}} \equiv \left(V_L^{u\dagger} V_L^d \right)_{ij}, \quad (2.87)$$

called the Cabibbo-Kobayashi-Maskawa (CKM) matrix, is defined. The elements of the CKM matrix, characterizing the coupling strength between u_{iL} and d_{jL} , are parameters to be determined by experiment.

When introducing the Yukawa terms for leptons in Eq. (2.60), we did not run into the complication of mixing. The reason for this is that the lepton flavors are *defined* by the charged lepton mass states. In the Standard Model, mass is the only property differentiating e , μ and τ , and the neutrino states are defined by which of these mass eigenstates they couple to in the weak charged current interactions. Thus, the neutrino ν_α only couples to ℓ_α , by definition. Since the neutrinos are massless in every basis, there is no reason to transform the lepton fields. For quarks, we do not have this luxury; there is no a priori reason that the eigenstates of the weak interactions and the mass eigenstates that define their flavor should coincide.

We have now discussed the ingredients of the Standard Model, which, putting everything together, is the gauge theory of $SU(3)_c \times SU(2)_L \times U(1)_Y$, with spontaneous breaking of the symmetry to $SU(3)_c \times U(1)_{\text{em}}$. In its original formulation, the neutrino sector of the Standard Model describes three massless states, but is readily extended to include massive neutrinos. This extension of the electroweak theory can be done in a straightforward way, analogously to the charged lepton masses, by introducing right-chiral components of the neutrino fields. This would be restrictive, however; neutrinos are not obligated to obtain mass only through Yukawa couplings to the Higgs vev. The topic of neutrino masses requires a more detailed discussion, which is given in the following section.

2.4 Neutrino Masses

With the observation of neutrino oscillations [9], it is an established fact that neutrinos are massive. Similarly to the quark sector, the neutrinos of definite mass are in general superpositions of flavor eigenstates, which are defined by their charged current interactions. Roughly speaking, due to their different masses the massive neutrinos propagate with different frequencies, allowing interference between the flavor components of the mass eigenstate. Thus, a neutrino emitted in the electron flavor eigenstate has a non-zero probability to be observed as a muon or tau neutrino on detection. Neutrino oscillations will be described in more detail in Section 2.6.

One way to incorporate neutrino masses into the Standard Model is to introduce new right-chiral singlet fields N_{sR} . As the name suggests, these fields are singlets under the Standard Model gauge group, in contrast to the active, left-chiral neutrinos $\nu_{\alpha L}$ which partake in the weak interactions. The most general mass Lagrangian for neutrinos after electroweak symmetry breaking is [3, p. 130]

$$\mathcal{L}_{\text{Mass}} = - \sum_{s=1}^n \sum_{\alpha=e,\mu,\tau} \overline{N_{sR}} M_{s\alpha}^D \nu_{\alpha L} + \frac{1}{2} \sum_{s,s'=1}^n N_{sR}^T C^\dagger M_{ss'}^R N_{s'R} + H.c. \quad (2.88)$$

The number of active neutrinos is constrained to three by the invisible Z boson decay width [10],

but the number of singlet neutrinos is unconstrained. Thus, for the sake of generality we include n such fields.

The first term in Eq. (2.88) is a Dirac mass term with the $n \times 3$ Dirac mass matrix M^D , arising after electroweak symmetry breaking from the $SU(2)_L \times U(1)_Y$ invariant Yukawa Lagrangian

$$\mathcal{L} \supset - \sum_{s=1}^N \sum_{\alpha=e,\mu,\tau} \overline{L_{\alpha L}} \tilde{\phi} Y_{s\alpha}^\nu N_{sR} - \sum_{\alpha=e,\mu,\tau} \overline{L_{\alpha L}} \phi Y_{\alpha\beta}^\ell \ell_{\beta R} + H.c., \quad (2.89)$$

where Y^ν and Y^ℓ are matrices of Yukawa couplings. If we take $M_{ss'}^R = 0$ and assume $n = 3$, the singlet fields can be incorporated as the right-chiral components of the flavor neutrinos, i.e. $N_{sR} \rightarrow \nu_{\alpha R}$. We then find the familiar-looking Yukawa term

$$\begin{aligned} \mathcal{L} \supset & - \sum_{\alpha=e,\mu,\tau} \left(\overline{L_{\alpha L}} \tilde{\phi} Y_{\alpha\beta}^\nu \nu_{\beta R} + \overline{L_{\alpha L}} \phi Y_{\alpha\beta}^\ell \ell_{\beta R} \right) + H.c. \\ & = - \frac{v+H}{\sqrt{2}} \sum_{\alpha=e,\mu,\tau} \left(Y_{\alpha\beta}^\nu \overline{\nu_{\alpha L}} \nu_{\beta R} + Y_{\alpha\beta}^\ell \overline{\ell_{\alpha L}} \ell_{\beta R} \right) + H.c. \end{aligned} \quad (2.90)$$

In this case, the mechanism of neutrino mass is exactly analogous to the case of up-type quarks. As discussed in Section 2.3.3, the flavor states of the charged leptons are defined by their mass, so we take Y^ℓ to be diagonal without loss of generality. Meanwhile, to find the neutrino mass eigenstates we must do a change of basis. The Yukawa matrix is diagonalized,

$$U_L^\dagger Y^\nu U_R = Y^{\nu,\text{diag}}, \quad (2.91)$$

where $U_{L,R}$ are unitary matrices such that $Y_{ij}^{\nu,\text{diag}} = y_i^\nu \delta_{ij}$. The neutrino mass eigenstates are linear combinations of the flavor states, the coefficients being the elements of the matrices $U_{L,R}^\dagger$,

$$\nu_{iL} = (U_L^\dagger)_{i\alpha} \nu_{\alpha L}, \quad \nu_{iR} = (U_R^\dagger)_{i\alpha} \nu_{\alpha R}. \quad (2.92)$$

As in the case for quarks, the observable consequence of neutrino mixing is manifested in the charged current weak interactions, the neutral current interactions being invariant under the change of bases. Writing the leptonic charged weak current J^μ in the neutrino mass basis, we have

$$J^\mu = 2\overline{\nu_{\alpha L}} \gamma_\mu \ell_{\alpha L} = 2\overline{\nu_{iL}} (U_L^\dagger)_{i\alpha} \gamma_\mu \ell_{\alpha L}. \quad (2.93)$$

The physical effects of neutrino mixing are thus encoded in the unitary matrix

$$(U_L)_{\alpha i} \equiv U_{\alpha i}^{\text{PMNS}}, \quad (2.94)$$

called the Pontecorvo-Maki-Nakagawa-Sakata (PMNS) matrix. As mentioned, we assumed here that the three active neutrinos are Dirac particles; they are accompanied by three right-chiral singlet fields $\nu_{\alpha R}$. If this is not the case and there are more singlet neutrinos, the mixing matrix must be extended to accommodate the extra states, as we will see below.

Inserting the expression for $\tilde{\phi}$ in the unitary gauge given in Eq. (2.80) into the Yukawa La-

grangian Eq. (2.90) and using Eq. (2.91) and Eq. (2.92), we find the mass term

$$\mathcal{L} \supset - \sum_{i=1}^3 \frac{y_i^\nu v}{\sqrt{2}} \overline{\nu_{iL}} \nu_{iR} + H.c. . \quad (2.95)$$

Thus, the neutrino masses are $m_i = y_i^\nu v / \sqrt{2}$. To obtain masses in the acceptable range of ~ 0.1 eV [10], the Yukawa couplings must be $\sim 10^{-12}$, six orders of magnitude below even the electron Yukawa coupling, $y_e \approx 2.9 \times 10^{-6}$. Although the masses of neutrinos can be described in this way, their smallness is left unexplained. It is desirable to find a mechanism by which small neutrino masses are obtained in a more natural way.

The second term of Eq. (2.88) is a mass term for the singlet neutrinos. Note that the term can be written in the form

$$-\frac{1}{2} \overline{N_s} M_{ss'}^R N_{s'}, \quad (2.96)$$

where the Hermitian conjugate was included, and we defined the field $N_s = N_{sR} + N_{sR}^c$. This field satisfies the Majorana condition $N_s^c = N_s$, and Eq. (2.96) is therefore called a Majorana mass term. An analogous term could be written for the active neutrinos, but it would violate electroweak gauge symmetry and is therefore forbidden.

To obtain the neutrino mass eigenstates when both terms in Eq. (2.88) are present, we start by defining the array of left-chiral fields

$$\Psi_L = \left(\nu_{eL} \quad \nu_{\mu L} \quad \nu_{\tau L} \quad N_{1R}^c \quad \dots \quad N_{nR}^c \right)^T . \quad (2.97)$$

Then we can write the mass Lagrangian in the form

$$\mathcal{L}_{\text{Mass}} = \frac{1}{2} \Psi_L^T C^\dagger \mathcal{M} \Psi_L + H.c. , \quad (2.98)$$

where \mathcal{M} is the $(3+n) \times (3+n)$ mass matrix

$$\mathcal{M} = \begin{pmatrix} 0 & M^{DT} \\ M^D & M^R \end{pmatrix} . \quad (2.99)$$

We can now diagonalize the combined mass term by writing Ψ_L as a linear combination of the fields ν_{iL} ,

$$\Psi_{\alpha L} = U_{\alpha j} \nu_{jL} . \quad (2.100)$$

α here refers to both active and singlet flavors¹. The unitary matrix U is chosen such that

$$U^T \mathcal{M} U = \mathcal{M}^{\text{diag}}, \quad (2.101)$$

where $\mathcal{M}_{ij}^{\text{diag}} = m_i \delta_{ij}$. Thus, the fields ν_{iL} are $3+n$ mass eigenstates, and the mass Lagrangian can be written as

$$\mathcal{L}_{\text{Mass}} = \frac{1}{2} \sum_{i=1}^{3+n} m_i \nu_{iL}^T C^\dagger \nu_{iL} + H.c. = -\frac{1}{2} \sum_{i=1}^{3+n} m_i \overline{\nu_{iL}^c} \nu_{iL} + H.c. \quad (2.102)$$

¹The terminology of ‘‘flavor’’ to distinguish between the neutrino states participating in the weak charged current, is expanded to include the ‘‘singlet flavors’’ $s = 1, \dots, n$.

This Lagrangian takes the form of a Majorana mass term. Indeed, as for the singlet neutrino mass term we can write

$$\mathcal{L}_{\text{Mass}} = -\frac{1}{2} \sum_{i=1}^{3+n} m_i \bar{\nu}_i \nu_i, \quad (2.103)$$

where $\nu_i = \nu_{iL} + \nu_{iL}^c$ are massive fields satisfying the constraint $\nu_i^c = \nu_i$. Thus, when singlet Majorana fields N_s are present, the massive neutrinos are Majorana particles. As we shall see, this fact has important implications for the magnetic moments of neutrinos.

Again, the effects of mixing show up in the weak interactions. Now, we have $3 + n$ mass states which can be rotated to flavor eigenstates, 3 of which participate in the weak interaction. Recall the leptonic weak charged current,

$$J_\mu = 2\bar{\nu}_{\alpha L} \gamma_\mu \ell_{\alpha L}. \quad (2.104)$$

Rotating to the mass eigenstates requires only using a part of the mixing matrix U . Defining the non-unitary matrix

$$\tilde{U} = U|_{3 \times (3+n)} \quad (2.105)$$

as the $3 \times (3 + n)$ matrix obtained by taking the 3 first rows of U , we have

$$\nu_{\alpha L} = \sum_{\alpha=e,\mu,\tau} \tilde{U}_{\alpha j} \nu_{jL}, \quad (2.106)$$

so the leptonic weak charged current can be written as

$$J_\mu = 2\bar{\nu}_{jL} (\tilde{U}^\dagger)_{j\alpha} \gamma_\mu \ell_{\alpha L}. \quad (2.107)$$

Since the mixing matrix is non-unitary, the leptonic weak neutral current is affected as well,

$$\begin{aligned} J_\mu^3 &\supset \frac{1}{2} \bar{\nu}_{\alpha L} \gamma_\mu \nu_{\alpha L} \\ &= \frac{1}{2} \bar{\nu}_{iL} \gamma_\mu (\tilde{U}^\dagger)_{i\alpha} \tilde{U}_{\alpha j} \nu_{jL}. \end{aligned} \quad (2.108)$$

If mixing between the active flavors and the singlet states is negligible, \tilde{U} reduces to the unitary U^{PMNS} and the active and singlet flavors are isolated. Thus, testing the unitarity of the PMNS matrix is a probe for searching for singlet neutrinos.

It should be noted that a lepton number L assigned to the Majorana neutrinos ν_i is not conserved. In the Standard Model, lepton number is a Noether charge associated with the symmetry under a global $U(1)$ transformation

$$\psi \rightarrow e^{i\phi} \psi, \quad (2.109)$$

where ψ denotes the charged leptons and the standard left-chiral flavor neutrinos. Leptons have $L = +1$, while antileptons have $L = -1$. Clearly, such an assignment is problematic for Majorana neutrinos since the particles and antiparticles coincide. Majorana neutrinos allow for processes with $\Delta L = 2$, such as neutrinoless double beta decay ($0\nu\beta\beta$). Searching for $0\nu\beta\beta$ and other processes which similarly violate lepton number is an active field of research. Very recently, the CMS collaboration performed a search for vector boson fusion events with two muons of the same charge and no neutrinos in the final state [11]. In this process, the initial

state consists of hadrons with $L = 0$, while the final state has $L = \pm 2$. No deviation from the Standard model was found, allowing upper bounds to be set on mixing between ν_μ and N_R^c for a singlet mass in the 100 MeV - 10 TeV range.

2.5 The See-Saw Mechanism

With the mass matrix in Eq. (2.99), an opportunity arises to explain the smallness of the active neutrino masses. The Dirac mass matrix M^D is generated by the Higgs mechanism, and its entries are therefore expected to be of the order of the other fermion masses. Meanwhile, it is possible that M^R is generated by new physics at a high energy scale. The fields N_s could be parts of multiplets of some gauge symmetry in a high-energy theory, in which case M^R is related to the energy scale at which that symmetry breaks down to the Standard Model gauge group.

Let us first consider the simple case of one active, left-chiral neutrino $\nu_{\alpha L}$, and one singlet, right-chiral neutrino N_R . Thus, $\Psi_L = (\nu_{\alpha L} \quad N_R^c)^T$, and the mass matrix is

$$\mathcal{M}_{2 \times 2} = \begin{pmatrix} 0 & m_D \\ m_D & m_R \end{pmatrix}, \quad (2.110)$$

whose entries are real numbers. As in the general case, this mass matrix is diagonalized with the help of a unitary matrix U such that

$$U^T \mathcal{M}_{2 \times 2} U = \begin{pmatrix} m_1 & 0 \\ 0 & m_2 \end{pmatrix}, \quad (2.111)$$

and the mass eigenstates ν_{iL} are related to the flavor eigenstates by the unitary transformation

$$\Psi_{\alpha L} = U_{\alpha j} \nu_{jL}. \quad (2.112)$$

The mixing matrix U can be parameterized as

$$U = \begin{pmatrix} \cos \theta & \sin \theta \\ -\sin \theta & \cos \theta \end{pmatrix}, \quad (2.113)$$

where the mixing angle θ , which specifies the admixture of flavor states in the massive neutrinos, can be shown to be

$$\tan 2\theta = \frac{2m_D}{m_R}. \quad (2.114)$$

The masses are

$$m_{1,2} = \frac{1}{2} m_R \left(1 \mp \sqrt{1 + 4 \left(\frac{m_D}{m_R} \right)^2} \right). \quad (2.115)$$

Now, if we assume $m_R \gg m_D$ and expand in the small ratio m_D/m_R , we obtain to leading order

$$m_1 \approx \frac{m_D^2}{m_R}, \quad m_2 \approx m_R, \quad (2.116)$$

and the mixing angle is very small. Thus, we find one heavy state mainly composed of N_R^c and one light state mainly composed of $\nu_{\alpha L}$. Because of the negligible mixing, the masses $m_{1,2}$ are sometimes sloppily referred to as the masses of the flavor neutrinos ν_α and N_R^c .

The small mass m_1 is suppressed by m_R ; as increasing the mass of the heavy state results in the lighter mass becoming smaller. Hence, the “see-saw mechanism”. Taking Yukawa couplings of the order unity, we have $m_D \sim v$ and the desirable light mass $m_1 \sim 0.1 \text{ eV}$ is obtained by taking $m_R \sim 10^{14} \text{ GeV}$.

The see-saw mechanism works as long as the approximation $m_R \gg m_D$ holds. For example, allowing the neutrino Yukawa coupling to be on the order of the electron Yukawa coupling, m_R is lowered to 10^2 GeV . Of relevance to this thesis is the assumption that the singlet neutrino is kinematically reachable by neutrinos produced in the sun, which have energies up to $\sim 10 \text{ MeV}$ [12]. Singlet neutrinos with masses not too far from the active neutrino masses are also called sterile neutrinos, and in this case we are interested in sterile neutrinos with mass of order 1 MeV or lower, far below the conventional see-saw scale. For m_R at this scale, a Yukawa coupling of the order 10^{-8} is needed to obtain the correct active mass, and the see-saw mechanism loses much of its appeal. Nevertheless, the formulae in Eq. (2.116) are generic consequences of the assumption $m_R \gg m_D$ when both terms in Eq. (2.88) are present.

Let us now outline the see-saw mechanism in the general case of $3 + n$ neutrino flavors. The entries of M^R are taken to be much larger than the entries of M^D , and the mass matrix can be block-diagonalized by a matrix \mathcal{U} ,

$$\mathcal{U}^T \mathcal{M} \mathcal{U} = \begin{pmatrix} M_{\text{light}} & 0 \\ 0 & M_{\text{heavy}} \end{pmatrix} + \mathcal{O}((M^R)^{-1} M^D), \quad (2.117)$$

where

$$M_{\text{light}} \approx -M^{DT} (M^R)^{-1} M^D \quad (2.118)$$

is a 3×3 matrix whose eigenvalues give the light neutrino masses, and

$$M_{\text{heavy}} \approx M^R \quad (2.119)$$

is an $n \times n$ matrix whose eigenvalues are the masses of n heavy neutrinos. Thus, we obtain 3 light and n heavy neutrino mass eigenstates. The mixing matrix \mathcal{U} has off-diagonal blocks of the order $(M^R)^{-1} M^D$ [13], which we have assumed to be small. This means there is little mixing between the blocks. The 3 light neutrinos are mainly composed of the active flavors ν_e, ν_μ, ν_τ , while the n heavy states are mainly composed of the singlets. Thus, in low-energy situations we effectively have mixing of three massive Majorana neutrinos.

2.6 Neutrino Oscillations

Having seen how neutrino flavor states are superpositions of mass eigenstates, we are now able to discuss neutrino oscillations. Neutrino oscillations are important in the discussion of experimentally measuring neutrino magnetic moments. Therefore, the simple case of neutrino oscillations in vacuum, using the plane wave approximation, is presented here. The derivation closely follows Ref. [3]. For a recent review on neutrino oscillations, see Ref. [14].

Neutrinos produced in weak interactions are in one of three flavor states, which are superpositions of mass eigenstates. Thus, the state describing the emitted neutrino is

$$|\nu_\alpha\rangle = \sum_i U_{\alpha i}^* |\nu_i\rangle, \quad (2.120)$$

where $\alpha = e, \mu, \tau$ and $U_{\alpha i}^*$ are coefficients stemming from the mixing matrix which enters the leptonic weak charged current. The states $|\nu_i\rangle$ describe neutrinos of definite mass, and are therefore eigenvalues of the Hamiltonian,

$$H |\nu_i\rangle = E_i |\nu_i\rangle. \quad (2.121)$$

The time evolution of the mass states is determined by the Schrödinger equation

$$i \frac{d}{dt} |\nu_i(t)\rangle = H |\nu_i(t)\rangle, \quad (2.122)$$

leading to the plane wave solutions

$$|\nu_i(t)\rangle = e^{-iE_i t} |\nu_i\rangle. \quad (2.123)$$

Thus, inserting into Eq. (2.120), a state initially created in the flavor α at $t = 0$ evolves as

$$|\nu_\alpha(t)\rangle = \sum_i U_{\alpha i}^* e^{-iE_i t} |\nu_i\rangle. \quad (2.124)$$

Projecting the evolved state onto another state of definite flavor $|\nu_\beta\rangle$, the transition amplitude for $\nu_\alpha \rightarrow \nu_\beta$ is obtained as a function of time,

$$\langle \nu_\beta | \nu_\alpha(t) \rangle = \sum_{ij} U_{\alpha i}^* U_{\beta j} e^{-iE_i t} \langle \nu_j | \nu_i \rangle = \sum_i U_{\alpha i}^* U_{\beta i} e^{-iE_i t}, \quad (2.125)$$

where the mass states were assumed to be orthonormal. The transition probability is obtained by squaring the amplitude,

$$P_{\nu_\alpha \rightarrow \nu_\beta}(t) = |\langle \nu_\beta | \nu_\alpha(t) \rangle|^2 = \sum_{ij} U_{\alpha i}^* U_{\beta i} U_{\alpha j} U_{\beta j}^* e^{-i(E_i - E_j)t}. \quad (2.126)$$

For ultra-relativistic neutrinos, the energy eigenvalues are

$$E_i = \sqrt{\mathbf{p}^2 + m_i^2} \approx E + \frac{m_i^2}{2E}, \quad (2.127)$$

where $E = |\mathbf{p}|$ is the energy of the neutrino, neglecting the mass contribution. The difference which enters the exponent in Eq. (2.126) is then

$$E_i - E_j \approx \frac{m_i^2 - m_j^2}{2E} \equiv \frac{\Delta m_{ij}^2}{2E}, \quad (2.128)$$

where the squared-mass difference Δm_{ij}^2 was defined. Furthermore, since the propagation time t is not measured, it is useful to make the approximation $t \approx L$, where L is the distance between the neutrino source and the detector. This approximation holds since ultrarelativistic neutrinos travel at nearly the speed of light. With these approximations we obtain the useful formula for

the transition probability,

$$P_{\nu_\alpha \rightarrow \nu_\beta}(L, E) = \sum_{ij} U_{\alpha i}^* U_{\beta i} U_{\alpha j} U_{\beta j}^* \exp\left(-i \frac{\Delta m_{ij}^2 L}{2E}\right). \quad (2.129)$$

The ratio L/E depends on the experiment, and the mixing matrix and squared mass differences are constants of nature to be measured. Clearly, if all neutrinos are massless, neutrino oscillations would not be observed. Unfortunately, however, oscillation experiments cannot probe absolute neutrino masses, only their squared differences.

In the above derivation the neutrinos were assumed to be ultrarelativistic. But if neutrinos are massive, they can in principle travel at any velocity relative to the detector. Consider the processes by which the neutrinos are detected. One option is processes like

$$\nu + A \rightarrow \sum_i X_i, \quad (2.130)$$

proceeding through charged or neutral weak current interactions, where A and X_i are the target particle in the detector and the daughter particles, respectively. The threshold neutrino energy for such processes to occur is $E \gtrsim \mathcal{O}(100 \text{ keV})$ [3, p. 143]. Another option is scattering off an atomic electron, $\nu + e^- \rightarrow \nu + e^-$, which has the cross section $\sigma \propto E$. This sets sensitivity limits on the neutrino energy for detectors using this process. Even ignoring this, the characteristic energies for atomic electrons is on the order of a few eV. In any case, for the present limits on neutrino masses at $\mathcal{O}(0.1 \text{ eV})$ [10], the detectable neutrinos satisfy $E \gg m$, and the ultrarelativistic approximation is not restrictive.

Chapter 3

Magnetic Moments

3.1 The Classical Description

The behavior of a system of charged particles in an electromagnetic field is described by the Lagrangian [15, p. 22]

$$L = \frac{1}{2}m_i v_i^2 + q_i \vec{\mathbf{A}}(\vec{\mathbf{r}}_i) \cdot \vec{\mathbf{v}}_i - q_i \phi(\vec{\mathbf{r}}_i), \quad (3.1)$$

where m_i , $\vec{\mathbf{v}}_i$ and q_i are the mass, velocity and charge of particle i , respectively, $\vec{\mathbf{A}}(\vec{\mathbf{r}})$ is the magnetic vector potential, and $\phi(\vec{\mathbf{r}})$ is the electric scalar potential. The magnetic field $\vec{\mathbf{B}}$ is given by $\vec{\mathbf{B}} = \vec{\nabla} \times \vec{\mathbf{A}}$. For a uniform magnetic field, we can use the vector potential $\vec{\mathbf{A}} = \frac{1}{2} \vec{\mathbf{B}} \times \vec{\mathbf{r}}$, since

$$\begin{aligned} \vec{\nabla} \times \vec{\mathbf{A}} &= \frac{1}{2} \vec{\nabla} \times (\vec{\mathbf{B}} \times \vec{\mathbf{r}}) \\ &= \frac{1}{2} \left[(\vec{\mathbf{r}} \cdot \vec{\nabla}) \vec{\mathbf{B}} - (\vec{\mathbf{B}} \cdot \vec{\nabla}) \vec{\mathbf{r}} + \vec{\mathbf{B}} (\vec{\nabla} \cdot \vec{\mathbf{r}}) - \vec{\mathbf{r}} (\vec{\nabla} \cdot \vec{\mathbf{B}}) \right] \\ &= \frac{1}{2} \left[-\vec{\mathbf{B}} + 3\vec{\mathbf{B}} \right] = \vec{\mathbf{B}}, \end{aligned} \quad (3.2)$$

where in the second line, the first term vanishes by uniformity and the fourth term vanishes since $\vec{\mathbf{B}}$ is divergence-free. Assuming that every particle in the system has the same ratio q/m , the Lagrangian can be rewritten as

$$\begin{aligned} L &= \frac{1}{2}m_i v_i^2 + \frac{q}{2m} (\vec{\mathbf{B}} \times \vec{\mathbf{r}}_i) \cdot m_i \vec{\mathbf{v}}_i - q_i \phi(\vec{\mathbf{r}}_i) \\ &= \frac{1}{2}m_i v_i^2 + \frac{q\vec{\mathbf{B}}}{2m} \cdot (\vec{\mathbf{r}}_i \times m_i \vec{\mathbf{v}}_i) - q_i \phi(\vec{\mathbf{r}}_i). \end{aligned} \quad (3.3)$$

The quantity in the brackets is the angular momentum $\vec{\mathbf{L}}$ of the system. Thus, the interaction between the system and an external uniform magnetic field is described by the potential

$$V = -\frac{q}{2m} \vec{\mathbf{L}} \cdot \vec{\mathbf{B}} \equiv -\vec{\mu} \cdot \vec{\mathbf{B}}. \quad (3.4)$$

The vector $\vec{\mu}$ is the magnetic moment vector of the system, characterizing the strength of the interaction of the system with the external magnetic field. The sign choice in Eq. (3.4) is such that a magnetic dipole tends to align itself with the external magnetic field.

The above description can be used to calculate the magnetic moment of a system of charged particles. Consider, for example, a collection of uniformly distributed particles of charge q and mass m , travelling around a circular loop of radius R at an angular speed $\omega = v/R$. The system is illustrated in Fig. 3.1.

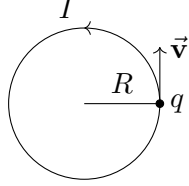


Figure 3.1: A system consisting of uniformly distributed particles with charge q , travelling in a circular loop of radius R . The particles all have the same angular velocity, and constitute a current I .

The angular momentum of the system is

$$\vec{\mathbf{L}} = \sum_i m_i R^2 \omega \hat{\mathbf{n}}, \quad (3.5)$$

where $\hat{\mathbf{n}}$ is the unit vector perpendicular to the loop. The motion of the particles constitute a steady electrical current I . With the linear charge density $\sum_i q_i / 2\pi R$, the current is

$$I = \frac{\sum_i q_i v}{2\pi R} = \frac{\sum_i q_i \omega}{2\pi}. \quad (3.6)$$

Using Eq. (3.4) and Eq. (3.5), the magnetic moment of the system is then

$$\begin{aligned} \vec{\mu} &= \frac{q}{2m} \sum_i m_i R^2 \omega \hat{\mathbf{n}} \\ &= \frac{1}{2} \sum_i q_i R^2 \omega \hat{\mathbf{n}} \\ &= I \pi R^2 \hat{\mathbf{n}} = IA \hat{\mathbf{n}}, \end{aligned} \quad (3.7)$$

where A is the area of the circular loop.

Elementary particles carry intrinsic angular momenta called spin. For example, as already discussed, the electron is a fermion with spin-1/2. It is tempting to apply the above description to calculate the magnetic moment of the electron, treating it as a rotating spherical charge distribution. However, in doing so we would consider the electron as a classical system, which it certainly is not. To correctly calculate the magnetic moment of elementary particles, we need a quantum mechanical description.

3.2 The Quantum Mechanical Description

For a classical system of particles with charge q and mass m , we found $\vec{\mu} = q\vec{\mathbf{L}}/2m$. In general,

$$\vec{\mu} = \gamma \vec{\mathbf{L}}, \quad (3.8)$$

where γ is called the gyromagnetic ratio. Any particle with an intrinsic angular momentum also has an associated magnetic moment, with the gyromagnetic ratio depending on the particle. We shall restrict ourselves to spin-1/2 fermions, whose free propagation is described by the Dirac equation Eq. (2.1). As in Eq. (2.25), to introduce interactions between the fermion and the electromagnetic field, we make the minimal substitution

$$\partial_\mu \rightarrow D_\mu = \partial_\mu + iqA_\mu, \quad (3.9)$$

where q is the charge of the fermion and $A^\mu = (\phi, \vec{\mathbf{A}})$ is the electromagnetic 4-potential. The Dirac equation for a charged fermion in an electromagnetic field becomes

$$\left[\gamma^\mu (i\partial_\mu - qA_\mu) - m\psi \right] = 0. \quad (3.10)$$

Now, applying the operator $[\gamma^\nu (i\partial_\nu - qA_\nu) + m]$ from the left, we obtain

$$\left[(i\partial_\mu - qA_\mu) (i\partial_\nu - qA_\nu) \gamma^\mu \gamma^\nu - m^2 \right] \psi = 0. \quad (3.11)$$

But for a vector T_μ , it holds that

$$T_\mu T_\nu \gamma^\mu \gamma^\nu = \frac{1}{4} \left(\{T_\mu, T_\nu\} \{\gamma^\mu, \gamma^\nu\} + [T_\mu, T_\nu] [\gamma^\mu, \gamma^\nu] \right). \quad (3.12)$$

Here, we need

$$\begin{aligned} \{i\partial_\mu - qA_\mu, i\partial_\nu - qA_\nu\} \{\gamma^\mu, \gamma^\nu\} &= 2g^{\mu\nu} \{i\partial_\mu - qA_\mu, i\partial_\nu - qA_\nu\} \\ &= 4 (i\partial_\mu - qA_\mu)^2, \end{aligned} \quad (3.13)$$

and

$$\begin{aligned} [i\partial_\mu - qA_\mu, i\partial_\nu - qA_\nu] [\gamma^\mu, \gamma^\nu] &= -2i\sigma^{\mu\nu} \left(-\partial_\mu \partial_\nu - iq (\partial_\mu A_\nu) - iq A_\nu \partial_\mu - iq A_\mu \partial_\nu + q^2 A_\mu A_\nu \right. \\ &\quad \left. + \partial_\nu \partial_\mu + iq (\partial_\nu A_\mu) + iq A_\mu \partial_\nu + iq A_\nu \partial_\mu - q^2 A_\nu A_\mu \right) \\ &= -2qF_{\mu\nu} \sigma^{\mu\nu}, \end{aligned} \quad (3.14)$$

where $F_{\mu\nu} = \partial_\mu A_\nu - \partial_\nu A_\mu$ is the electromagnetic field strength tensor, and we used the definition $\sigma^{\mu\nu} = -\frac{i}{2} [\gamma^\mu, \gamma^\nu]$. Eq. (3.11) then becomes

$$\left[(i\partial_\mu - qA_\mu)^2 - \frac{q}{2} F_{\mu\nu} \sigma^{\mu\nu} - m^2 \right] \psi = 0. \quad (3.15)$$

This result can be written compactly as $(\mathcal{D}^2 + m^2)\psi = 0$, where we have found $\mathcal{D}^2 = D_\mu^2 - qF_{\mu\nu} \sigma^{\mu\nu}/2$. The magnetic moment is contained in the term $qF_{\mu\nu} \sigma^{\mu\nu}/2$, as we shall now see.

To locate the magnetic moment interaction, we need to identify the Hamiltonian and take the non-relativistic limit. Since $i\partial_t \psi = H_D \psi$, where H_D is the Dirac Hamiltonian, we isolate the time component of the kinetic term in Eq. (3.15),

$$(i\partial_t - qA_0)^2 \psi = \left[(i\partial_i - qA_i)^2 + \frac{q}{2} F_{\mu\nu} \sigma^{\mu\nu} + m^2 \right] \psi. \quad (3.16)$$

Making the substitutions $i\partial_t \rightarrow H$, $i\partial_i \rightarrow -\vec{\mathbf{p}}$, we obtain

$$(H_D - q\phi)^2 \psi = \left[(\vec{\mathbf{p}} - q\vec{\mathbf{A}})^2 + \frac{q}{2} F_{\mu\nu} \sigma^{\mu\nu} + m^2 \right] \psi. \quad (3.17)$$

We now reintroduce factors of \hbar and c , so that the non-relativistic limit can be taken by letting $1/c \rightarrow 0$. Factoring out the mass term, we have

$$(H_D - q\phi)^2 = m^2 c^4 \left[1 + \frac{1}{c^2} \left(\frac{(\vec{\mathbf{p}} - q\vec{\mathbf{A}})^2}{m^2} + \frac{\hbar q}{2m^2} F_{\mu\nu} \sigma^{\mu\nu} \right) \right]. \quad (3.18)$$

Taking the square root and keeping terms up to order c^0 , we obtain the non-relativistic approximation

$$H_D - q\phi \approx mc^2 + \frac{(\vec{\mathbf{p}} - q\vec{\mathbf{A}})^2}{2m} + \frac{\hbar q}{4m} F_{\mu\nu} \sigma^{\mu\nu}, \quad (3.19)$$

and subtracting the mass energy we obtain

$$H = H_D - mc^2 \approx \frac{(\vec{\mathbf{p}} - q\vec{\mathbf{A}})^2}{2m} + \frac{\hbar q}{4m} F_{\mu\nu} \sigma^{\mu\nu} + q\phi, \quad (3.20)$$

where magnetic moment interaction is described by the second term. Note that this term is proportional to \hbar . Thus, taking the classical limit $\hbar \rightarrow 0$, the intrinsic magnetic moment vanishes, indicating its quantum mechanical nature. In order to compare to the interaction potential in Eq. (3.4), we expand the second term and use the relations $F_{0i} = -E^i/c$ and $F_{ij} = \epsilon_{kij} B^k$,

$$\begin{aligned} F_{\mu\nu} \sigma^{\mu\nu} &= 2F_{0i} \sigma^{0i} + F_{ij} \sigma^{ij} \\ &= -\frac{2}{c} E^i \sigma^{0i} + \epsilon_{kij} B^k \sigma^{ij} \\ &= -\frac{2}{c} E^i \sigma^{0i} - 4B^k S^k \\ &\approx -4B^k S^k, \end{aligned} \quad (3.21)$$

where $S^k = \epsilon^{kij} \sigma^{ij}/4$ are the spin operators acting on Dirac spinors, satisfying the rotation algebra $[S^i, S^j] = i\hbar \epsilon^{ijk} S^k$. Substituting into Eq. (3.20) and returning to natural units, the non-relativistic Hamiltonian is

$$H \approx \frac{(\vec{\mathbf{p}} - q\vec{\mathbf{A}})^2}{2m} - \frac{q}{m} \vec{\mathbf{B}} \cdot \vec{\mathbf{S}} + q\phi. \quad (3.22)$$

Comparing to Eq. (3.4), we find the magnetic moment $\vec{\mu} = q\vec{\mathbf{S}}/m$, or the gyromagnetic ratio

$$\gamma = \frac{q}{m} \quad (3.23)$$

for spin-1/2 particles with charge q . The factor missing in the classical prediction $\gamma = q/2m$ is called the g-factor, and so the Dirac equation predicts $g = 2$. The electron, having charge

$q = -e$, has a magnetic moment

$$\begin{aligned}\vec{\mu}_e &= -g_e \frac{e}{2m_e} \vec{\mathbf{S}} \\ &= -g_e \mu_B \vec{\mathbf{S}},\end{aligned}\tag{3.24}$$

where $\mu_B = e/2m_e$ is the Bohr magneton.

The $g = 2$ result is a remarkable prediction of the Dirac equation, but it does not agree with the experimental value of $g_e \approx 2.0023$ [10]. The deviation from $g = 2$, called the anomalous magnetic moment, arises from quantum loop effects and requires quantum field theory to calculate.

3.3 Anomalous Magnetic Moment of a Charged Lepton

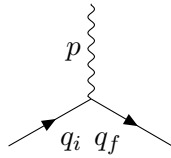
We have seen that a charged spinor ψ satisfies

$$(\not{D}^2 + m^2)\psi = 0.\tag{3.25}$$

Specializing to the case of a charged lepton with $q = -e$ gives $\not{D}^2 = D_\mu^2 + \frac{e}{2}F_{\mu\nu}\sigma^{\mu\nu}$. The magnetic moment stems from the term $\frac{e}{2}F_{\mu\nu}\sigma^{\mu\nu}$, which connects the spin of the charged lepton to the magnetic field. The $g = 2$ result is contained in the coefficient of this term, $g\frac{e}{4}F_{\mu\nu}\sigma^{\mu\nu}$. When calculating the magnetic moment in quantum field theory, we therefore look for terms proportional to $F_{\mu\nu}\sigma^{\mu\nu}$, which make corrections to this coefficient. The field strength tensor contains derivatives of the photon field, so in momentum space the term will look like $\bar{u}(q_f)p_\nu\sigma^{\mu\nu}u(q_i)$.

We will now calculate the one-loop contribution to the g-factor of a charged lepton in QED, illustrating how magnetic moments are obtained in quantum field theory. This calculation was first done by Schwinger in 1948 [16], and its agreement with experiment was an important success of quantum field theory.

The relevant process at tree-level is



$$= \mathcal{M}_0^\mu = ie \bar{u}(q_f) \gamma^\mu u(q_i).\tag{3.26}$$

The photon corresponds to an external electromagnetic field and is off-shell, its momentum constrained to be $p^\mu = q_f^\mu - q_i^\mu$. We use the Gordon identity,

$$\bar{u}(q_f)(q_i^\mu + q_f^\mu)u(q_i) = (2m)\bar{u}(q_f)\gamma^\mu u(q_i) + i\bar{u}(q_f)\sigma^{\mu\nu}(q_i^\nu - q_f^\nu)u(q_i)\tag{3.27}$$

to rewrite the amplitude,

$$\mathcal{M}_0^\mu = ie \frac{\bar{u}(q_f)(q_i^\mu + q_f^\mu)u(q_i)}{2m} - \frac{e}{2m} \bar{u}(q_f)p_\nu\sigma^{\mu\nu}u(q_i).\tag{3.28}$$

The second term has a coefficient $C = \frac{e}{2m}$, and the $g = 2$ result is identified with $\frac{4m}{e}C$. To calculate corrections to g , we thus calculate the coefficient to this term in a given order of perturbation theory.

In general, we look at graphs like



$$(3.29)$$

Later we will carefully decompose this vertex into Lorentz invariant form factors, in the case of incoming and outgoing neutrinos. For now, using all possible Lorentz vectors which may appear in QED, we parameterize the amplitude as

$$\mathcal{M}^\mu = \bar{u}(q_f)(f_1\gamma^\mu + f_2p^\mu + f_3q_i^\mu + f_4q_f^\mu)u(q_i) \quad (3.30)$$

where the form factors f_i are matrices in spinor space which depend on scalars such as $p \cdot q$, p^2 or \not{p} . Using momentum conservation we can substitute out the p^μ dependence and let $f_2 = 0$. Further we can substitute all q_i and q_f dependence in favor of m by using the momentum space Dirac equation. Thus, f_i can only depend on contractions of q_i and q_f , i.e. $q_i q_f$ and m . Conventionally, the dependence is taken to be on $p^2 = (q_f - q_i)^2 = 2m^2 - 2q_i q_f$ and m^2 .

Now, using the Ward identity,

$$\begin{aligned} 0 &= p_\mu \mathcal{M}^\mu \\ &= p_\mu \bar{u}(q_f)(f_1\gamma^\mu + f_3q_i^\mu + f_4q_f^\mu)u(q_i) \\ &= f_1\bar{u}(q_f)\not{p}u(q_i) + (p \cdot q_i) f_3\bar{u}(q_f)u(q_i) + (p \cdot q_f) f_4\bar{u}(q_f)u(q_i), \end{aligned} \quad (3.31)$$

and using the Dirac equation, $\bar{u}(q_f)\not{p}u(q_i) = \bar{u}(q_f)(\not{q}_f - \not{q}_i)u(q_i) = \bar{u}(q_f)(m - m)u(q_i) = 0$, so

$$\begin{aligned} (p \cdot q_i) f_3\bar{u}(q_f)u(q_i) &= -(p \cdot q_f) f_4\bar{u}(q_f)u(q_i) \\ (q_f \cdot q_i - q_i \cdot q_i) f_3\bar{u}(q_f)u(q_i) &= -(q_f \cdot q_f - q_i \cdot q_f) f_4\bar{u}(q_f)u(q_i) \\ (q_f \cdot q_i - m^2) f_3\bar{u}(q_f)u(q_i) &= (q_i \cdot q_f - m^2) f_4\bar{u}(q_f)u(q_i). \end{aligned} \quad (3.32)$$

Thus, $f_3 = f_4$. Now we have reduced the number of form factors down to two, and we are left with

$$\mathcal{M}^\mu = \bar{u}(q_f)(f_1\gamma^\mu + f_3(q_i^\mu + q_f^\mu))u(q_i) \quad (3.33)$$

To extract the magnetic moment, we use the Gordon identity to rewrite the second term,

$$f_3\bar{u}(q_f)(q_i^\mu + q_f^\mu)u(q_i) = f_3(2m)\bar{u}(q_f)\gamma^\mu u(q_i) + f_3i\bar{u}(q_f)\sigma^{\mu\nu}(q_i^\nu - q_f^\nu)u(q_i), \quad (3.34)$$

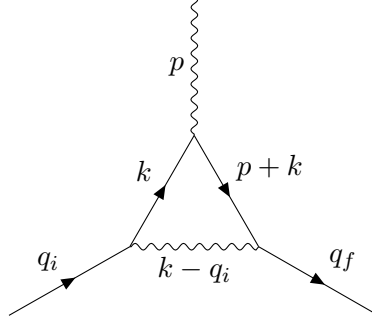
which when substituted into the amplitude gives

$$\begin{aligned} \mathcal{M}^\mu &= \bar{u}(q_f) [f_1 + 2mf_3] \gamma^\mu u(q_i) + \bar{u}(q_f) [if_3\sigma^{\mu\nu}(q_i^\nu - q_f^\nu)] u(q_i) \\ &= ie\bar{u}(q_f) \left[F_1 \left(\frac{p^2}{m^2} \right) \gamma^\mu + \frac{i\sigma^{\mu\nu} p_\nu F_2 \left(\frac{p^2}{m^2} \right)}{2m} \right] u(q_i), \end{aligned} \quad (3.35)$$

where we introduced the new form factors F_1 and F_2 . F_1 corresponds to the renormalization of the electric charge of the lepton, while F_2 contributes to the magnetic moment. Observing that the tree-level result is recovered for $F_1 = 1$ and $F_2 = 0$, we identify $g \rightarrow 2(1 + F_2(p^2/m^2))$. Since the magnetic moment is measured at non-relativistic energies, the quantity we wish to

calculate is $F_2(0)$ for the desired order of perturbation theory.

Only one-particle irreducible vertex graphs contribute to the magnetic moment correction. At 1-loop order, the only such graph is



which has the amplitude

$$\mathcal{M}_2^\mu = e^3 \bar{u}(q_f) \int \frac{d^4 k}{(2\pi)^4} \frac{\gamma^\nu (\not{p} + \not{k} + m) \gamma^\mu (\not{k} + m) \gamma_\nu}{[(k - q_i)^2 + i\varepsilon][(p + k)^2 - m^2 + i\varepsilon][k^2 - m^2 + i\varepsilon]} u(q_i) \quad (3.36)$$

We use Feynman parameters to simplify the denominator,

$$\frac{1}{ABC} = 2 \int_0^1 dx dy dz \delta(x + y + z - 1) \frac{1}{[xA + yB + zC]^3} \quad (3.37)$$

Here,

$$A = k^2 - m^2 + i\varepsilon, \quad B = (p + k)^2 - m^2 + i\varepsilon, \quad C = (k - q_i)^2 + i\varepsilon, \quad (3.38)$$

such that

$$\begin{aligned} xA + yB + zC &= xk^2 - xm^2 + yp^2 + yk^2 + 2ypk - ym^2 + zk^2 + zq_i^2 - 2zkq_i + i\varepsilon \\ &= k^2 + 2k(y p - z q_i) + yp^2 + zq_i^2 - (x + y)m^2 + i\varepsilon. \end{aligned} \quad (3.39)$$

But

$$\begin{aligned} (k^\mu + yp^\mu - zq_i^\mu)^2 &= k^2 + y^2 p^2 + z^2 q_i^2 + 2ykp - 2zkq_i - 2yzpq_i \\ &= k^2 + 2k(y p - z q_i) + y^2 p^2 + z^2 m^2 - 2yzpq_i, \end{aligned} \quad (3.40)$$

so we obtain Eq. (3.39) if we subtract from this

$$\begin{aligned} \Delta &= y^2 p^2 + z^2 m^2 - 2yzpq_i - yp^2 - zq_i^2 + (x + y)m^2 \\ &= y(y - 1)p^2 + z^2 m^2 - 2yzpq_i - zm^2 + (1 - z)^2 m^2 \\ &= y(-x - z)p^2 - 2yzpq_i + (1 - z)^2 m^2 \\ &= -xyp^2 + (1 - z)^2 m^2 - yz[p^2 + 2pq_i], \end{aligned} \quad (3.41)$$

where the last term vanishes since $p^2 + 2pq_i = (p + q_i)^2 - q_i^2 = q_f^2 - q_i^2 = m^2 - m^2 = 0$. Thus, we have

$$xA + yB + zC = (k^\mu + yp^\mu - zq_i^\mu)^2 - \Delta + i\varepsilon, \quad (3.42)$$

which we can exploit by doing the substitution $k^\mu \rightarrow k^\mu - yp^\mu + zq_i^\mu$, making the denominator $(k^2 - \Delta)^3$ and leaving $d^4 k$ unchanged.

We now turn to the numerator of the amplitude, which is

$$\begin{aligned}
N^\mu &= \bar{u}(q_f)\gamma^\nu(\not{p} + \not{k} + m)\gamma^\mu(\not{k} + m)\gamma_\nu u(q_i) \\
&= \bar{u}(q_f) \left[\gamma^\nu \not{p} \gamma^\mu \not{k} \gamma_\nu + \gamma^\nu \not{k} \gamma^\mu \not{k} \gamma_\nu + \gamma^\nu \not{p} \gamma^\mu \gamma_\nu m + \gamma^\nu \not{k} \gamma^\mu \gamma_\nu m + \gamma^\nu \gamma^\mu \not{k} \gamma_\nu m + \gamma^\nu \gamma^\mu \gamma_\nu m^2 \right] u(q_i) \\
&= \bar{u}(q_f) \left[-2\not{k} \gamma^\mu \not{p} - 2\not{k} \gamma^\mu \not{k} + 4p_\sigma g^{\sigma\mu} m + 4k_\sigma g^{\sigma\mu} m + 4k_\sigma g^{\mu\sigma} m - 2\gamma^\mu m^2 \right] u(q_i) \\
&= -2\bar{u}(q_f) \left[\not{k} \gamma^\mu \not{p} + \not{k} \gamma^\mu \not{k} + m^2 \gamma^\mu - 2m(2k^\mu + p^\mu) \right] u(q_i). \tag{3.43}
\end{aligned}$$

Making the substitution $k^\mu \rightarrow k^\mu - yp^\mu + zq_i^\mu$, we obtain

$$\begin{aligned}
-\frac{1}{2}N^\mu &= \bar{u}(q_f) \left[m^2 \gamma^\mu + (\not{k} - y\not{p} + z\not{q}_i)\gamma^\mu \not{p} + (\not{k} - y\not{p} + z\not{q}_i)\gamma^\mu (\not{k} - y\not{p} + z\not{q}_i) \right. \\
&\quad \left. - 2m(2k^\mu - 2yp^\mu + 2zq_i^\mu + p^\mu) \right] u(q_i). \tag{3.44}
\end{aligned}$$

We wish to extract from this the term proportional to $p_\nu \bar{u}(q_f) \sigma^{\mu\nu} u(q_i)$. To accomplish this, the numerator will be rewritten in the form $Ap^\mu + B(q_i^\mu + q_f^\mu) + C\gamma^\mu$. From there the Gordon identity can be used to obtain the $p_\nu \bar{u}(q_f) \sigma^{\mu\nu} u(q_i)$ term. After some tedious algebra (see Appendix D), we find the relevant part of the numerator

$$N^\mu \supset -2imz(1-z)p_\nu \bar{u}(q_f) \sigma^{\mu\nu} u(q_i). \tag{3.45}$$

Substituting Eq. (3.45) and the denominator $(k^2 - \Delta + i\varepsilon)^3$ into Eq. (3.36), the term in the amplitude contributing to the magnetic moment is

$$\begin{aligned}
\mathcal{M}_2^\mu &\supset e^3 \int \frac{d^4k}{(2\pi)^4} \times 2 \int_0^1 dx dy dz \delta(x+y+z-1) \frac{-2imz(1-z)p_\nu \bar{u}(q_f) \sigma^{\mu\nu} u(q_i)}{(k^2 - \Delta + i\varepsilon)^3} \\
&= -p_\nu \bar{u}(q_f) \sigma^{\mu\nu} u(q_i) \left[4ime^3 \int_0^1 dx dy dz \delta(x+y+z-1) \int \frac{d^4k}{(2\pi)^4} \frac{z(1-z)}{(k^2 - \Delta + i\varepsilon)^3} \right] \tag{3.46}
\end{aligned}$$

Our goal is to obtain the form factor F_2 . Comparing to Eq. (3.35), we have at 1-loop order

$$F_2(p^2) = 8im^2 e^2 \int_0^1 dx dy dz \delta(x+y+z-1) z(1-z) \int \frac{d^4k}{(2\pi)^4} \frac{1}{(k^2 - \Delta + i\varepsilon)^3}. \tag{3.47}$$

The k integral is evaluated using Wick rotation (see e.g. Appendix B.2 of [7]),

$$\int \frac{d^4k}{(2\pi)^4} \frac{1}{(k^2 - \Delta + i\varepsilon)^3} = \frac{-i}{32\pi^2 \Delta} = \frac{-i}{32\pi^2 (-xyp^2 + (1-z)^2 m^2)}. \tag{3.48}$$

Note that the form factor now can be written as

$$F_2(p^2) = 8ie^2 \int_0^1 dx dy dz \delta(x+y+z-1) z(1-z) \left[\frac{-im^2/p^2}{32\pi^2 (-xy + (1-z)^2 m^2/p^2)} \right], \tag{3.49}$$

and thus in the high-energy limit $p^2/m^2 \rightarrow \infty$, the form factor is zero. As we shall see, the magnetic moment operator is chirality flipping. This behavior is therefore expected, as the left- and right-chiral fields decouple in the massless limit of QED.

Meanwhile, in the low-energy limit we have

$$\begin{aligned}
F_2(0) &= \frac{im^2e^2}{4} \int_0^1 dx dy dz \delta(x+y+z-1) z(1-z) \frac{-i}{\pi^2(1-z)^2m^2} \\
&= \frac{e^2}{4\pi^2} \int_0^1 dz \int_0^1 dy \frac{z}{1-z} \int_0^1 dx \delta(x+y+z-1).
\end{aligned} \tag{3.50}$$

The integral over x is only non-zero if $x+y+z-1=0$ inside the integration interval, which means that $y+z=1-x$ must be in the interval $[0,1]$. This reduces the upper limit in y to $1-z$, and we have

$$\begin{aligned}
F_2(0) &= \frac{e^2}{4\pi^2} \int_0^1 dz \int_0^{1-z} dy \frac{z}{1-z} \\
&= \frac{e^2}{4\pi^2} \int_0^1 dz z \\
&= \frac{e^2}{8\pi^2} \\
&= \frac{\alpha}{2\pi},
\end{aligned} \tag{3.51}$$

where $\alpha = e^2/2\pi$ is the fine structure constant. The g-factor of a charged lepton to one-loop order in QED is thus

$$g = 2(1 + F_2(0)) = 2 + \frac{\alpha}{\pi}, \tag{3.52}$$

or in terms of the anomalous magnetic moment, $a \equiv \frac{g-2}{2} = \frac{\alpha}{2\pi} \approx 0.00116$. To obtain a more accurate prediction, one must calculate higher-order loop diagrams, including electroweak and hadronic effects. The QED calculation for the electron has been done to 5th order in α , obtaining a_e in terms of the fine structure constant [17].

Because of the possibility of extremely precise measurement, the magnetic moment of charged leptons can be used as precision tests of the Standard Model. To compare the measured g-factor to the theoretical prediction, one needs an independent measurement of α with equivalent or better precision to the measurement of g . Using measurements of the velocity of rubidium atoms that absorb a photon [18], an experimental value of α has been obtained that disagrees with measurements of the electron anomalous magnetic moment at a significance of 1.6σ [18, 19]. This is a reduction from the 2.5σ deviation when comparing to previous measurements of α using cesium atoms [20].

The muon magnetic moment has a larger discrepancy between theory and experiment. As of 2022, there is a tension of 4.2σ between the measured value and the theoretical prediction [21]. If the discrepancy persists in future experiments, this could be a strong hint toward physics beyond the Standard Model.

3.4 Effective Lagrangian for the Magnetic Moment

We have seen how the magnetic moment is contained in the amplitude of processes like



(3.53)

in the limit $p^2 \rightarrow 0$. To find corrections to the magnetic moment of a charged lepton, we looked for terms proportional to $p_\nu \sigma^{\mu\nu}$ in the amplitude. Such an amplitude is obtained directly from the effective Lagrangian

$$\mathcal{L}_{\text{eff}} \propto F_{\mu\nu} \bar{\psi} \sigma^{\mu\nu} \psi. \quad (3.54)$$

Consider the process $f\gamma \rightarrow f$, described by this Lagrangian. The fermion field operators do their usual job of annihilating the initial state fermion and creating the final state fermion. Since the electromagnetic tensor contains a derivative, we obtain a factor of p from the photon field. $F^{\mu\nu}$ and $\sigma^{\mu\nu}$ are both antisymmetric, so we obtain an amplitude proportional to $\bar{u}(q_i) \sigma^{\mu\nu} p_\mu \epsilon_\nu u(q_f)$, which is what we're after.

3.4.1 Chirality Flip

We can write the effective Lagrangian in terms of the left- and right-chiral parts of the fields,

$$\begin{aligned} \mathcal{L}_{\text{eff}} &\propto F_{\mu\nu} (\bar{\psi}_L + \bar{\psi}_R) \sigma^{\mu\nu} (\psi_L + \psi_R) \\ &= F_{\mu\nu} (\bar{\psi}_L P_R + \bar{\psi}_R P_L) \sigma^{\mu\nu} (P_L \psi_L + P_R \psi_R). \end{aligned} \quad (3.55)$$

Since γ_5 anticommutes with γ^μ , the chirality projectors commute with $\sigma^{\mu\nu} = \frac{i}{2} [\gamma^\mu, \gamma^\nu]$. Then since $P_R P_L = P_L P_R = 0$, we are left with the terms

$$\mathcal{L}_{\text{eff}} \propto F_{\mu\nu} \bar{\psi}_L \sigma^{\mu\nu} \psi_R + F_{\mu\nu} \bar{\psi}_R \sigma^{\mu\nu} \psi_L, \quad (3.56)$$

which shows that the interaction induces a chirality flip. Thus, to have neutrino magnetic moments, one needs to introduce fields to play the part of right-chiral neutrinos. There are several options:

- Right-handed gauge singlet fields $\nu_{\alpha R}$, appearing in a Dirac mass term $\bar{\nu}_{\alpha L} M_{\alpha\beta}^D \nu_{\beta R} + H.c.$. The two chiral fields are parts of a single Dirac spinor $\nu_\alpha = \nu_{\alpha L} + \nu_{\alpha R}$.
- Heavier singlet neutrinos N_{sR} , which in addition to the Dirac mass term have a Majorana mass term $\bar{N}_{sR}^c M_{ss'}^R N_{s'R} + H.c.$. Since this field has a different mass than the active neutrino, it does not combine with ν_L into a Dirac spinor. Naturally small active neutrino masses can be generated with the help of the heavy states N_s through the see-saw mechanism.
- The charge conjugated neutrino ν_L^c , which is part of the Majorana field $\nu = \nu_L + \nu_L^c$. The magnetic moments of Majorana neutrinos are discussed in Section 3.4.3.

The chirality flip has an important implication for the magnetic moment of neutrinos with only Standard Model interactions. In that case, the contributing 1-loop diagrams are [22]

$$(3.57)$$

These diagrams involve electroweak vertices, which only occur for left-chiral neutrinos. Thus, the chirality flip occurs on the incoming or outgoing neutrino with a mass insertion, from $\mathcal{L} \supset m\bar{\psi}_L\psi_R + H.c.$ Therefore, one has $\mu_\nu \propto m_\nu$. Since (3.57) contain two weak vertices and one electromagnetic vertex, we obtain

$$\mu_\nu \sim eG_F m_\nu = 2m_e\mu_B G_F m_\nu \sim 10^{-18} \mu_B \left(\frac{m_\nu}{10^{-1} \text{ eV}} \right), \quad (3.58)$$

where $\mu_B = e/2m_e$ is the Bohr magneton. Thus, the neutrino magnetic moment in the Standard Model is heavily suppressed by the small mass of the neutrinos. The explicit calculation of the neutrino magnetic moment in the standard electroweak theory will be shown in Chapter 5.

3.4.2 Effective Lagrangian in the Non-Relativistic Limit

In general, we are interested in processes like Eq. (3.53) with an incoming fermion ψ_i and an outgoing fermion ψ_f , not necessarily in the same state, i.e. it is possible that $f \neq i$. The effective Lagrangian is therefore generalized to

$$\mathcal{L}_{\text{eff}} = -\frac{1}{2} \sum_{f,i=1}^N \mu_{fi} F_{\mu\nu} \bar{\psi}_f \sigma^{\mu\nu} \psi_i, \quad (3.59)$$

where the coupling μ_{fi} is an element of a matrix in the space of N fermion states, here taken to be mass eigenstates. We have seen how this Lagrangian gives an amplitude proportional to $\sigma^{\mu\nu} p_\mu \epsilon_\nu$, thus contributing to the magnetic moment. Let us now justify the name of the coupling μ_{fi} by making the connection to the non-relativistic interaction Hamiltonian $H = -\vec{\mu} \cdot \vec{B}$. We work in the Pauli-Dirac representation, which is convenient for taking the non-relativistic limit, and hold f, i fixed. In the rest frame we have the plane wave spinor solutions

$$\begin{aligned} \psi_i &\approx \begin{pmatrix} \phi_s \\ 0 \end{pmatrix} e^{-im_i t} \\ \bar{\psi}_f &= \psi_f^\dagger \gamma^0 \approx \begin{pmatrix} \phi_r^T & 0 \end{pmatrix} e^{im_f t}, \end{aligned} \quad (3.60)$$

where $r = 1, 2$, $\phi_1 = (1, 0)^T$ and $\phi_2 = (0, 1)^T$. Splitting Eq. (3.59) into terms with $\mu = j$ and $\mu = 0$ and inserting the spinor solutions, we have

$$\mathcal{L}_{\text{eff}} \approx -e^{i(m_f - m_i)} \left[\frac{\mu_{fi}}{2} F_{jk} \begin{pmatrix} \phi_r^T & 0 \end{pmatrix} \sigma^{jk} \begin{pmatrix} \phi_s \\ 0 \end{pmatrix} + \mu_{fi} F_{0k} \begin{pmatrix} \phi_r^T & 0 \end{pmatrix} \sigma^{0k} \begin{pmatrix} \phi_s \\ 0 \end{pmatrix} \right]. \quad (3.61)$$

In the Dirac-Pauli representation, the gamma matrices are

$$\gamma^0 = \begin{pmatrix} \mathbb{1} & 0 \\ 0 & -\mathbb{1} \end{pmatrix}, \quad \gamma^k = \begin{pmatrix} 0 & \sigma^k \\ -\sigma^k & 0 \end{pmatrix}, \quad (3.62)$$

so

$$\sigma^{jk} = -\frac{i}{2}[\sigma^j, \sigma^k] \mathbb{1}_{4 \times 4} = \epsilon^{jkl} \sigma^l \mathbb{1}_{4 \times 4}, \quad \sigma^{0k} = i \begin{pmatrix} 0 & \sigma^k \\ \sigma^k & 0 \end{pmatrix}. \quad (3.63)$$

The second term in Eq. (3.61) vanishes, and we're left with

$$\begin{aligned} \mathcal{L}_{\text{eff}} &\approx -\frac{\mu_{fi}}{2} e^{i(m_f - m_i)t} F_{jk} \epsilon^{jkl} \begin{pmatrix} \phi_r^T & 0 \end{pmatrix} \sigma^l \mathbb{1}_{4 \times 4} \begin{pmatrix} \phi_s \\ 0 \end{pmatrix} \\ &= \mu_{fi} e^{i(m_f - m_i)t} B^l \phi_r^T \sigma^l \phi_s, \end{aligned} \quad (3.64)$$

where we used the relation $B^l = -\frac{1}{2} \epsilon^{jkl} F_{jk}$ to rewrite in terms of the magnetic field. At this point, we are describing the generalization of the magnetic moment, where the concept is extended to transition processes where $i \neq f$. To connect with the non-relativistic theory, we now take $i = f$, such that we are describing the magnetic moment interaction of a single fermion ψ . The spin operator for a non-relativistic fermion is [23, equation (3.111)] $\vec{\mathbf{S}} = \int d^3x \psi^\dagger \left(\frac{1}{2} \vec{\Sigma} \right) \psi$, where $\Sigma^k = \sigma^k \mathbb{1}$. Inserting our spinor solutions, we have

$$\begin{aligned} S^k &= \frac{1}{2} \int d^3x \begin{pmatrix} \phi_r^T & 0 \end{pmatrix} \begin{pmatrix} \sigma^k & 0 \\ 0 & \sigma^k \end{pmatrix} \begin{pmatrix} \phi_s \\ 0 \end{pmatrix} \\ &= \frac{1}{2} \int d^3x \phi_r^T \sigma^k \phi_s. \end{aligned} \quad (3.65)$$

Thus,

$$-\int d^3x \mathcal{L}_{\text{eff}} = H = -2\mu \vec{\mathbf{S}} \cdot \vec{\mathbf{B}} \implies \vec{\mu} = 2\mu \vec{\mathbf{S}} = \mu \vec{\sigma}. \quad (3.66)$$

The quantity μ thus determines the amplitude of the magnetic moment vector. We call μ_{fi} “the magnetic moment”, defined through the effective Lagrangian Eq. (3.59), while $\vec{\mu}$ is referred to as “the magnetic moment vector”. Note that in Eq. (3.66), we assumed that the spinors ψ describe neutrinos. In the case of charged leptons, $-\int d^3x \mathcal{L}_{\text{eff}}$ is added to the tree-level contribution $H_0 = 2e \vec{\mathbf{S}} \cdot \vec{\mathbf{B}} / 2m_\ell$. Then, the coupling should be $a_\ell e / 4m_\ell$, a_ℓ being the anomalous magnetic moment, in order to produce $\vec{\mu}_\ell = -ge / 2m_\ell \vec{\mathbf{S}}$.

3.4.3 Magnetic Moment of Majorana Neutrinos

Majorana fermions are defined by the property $\psi = \psi^c$, where

$$\psi^c = C \bar{\psi}^T \quad (3.67)$$

denotes charge conjugation and C is the charge conjugation matrix. For the Dirac adjoint field we have

$$\overline{\psi^c} = -\psi^T C^{-1}. \quad (3.68)$$

Thus in the case of Majorana fermions we can rewrite the effective Lagrangian as

$$\mathcal{L}_{\text{eff}}^{\text{Majorana}} = -\frac{\mu_{fi}}{4} F_{\mu\nu} \left(\overline{\psi}_f \sigma^{\mu\nu} \psi_i + \overline{\psi}_f^c \sigma^{\mu\nu} \psi_i^c \right) \quad (3.69)$$

Using equations (3.67) and (3.68), we can rewrite the second term in the brackets:

$$\begin{aligned} \overline{\psi}_f^c \sigma^{\mu\nu} \psi_i^c &= -\psi_f^T C^{-1} \sigma^{\mu\nu} C \overline{\psi}_i^T \\ &= -\frac{i}{2} \psi_f^T C^{-1} (\gamma^\mu \gamma^\nu - \gamma^\nu \gamma^\mu) C \overline{\psi}_i^T. \end{aligned} \quad (3.70)$$

Now, using the property $C \gamma^{\mu T} C^{-1} = -\gamma^\mu$,

$$\begin{aligned} \overline{\psi}_f^c \sigma^{\mu\nu} \psi_i^c &= -\frac{i}{2} \psi_f^T C^{-1} \left(C \gamma^{\mu T} C^{-1} C \gamma^{\nu T} C^{-1} - C \gamma^{\nu T} C^{-1} C \gamma^{\mu T} C^{-1} \right) C \overline{\psi}_i^T \\ &= -\frac{i}{2} \psi_f^T \left(\gamma^{\mu T} \gamma^{\nu T} - \gamma^{\nu T} \gamma^{\mu T} \right) \overline{\psi}_i^T \\ &= -\frac{i}{2} \psi_f^T (\gamma^\nu \gamma^\mu - \gamma^\mu \gamma^\nu)^T \overline{\psi}_i^T \\ &= -\psi_f^T \sigma^{\nu\mu T} \overline{\psi}_i^T \\ &= \psi_f^T \sigma^{\mu\nu T} \overline{\psi}_i^T \\ &= -\left(\overline{\psi}_i \sigma^{\mu\nu} \psi_f \right)^T, \end{aligned} \quad (3.71)$$

where we used the antisymmetry of $\sigma^{\mu\nu}$, and we gained a minus when exchanging spinors. The object inside the brackets is just a number, so we can take the transpose without changing it. Thus, we arrive at

$$\overline{\psi}_f^c \sigma^{\mu\nu} \psi_i^c = -\overline{\psi}_i \sigma^{\mu\nu} \psi_f. \quad (3.72)$$

Inserting into Eq. (3.69), we have

$$\mathcal{L}_{\text{eff}}^{\text{Majorana}} = -\frac{\mu_{fi}}{4} F_{\mu\nu} \left(\overline{\psi}_f \sigma^{\mu\nu} \psi_i - \overline{\psi}_i \sigma^{\mu\nu} \psi_f \right). \quad (3.73)$$

If $i = j$ the effective Lagrangian vanishes. Thus, Majorana fermions only have transition magnetic moments. Since the quantity in the brackets is antisymmetric on the exchange $i \leftrightarrow f$ while the Lagrangian is symmetric, we have

$$\mu_{if} = -\mu_{fi}, \quad (3.74)$$

i.e. the magnetic moment matrix for Majorana fermions is antisymmetric. Majorana fermions have half the number of degrees of freedom as Dirac fermions, so it should be expected that the magnetic moment matrix for Majorana neutrinos is more restricted.

Since Majorana spinors can be written as $\psi = \psi_L + \psi_L^c$, with $P_R \psi = \psi_L^c$, the charge conjugate spinor ψ_L^c plays the part of the right-chiral field in the magnetic moment interaction. Thus, for Majorana particles one finds transition magnetic moments for the processes $\psi_{iL} \gamma \rightarrow \psi_{fL}^c$ and $\psi_{iL}^c \gamma \rightarrow \psi_{fL}$, where $f \neq i$.

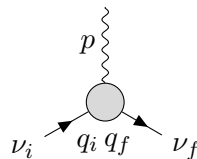
Chapter 4

Electromagnetic Form Factors

We have now seen how the magnetic moment μ_{fi} of neutrinos can be defined as the coupling in the effective Lagrangian in Eq. (3.59). To predict μ_{fi} in a given theory, we need a way of extracting it from the relevant amplitudes. Such a method is developed in this chapter. The amplitude resulting from an effective neutrino-photon vertex depends on various Lorentz covariant combinations of tensors. We wish to separate the dependence on these tensors into individual terms, the coefficients of which are the electromagnetic form factors. From the structure of the effective interaction described in the previous chapter, one of these form factors will be identified with the neutrino magnetic moment. The ensuing derivation closely follows those in [24] and [13].

4.1 Dirac Neutrinos

The neutrino magnetic moment is described by the interaction with a single photon in the low energy limit. In the case of the electron, we were able to write down the QED vertex function in terms of two form factors. Using the Gordon identity, the vertex function could be rewritten such that one term was proportional to $\sigma^{\mu\nu}$, allowing us to read off the magnetic moment. In the case of neutrinos, we are interested in the amplitude



$$= \bar{u}_f(q_f)\Lambda_{fi}^\mu(q_i, q_f)u_i(q_i), \quad (4.1)$$

where the external photon polarization vector was not included. This process only has contributions from loop diagrams. Eq. (4.1) arises from an effective interaction Hamiltonian [13]

$$\mathcal{H} = \sum_{f,i=1}^N \bar{\nu}_f \Lambda_{fi}^\mu \nu_i A_\mu, \quad (4.2)$$

where ν_i and ν_f are on-shell neutrino mass eigenstates, i.e. $p_{i,f}^2 = m_{i,f}^2$, and momentum is conserved, $p = q_f - q_i$. The sum runs over all neutrino mass states. The vertex function Λ_{fi}^μ is a 4×4 matrix in spinor space. Unlike in the QED case, the loop contributions can come from parity-violating weak interactions, so Λ_{fi}^μ is a sum of polar and axial vector contributions.

Thus, we can write $\Lambda_{f_i}^\mu$ as a linear combination of the 16 basis matrices $\{\mathbb{1}, \gamma^\mu, \sigma^{\mu\nu}, \gamma_5, \gamma^\mu \gamma_5\}$. The Lorentz index in the vertex function can be carried by the available tensors, which are the momenta q_1^μ, q_2^μ , the metric $g^{\mu\nu}$ and the Levi-Civita symbol $\epsilon^{\mu\nu\lambda\rho}$, where dependence on p^μ was eliminated using momentum conservation. For convenience, we choose the momentum dependence to be on p and $r \equiv q_i + q_f$. Then $\Lambda_{f_i}^\mu$ can be expressed in terms of the combinations of tensors and basis matrices which carry one Lorentz index.

We can immediately eliminate contractions of the momenta with γ^μ , such as \not{p}, \not{r} and $\sigma_{\lambda\rho} p^\lambda r^\rho$, by using the momentum-space Dirac equation,

$$\not{q}_i u(q_i) = m_i u(q_i), \quad \bar{u}(q_f) \not{q}_f = m_f \bar{u}(q_f). \quad (4.3)$$

The remaining terms where the Lorentz index is carried by p^μ or r^μ are

$$\{p^\mu \mathbb{1}, r^\mu \mathbb{1}, p^\mu \gamma_5, r^\mu \gamma_5\}. \quad (4.4)$$

There are also terms where the basis matrix carries the Lorentz index. These are

$$\{\gamma^\mu, \gamma^\mu \gamma_5, \sigma^{\mu\nu} p_\nu, \sigma^{\mu\nu} r_\nu\}. \quad (4.5)$$

Finally, we have the terms where the Lorentz index is carried by the Levi-Civita symbol,

$$\{\epsilon^{\mu\nu\lambda\rho} \sigma_{\lambda\rho} p_\nu, \epsilon^{\mu\nu\lambda\rho} \sigma_{\lambda\rho} r_\nu, \epsilon^{\mu\nu\lambda\rho} p_\lambda r_\rho \gamma_\nu, \epsilon^{\mu\nu\lambda\rho} p_\lambda r_\rho \gamma_5 \gamma_\nu, \epsilon^{\mu\nu\lambda\rho} p_\lambda r_\rho \sigma_{\nu\kappa} p^\kappa, \epsilon^{\mu\nu\lambda\rho} p_\lambda r_\rho \sigma_{\nu\kappa} r^\kappa\}. \quad (4.6)$$

These 14 terms are not linearly independent. Our next task is to reduce the number of terms down to the set of 6 matrices

$$S = \{p^\mu \mathbb{1}, p^\mu \gamma_5, \gamma^\mu, \gamma^\mu \gamma_5, \sigma^{\mu\nu} p_\nu, \epsilon^{\mu\nu\lambda\rho} \sigma_{\lambda\rho} p_\nu\}. \quad (4.7)$$

Firstly, we can rewrite the matrix $\sigma^{\mu\nu}$ as

$$\sigma^{\mu\nu} = i\gamma^\mu \gamma^\nu - ig^{\mu\nu}. \quad (4.8)$$

Thus, we have

$$\begin{aligned} \bar{u}(q_f) i\sigma^{\lambda\rho} (q_f - q_i)_\rho u(q_i) &= \bar{u}(q_f) (-\gamma^\lambda \gamma^\rho + g^{\lambda\rho}) (q_f - q_i)_\rho u(q_i) \\ &= \bar{u}(q_f) \left[-\gamma^\lambda (\not{q}_f - \not{q}_i) + q_f^\lambda - q_i^\lambda \right] u(q_i) \\ &= \bar{u}(q_f) \left[\not{q}_f \gamma^\lambda - 2(q_f)_\rho g^{\lambda\rho} + \gamma^\lambda m_i + q_f^\lambda - q_i^\lambda \right] u(q_i) \\ &= \bar{u}(q_f) \left[(m_f + m_i) \gamma^\lambda - (q_f + q_i)^\lambda \right] u(q_i). \end{aligned} \quad (4.9)$$

Using this relation we can eliminate the $r^\mu \mathbb{1}$ term in favor of $\sigma^{\mu\nu} p_\nu$ and γ^μ . Using $q_f + q_i$ instead of $q_f - q_i$ in the above derivation, we arrive at

$$\bar{u}(q_f) i\sigma^{\lambda\rho} (q_f + q_i)_\rho u(q_i) = \bar{u}(q_f) \left[(m_f - m_i) \gamma^\lambda - (q_f - q_i)^\lambda \right] u(q_i), \quad (4.10)$$

which we can use to eliminate $\sigma^{\mu\nu} r_\nu$ in favor of γ^μ and $p^\mu \mathbb{1}$. Furthermore, exchanging $u(q_i)$ for $\gamma_5 u(q_i)$ in Eqs. (4.9) and (4.10) has the effect of flipping the sign of m_i , since $\{\gamma^\mu, \gamma_5\} = 0$.

Thus, we have the identities

$$\bar{u}(q_f) i \sigma^{\lambda\rho} (q_f - q_i)_\rho \gamma_5 u(q_i) = \bar{u}(q_f) \left[(m_f - m_i) \gamma^\lambda - (q_f + q_i)^\lambda \right] \gamma_5 u(q_i), \quad (4.11)$$

$$\bar{u}(q_f) i \sigma^{\lambda\rho} (q_f + q_i)_\rho \gamma_5 u(q_i) = \bar{u}(q_f) \left[(m_f + m_i) \gamma^\lambda - (q_f - q_i)^\lambda \right] \gamma_5 u(q_i). \quad (4.12)$$

The left-hand side of these equations can be rewritten using the relation

$$\sigma^{\lambda\rho} \gamma_5 = \frac{i}{2} \epsilon^{\mu\nu\lambda\rho} \sigma_{\mu\nu}, \quad (4.13)$$

which allows us to use Eq. (4.11) to rewrite $r^\mu \gamma_5$ in terms of $\gamma^\mu \gamma_5$ and $\epsilon^{\mu\nu\lambda\rho} \sigma_{\lambda\rho} p_\nu$, and Eq. (4.12) to rewrite $\epsilon^{\mu\nu\lambda\rho} \sigma_{\lambda\rho} r_\nu$ in terms of $\gamma^\mu \gamma_5$ and $p^\mu \gamma_5$.

There are 4 more terms involving the Levi-Civita symbol which need to be rewritten in terms of the set S . All of them contain the contraction $\epsilon^{\mu\nu\lambda\rho} \gamma_\nu$, so we use the identity

$$\epsilon^{\mu\nu\lambda\rho} \gamma_\nu = i \left(g^{\mu\lambda} g^{\nu\rho} - g^{\mu\rho} g^{\nu\lambda} \right) \gamma_\nu \gamma_5 - \gamma^\mu \sigma^{\lambda\rho} \gamma_5. \quad (4.14)$$

This must be contracted with $p_\lambda r_\rho$, yielding

$$\epsilon^{\mu\nu\lambda\rho} p_\lambda r_\rho \gamma_\nu = i \not{p} p^\mu \gamma_5 - i \not{p} r^\mu \gamma_5 - \frac{i}{2} \gamma^\mu \gamma_5 (\not{p} \not{r} - \not{r} \not{p}). \quad (4.15)$$

As stated before, \not{r} and \not{p} can be exchanged in favor of masses. Thus, Eq. (4.15) can be used to exchange $\epsilon^{\mu\nu\lambda\rho} p_\lambda r_\rho \gamma_\nu$ in favor of $p^\mu \gamma_5$, $\gamma^\mu \gamma_5$, and $\epsilon^{\mu\nu\lambda\rho} \sigma_{\lambda\rho} p_\nu$. The term $\epsilon^{\mu\nu\lambda\rho} p_\lambda r_\rho \sigma_{\nu\kappa} p^\kappa$ can be written as

$$\epsilon^{\mu\nu\lambda\rho} p_\lambda r_\rho \sigma_{\nu\kappa} p^\kappa = \frac{i}{2} \left[\epsilon^{\mu\nu\lambda\rho} p_\lambda r_\rho \gamma_\nu, \not{p} \right], \quad (4.16)$$

i.e. we obtain the same terms as in Eq. (4.15), but with an extra \not{p} on the left or right. Thus, we can still exchange $\epsilon^{\mu\nu\lambda\rho} p_\lambda r_\rho \sigma_{\nu\kappa} p^\kappa$ in favor of $p^\mu \gamma_5$, $\gamma^\mu \gamma_5$, and $\epsilon^{\mu\nu\lambda\rho} \sigma_{\lambda\rho} p_\nu$, and the same is true for $\epsilon^{\mu\nu\lambda\rho} p_\lambda r_\rho \sigma_{\nu\kappa} r^\kappa$. Finally, multiplying Eq. (4.15) by γ_5 and using $\gamma_5 \gamma_5 = \mathbb{1}$, we can write the term $\epsilon^{\mu\nu\lambda\rho} p_\lambda r_\rho \gamma_5 \gamma_\nu$ in terms of $p^\mu \mathbb{1}$, γ^μ and $\sigma^{\mu\nu} p_\nu$.

Summarizing, we have shown that the vertex function Λ_{fi}^μ can be written as a linear combination of the set S . The coefficients are Lorentz invariant functions of p and r , but since $r^2 = 2 \left(m_f^2 + m_i^2 \right) - p^2$, they can be written in terms of p^2 only. Thus, we can write the vertex function on the form

$$\Lambda_{fi}^\mu = f_1(p^2) p^\mu \mathbb{1} + f_2(p^2) p^\mu \gamma_5 + f_3(p^2) \gamma^\mu + f_4(p^2) \gamma^\mu \gamma_5 + f_5(p^2) \sigma^{\mu\nu} p_\nu + f_6(p^2) \epsilon^{\mu\nu\lambda\rho} \sigma_{\lambda\rho} p_\nu, \quad (4.17)$$

where the indices fi on the form factors f_j have been suppressed to avoid clutter. We can simplify further using conservation of the electromagnetic current, $\partial_\mu j^\mu$, where $j^\mu = \bar{\nu}_f \Lambda_{fi}^\mu \nu_i$. In momentum space this implies $p_\mu \bar{u}(q_f) \Lambda_{fi}^\mu(q_i, q_f) u(q_i) = 0$. The f_5 and f_6 terms vanish in this contraction, since $p_\mu p_\nu$ is symmetric in μ and ν while the relevant tensors are antisymmetric. Using the momentum space Dirac equation, the rest of the terms give

$$\begin{aligned} \bar{u}(q_f) \left[f_1(p^2) p_\mu p^\mu + f_2(p^2) p_\mu p^\mu \gamma_5 + f_3(p^2) \not{p} + f_4(p^2) \not{p} \gamma_5 \right] u(q_i) &= 0 \\ \implies \bar{u}(q_f) \left[f_1(p^2) p^2 + f_2(p^2) p^2 \gamma_5 + f_3(p^2) (m_f - m_i) + f_4(p^2) (m_f + m_i) \gamma_5 \right] u(q_i) &= 0 \end{aligned}$$

$$\begin{aligned} &\implies f_1(p^2)p^2 + f_3(p^2)(m_f - m_i) = 0 \\ &f_2(p^2)p^2 + f_4(p^2)(m_f + m_i) = 0, \end{aligned} \quad (4.18)$$

where we obtain two independent equations since γ_5 and the identity matrix are linearly independent. Substituting Eq. (4.18) back into Eq. (4.17), we have

$$\begin{aligned} \bar{u}(q_f)\Lambda_{fi}^\mu u(q_i) &\supset \bar{u}(q_f) \left[-f_3(p^2)\frac{m_f - m_i}{p^2}p^\mu + f_3(p^2)\gamma^\mu \right. \\ &\quad \left. - f_4(p^2)\frac{m_f + m_i}{p^2}p^\mu\gamma_5 + f_4(p^2)\gamma^\mu\gamma_5 \right] u(q_i) \\ &= \bar{u}(q_f) \left[F_Q(p^2) \left(\gamma^\mu - \frac{\not{p}p^\mu}{p^2} \right) + F_A(p^2) \left(\gamma^\mu - \frac{\not{p}p^\mu}{p^2} \right) \gamma_5 \right] u(q_i), \end{aligned} \quad (4.19)$$

where $F_Q(p^2) = f_3(p^2)$ is the form factor corresponding to charge renormalization, and $F_A(p^2) = f_4(p^2)$ is the anapole form factor.

Further, we use Eq. (4.13) to obtain

$$\begin{aligned} \sigma^{\mu\nu}\gamma_5 &= \frac{i}{2}\epsilon^{\lambda\rho\mu\nu}\sigma_{\lambda\rho} \\ &= \frac{i}{2}\epsilon^{\mu\nu\lambda\rho}\sigma_{\lambda\rho} \\ \implies \epsilon^{\mu\nu\lambda\rho}\sigma_{\lambda\rho} &= -2i\sigma^{\mu\nu}\gamma_5, \end{aligned} \quad (4.20)$$

which can be used to rewrite the f_6 term in Eq. (4.17) as proportional to $\sigma^{\mu\nu}p_\nu\gamma_5$. This term was not included in the original set S since it is a combination of two basis matrices. Together with Eq. (4.19), this enables us to write the vertex function on the conventional form

$$\Lambda_{fi}^\mu = \left(\gamma^\mu - \frac{\not{p}p^\mu}{p^2} \right) F_Q(p^2) + \frac{i\sigma^{\mu\nu}p_\nu}{m_f + m_i} F_M(p^2) + \left(\gamma^\mu - \frac{\not{p}p^\mu}{p^2} \right) \gamma_5 F_A(p^2) + \frac{i\sigma^{\mu\nu}p_\nu}{m_f + m_i} \gamma_5 F_E(p^2), \quad (4.21)$$

where $F_M = -i(m_f + m_i)f_5$ is the magnetic dipole form factor, and $F_E = -2(m_f + m_i)f_6$ is the electric dipole form factor. The form factor $F_M(p^2)$ in the on-shell limit is what we're interested in here, since it gives the magnetic moment. Recall the effective Lagrangian which describes the magnetic dipole moment interaction,

$$\mathcal{L}_{\text{eff}} = - \sum_{i,f=1}^N \frac{\mu_{fi}}{2} F_{\mu\nu} \bar{\nu}_f \sigma^{\mu\nu} \nu_i \quad (4.22)$$

For the process $\nu_i(q_i)\gamma(p) \rightarrow \nu_f(q_f)$ we find the S-matrix element

$$\begin{aligned} S_{fi} &= \langle \nu_f(q_f) | -i\frac{\mu_{fi}}{2} \int d^4x \text{N} \left\{ \left(\partial_\mu A_\nu^{(+)} - \partial_\nu A_\mu^{(+)} \right) \bar{\nu}^{(-)} \sigma^{\mu\nu} \nu^{(+)} \right\} | \gamma(p) \nu_i(q_i) \rangle \\ &= i\mu_{fi} \langle \nu_f(q_f) | \int d^4x \left(\bar{\nu}^{(-)} \sigma^{\mu\nu} \partial_\nu A_\mu^{(+)} \nu^{(+)} \right) | \gamma(p) \nu_i(q_i) \rangle \\ &= i\mu_{fi} \langle 0 | \int d^4x \bar{u}_f(q_f) \sigma^{\mu\nu} (-ip_\nu) \varepsilon_\mu(p) u_i(q_i) e^{i(q_f - q_i - p)x} | 0 \rangle \\ &= \mu_{fi} \bar{u}_f(q_f) \sigma^{\mu\nu} \varepsilon_\mu(p) p_\nu u_i(q_i) \times (2\pi)^4 \delta(q_f - q_i - p), \end{aligned} \quad (4.23)$$

i.e. the amplitude

$$\mathcal{M}^\mu = \mu_{fi} \bar{u}_f(q_f) \sigma^{\mu\nu} p_\nu u_i(q_i). \quad (4.24)$$

This must agree with Eq. (4.21) for an on-shell photon, so

$$\mu_{fi} = \frac{iF_M(0)}{m_f + m_i}. \quad (4.25)$$

Since the Hamiltonian in Eq. (4.2) is Hermitian and the photon field is real, it follows that

$$\begin{aligned} \sum_{f,i} \bar{\nu}_f \Lambda_{fi}^\mu \nu_i &= \sum_{f,i} \left(\bar{\nu}_f \Lambda_{fi}^\mu \nu_i \right)^\dagger \\ &= \sum_{f,i} \bar{\nu}_i \gamma^0 \left(\Lambda_{fi}^\mu \right)^\dagger \gamma^0 \nu_f \\ &= \sum_{f,i} \bar{\nu}_f \gamma^0 \left(\Lambda_{if}^\mu \right)^\dagger \gamma^0 \nu_i, \end{aligned} \quad (4.26)$$

where $\gamma^0 \gamma^0 = \mathbb{1}$ was inserted in the second line and the summation indices i, f were renamed in the third line. Thus, Hermiticity implies

$$\gamma^0 \left(\Lambda_{if}^\mu \right)^\dagger \gamma^0 = \Lambda_{fi}^\mu, \quad (4.27)$$

which means that $\gamma^0 (i\sigma^{\mu\nu} F_M)^\dagger \gamma^0 = i\sigma^{\mu\nu} F_M$. From this, we find that the magnetic moment matrix is Hermitian. This can also be seen from the Hermiticity of the effective Lagrangian in Eq. (4.22), which gives $\mu_{fi}^* = \mu_{if}$.

As we saw in Section 3.4.1, the magnetic moment operator is chirality flipping. The Lagrangian Eq. (4.22) and the amplitude Eq. (4.24) describes both the processes $\nu_L \gamma \rightarrow \nu_R$ and $\nu_R \gamma \rightarrow \nu_L$. When looking at a theory with active chiral neutrinos ν_L and heavier sterile chiral neutrinos N_R , it is more natural to consider the transition $\nu_L \gamma \rightarrow N_R$, but the resulting amplitude could then not be compared directly to Eq. (4.24). For simplicity, consider one active neutrino and one sterile neutrino. The effective Lagrangian is then

$$\mathcal{L}_{\text{eff}} = -\frac{\mu_{N\nu}}{2} F_{\mu\nu} \bar{N} \sigma^{\mu\nu} \nu - \frac{\mu_{\nu N}}{2} F_{\mu\nu} \bar{\nu} \sigma^{\mu\nu} N - \frac{\mu_{\nu\nu}}{2} F_{\mu\nu} \bar{\nu} \sigma^{\mu\nu} \nu - \frac{\mu_{NN}}{2} F_{\mu\nu} \bar{N} \sigma^{\mu\nu} N \quad (4.28)$$

Inserting the identity matrix $\mathbb{1} = P_L + P_R$, we obtain in total 8 terms. If the neutrinos are chiral, only two terms survive,

$$\mathcal{L}_{\text{eff}} = -\frac{\mu_{\nu N}}{2} F_{\mu\nu} \bar{N}_R \sigma^{\mu\nu} P_L \nu_L - \frac{\mu_{N\nu}}{2} F_{\mu\nu} \bar{\nu}_L \sigma^{\mu\nu} P_R N_R \quad (4.29)$$

The first term gives the interaction vertex $\nu_L \gamma \rightarrow N_R$. The relevant part of the resulting amplitude receives a factor 1/2 relative to Eq. (4.24) due to the chirality projector. Thus, Eq. (4.25) would need to be modified to

$$\mu_{\nu N} = \frac{2iF_M(0)}{m_f + m_i}. \quad (4.30)$$

Thus one uses either Eq. (4.25) or Eq. (4.30) to extract the magnetic moment, depending on

the situation at hand.

Having written the amplitude for a process like Eq. (4.1) in a given theory, one can obtain the magnetic moment by rewriting the amplitude in the form of Eq. (4.21), picking out $F_M(0)$, and using Eq. (4.25). We were able to do this for the 1-loop QED contribution to the electron magnetic moment, but in general it's very impractical. A more straightforward way to obtain $F_M(0)$ from the amplitude is to use a projector P_M^μ , such that

$$\text{tr} \left[P_{M\mu} \Lambda_{fi}^\mu \right] = F_M(p^2). \quad (4.31)$$

P_M^μ carries a Lorentz index and is a matrix in spinor space, such that contracting and taking the trace yields a scalar. Using the projection technique, one avoids having to calculate the entire loop integral, only picking out the relevant part. Throughout this thesis, the magnetic moment is calculated using PACKAGE-X [25] in MATHEMATICA [26]. Specifically, the form factor $F_M(p^2)$ is obtained using the function `Projector`, and loop integrals are carried out with the `LoopIntegrate` function.

4.2 Majorana Neutrinos

Majorana neutrinos are their own antiparticles, and thus the adjoint field $\bar{\nu}$ contains the same operators as ν . Therefore, the transition $\nu_i \gamma \rightarrow \nu_f$ can be obtained from two of the terms in the interaction Hamiltonian Eq. (4.2),

$$\mathcal{H} \supset \bar{\nu}_f \Lambda_{fi}^\mu \nu_i A_\mu + \bar{\nu}_i \Lambda_{if}^\mu \nu_f A_\mu. \quad (4.32)$$

These terms give the amplitude

$$\mathcal{M}^\mu = \bar{u}_f(q_f) \Lambda_{fi}^\mu(p) u_i(q_i) - \bar{v}_i(q_i) \Lambda_{if}^\mu(p) v_f(q_f), \quad (4.33)$$

where the relative minus comes from normal ordering. The first term is the amplitude in the case of Dirac neutrinos, Eq. (4.1). Using the relations $v = u^c = C\bar{u}^T$ and $\bar{v} = \bar{u}^c = -u^T C^{-1}$, the amplitude is written as

$$\begin{aligned} \mathcal{M}^\mu &= \bar{u}_f(q_f) \Lambda_{fi}^\mu(p) u_i(q_i) + u_i(q_i)^T C^{-1} \Lambda_{if}^\mu(p) C \bar{u}_f(q_f)^T \\ &= \bar{u}_f(q_f) \left(\Lambda_{fi}^\mu(p) + C \Lambda_{if}^\mu(p)^T C^{-1} \right) u_i(q_i), \end{aligned} \quad (4.34)$$

where the second term was transposed in spinor space and the properties $C^T = C^{-1} = -C$ were used. Defining the Majorana vertex function $\Lambda_{fi}^{M\mu}(p)$, we have

$$\Lambda_{fi}^{M\mu}(p) = \Lambda_{fi}^\mu(p) + C \Lambda_{if}^\mu(p)^T C^{-1}. \quad (4.35)$$

Specifically, the magnetic moment term for Majorana neutrinos is

$$\begin{aligned} \frac{i\sigma^{\mu\nu} p_\nu}{m_f + m_i} F_{Mfi}^M(p^2) &= \frac{i\sigma^{\mu\nu} p_\nu}{m_f + m_i} F_{Mfi}(p^2) + C \left(\frac{i\sigma^{\mu\nu} p_\nu}{m_f + m_i} F_{Mif}(p^2) \right)^T C^{-1} \\ &= \left(F_{Mfi}(p^2) - F_{Mif}(p^2) \right) \frac{i\sigma^{\mu\nu} p_\nu}{m_f + m_i}, \end{aligned} \quad (4.36)$$

where we used the property $C\sigma_{\mu\nu}^T C^{-1} = -\sigma_{\mu\nu}$, which follows from the defining property $C^{-1}\gamma_\mu C = -\gamma_\mu^T$ of the charge conjugation matrix. Thus, the magnetic moment matrix for Majorana neutrinos is obtained by

$$\mu_{fi}^M = \mu_{fi}^D - \mu_{if}^D. \quad (4.37)$$

As expected from Section 3.4.3, μ_{fi}^M is antisymmetric in the space of neutrino states, so only transition magnetic moments are allowed. Since the magnetic moment matrix is also Hermitian, the transition Majorana magnetic moments are imaginary.

4.3 Effective Neutrino Magnetic Moment

In detectors, one can look for neutrino magnetic moments by analyzing neutrino-electron scattering. In the Standard Model, weak neutral and charged current interactions contribute to this process. With a large neutrino magnetic moment, diagrams like Fig. 4.1 contribute significantly to the total cross section, which can be written as

$$\frac{d\sigma_{\nu_\alpha e^-}}{dT_e} = \left(\frac{d\sigma_{\nu_\alpha e^-}}{dT_e} \right)_w + \left(\frac{d\sigma_{\nu_\alpha e^-}}{dT_e} \right)_{\text{em}}, \quad (4.38)$$

where T_e is the kinetic energy of the final electron. The first term in Eq. (4.38) is the contribution from the Standard Model weak interactions, given by [13]

$$\left(\frac{d\sigma_{\nu_\alpha e^-}}{dT_e} \right)_w = \frac{G_F^2 m_e}{2\pi} \left\{ (g_V^{\nu_\alpha} + g_A^{\nu_\alpha})^2 + (g_V^{\nu_\alpha} - g_A^{\nu_\alpha})^2 \left(1 - \frac{T_e}{E_\nu} \right)^2 + [(g_A^{\nu_\alpha})^2 - (g_V^{\nu_\alpha})^2] \frac{m_e T_e}{E_\nu^2} \right\}, \quad (4.39)$$

where the couplings are

$$\begin{aligned} g_V^{\nu_e} &= 2 \sin^2 \theta_W + \frac{1}{2}, & g_A^{\nu_e} &= \frac{1}{2}, \\ g_V^{\nu_{\mu,\tau}} &= 2 \sin^2 \theta_W - \frac{1}{2}, & g_A^{\nu_{\mu,\tau}} &= -\frac{1}{2}, \end{aligned} \quad (4.40)$$

and for antineutrinos one must substitute $g_A \rightarrow -g_A$. The second term in Eq. (4.38) is the contribution from the neutrino-photon interaction, which in the lowest order in neutrino mass can be shown to be [27]

$$\left(\frac{d\sigma_{\nu_\alpha e^-}}{dT_e} \right)_{\text{em}} = \frac{\pi \alpha^2}{m_e^2} \left(\frac{1}{T_e} - \frac{1}{E_\nu} \right) \left(\frac{\mu_{\nu_\alpha}^{\text{eff}}}{\mu_B} \right)^2, \quad (4.41)$$

where E_ν is the energy of the incoming neutrino, and $\mu_{\nu_\alpha}^{\text{eff}}$ is the effective neutrino magnetic moment, which will be explained shortly. There is a cross term between the weak and electromagnetic terms in the cross section, but it is suppressed by m_ν/m_e at lowest order in neutrino mass, and we therefore neglect it [28]. Note the T_e dependence of Eq. (4.41), which is different from that of Eq. (4.39); the inverse proportionality means that the smaller electron energy can be measured, the smaller neutrino magnetic moments can be probed. This is illustrated in Fig. 4.2, where the weak and electromagnetic cross sections for a 1 MeV electron neutrino scattering elastically with an electron are shown as functions of the electron recoil energy. As is evident from Fig. 4.2, the electromagnetic contribution dominates at low recoil energies.

The neutrino-electron scattering cross section depends on an effective neutrino magnetic moment

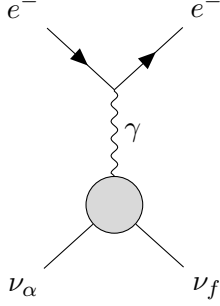


Figure 4.1: Diagram involving the neutrino electromagnetic interaction which contributes to neutrino-electron scattering. ν_α is an active neutrino flavor state emitted from a source, which oscillates on its way to the detector. ν_f is a mass eigenstate. The gray blob represents the neutrino electromagnetic interaction, including the magnetic moment, whose specific form depends on the model. In this diagram, the blob also includes the mixing and oscillation of the initial neutrino, as described by the effective neutrino magnetic moment in Eq. (4.42).

μ_ν^{eff} rather than the magnetic moment directly. There are two reasons for this. Firstly, the neutrino-photon interaction in Fig. 4.1 receives a contribution from the electric dipole moment in addition to the magnetic moment. Secondly, the neutrinos which participate in the neutrino-electron scattering in the detector are produced in flavor eigenstates, which are superpositions of mass eigenstates. Thus, the effective neutrino magnetic moment takes into account mixing and the oscillation that occurs between the source and the detector. Assuming vacuum oscillations as described in Section 2.6, the effective neutrino magnetic moment can be shown to be [13]

$$\left(\mu_{\nu_\alpha}^{\text{eff}}\right)^2 = \sum_f \left| \sum_k U_{\alpha k} e^{-iL\Delta m_{fk}^2/2E_\nu} (\mu_{fk} - i\epsilon_{fk}) \right|^2, \quad (4.42)$$

where ϵ_{fk} is the neutrino electric dipole moment. It can be extracted from the vertex function Eq. (4.21) as

$$\epsilon_{fk} = \frac{-iF_E(0)}{m_f + m_k}, \quad (4.43)$$

where $m_{f,k}$ are the masses of the neutrino eigenstates $\nu_{f,k}$. If the neutrinos pass through matter between the source and the detector, as in the case of solar neutrinos, one must take into account the effects of the surrounding matter on the neutrino oscillation. A description of neutrino oscillations in matter is beyond the scope of this thesis. Here, we only note that the effective magnetic moment for solar neutrinos can be written as [13]

$$\left(\mu_{\nu_{\text{solar}}}^{\text{eff}}\right)^2 = \sum_k |U_{ek}^M|^2 \sum_f |\mu_{fk} - i\epsilon_{fk}|^2, \quad (4.44)$$

where U^M is a mixing matrix taking into account matter effects, and the exponential terms in Eq. (4.42) are washed out by the finite energy resolution of the detector due to the large distance L in comparison to the oscillation length, $L \gg 4\pi E_\nu / \Delta m_{fk}^2$ [13].

In summary, the neutrino magnetic moment has an effect on the observable cross section of neutrino-electron scattering, where the μ_{fi} enters the description in the non-trivial way described by Eq. (4.41) and Eq. (4.42). By analyzing the recoil electron energy spectrum, one can

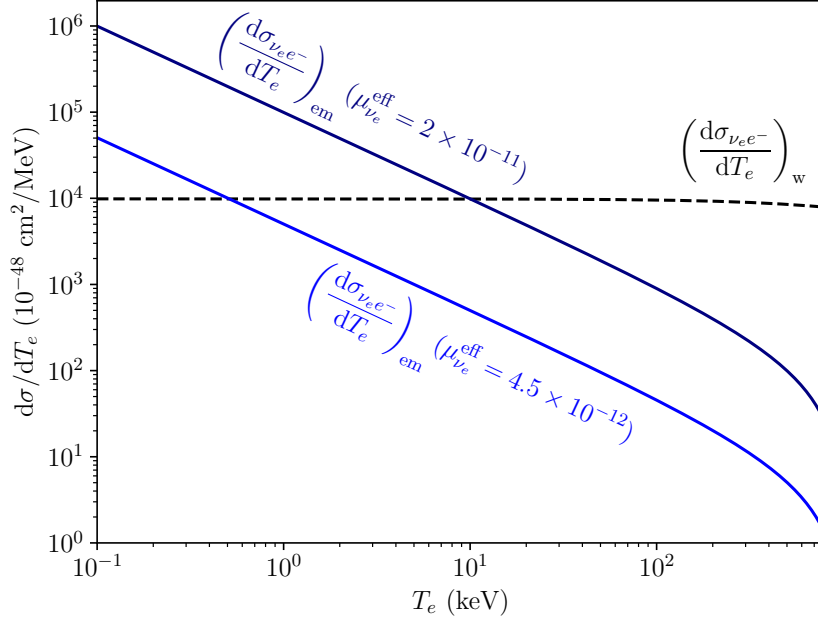


Figure 4.2: Weak (black dashed line) and electromagnetic (blue solid lines) contributions to the cross section of an electron neutrino scattering elastically with an electron, as a function of the recoil energy of the electron. The electromagnetic cross section is shown for two values of the effective magnetic moment, corresponding to terrestrial and astrophysical limits. At low recoil energies, the electromagnetic contribution dominates, distorting the spectrum relative to the Standard Model expectation.

look for a signal from neutrino magnetic moments.

4.4 The Experimental Situation

Having described how neutrino magnetic moments can be observed in detectors, let us now briefly discuss the current experimental status. The interested reader is referred to Ref. [13] for more details.

In the past, upper limits have been set on neutrino magnetic moments by the lack of deviations from the expected recoil electron spectrum. For example, in the 1990s data was taken on accelerator ν_μ and $\bar{\nu}_\mu$ scattering on e^- in the LSND detector. An upper limit of $\mu_{\nu_\mu}^{\text{eff}} < 6.8 \times 10^{-10} \mu_B$ was obtained [29]. In 2012, the GEMMA experiment reported the limit $\mu_{\nu_e}^{\text{eff}} < 2.9 \times 10^{-11} \mu_B$ from reactor $\bar{\nu}_e$ [30].

Solar neutrinos have also been used to look for neutrino magnetic moments. In 2017, the Borexino collaboration reported the limit $\mu_{\nu_{\text{solar}}}^{\text{eff}} < 2.8 \times 10^{-11} \mu_B$ [31]. More recently, the XENON1T experiment detected an excess in the low energy range of the electron recoil spectrum, which is shown in Fig. 4.3. Interpreted as a neutrino magnetic moment, the 90% confidence interval $\mu_{\nu_{\text{solar}}}^{\text{eff}} \in \{1.4, 2.9\} \times 10^{-11} \mu_B$ was obtained. The magnetic moment explanation is preferred over the Standard Model at a significance of 3.2σ [6]. One specific hypothesis to explain the XENON1T excess is a transition magnetic moment from ν_μ to a heavier sterile state [32]. BSM models in the context of this interpretation are discussed in Chapter 7 and Chapter 8. It should be noted that the XENON1T collaboration also have interpreted the excess as coming from solar axions, with a statistical significance of 3.4σ . The source of the excess may also be small

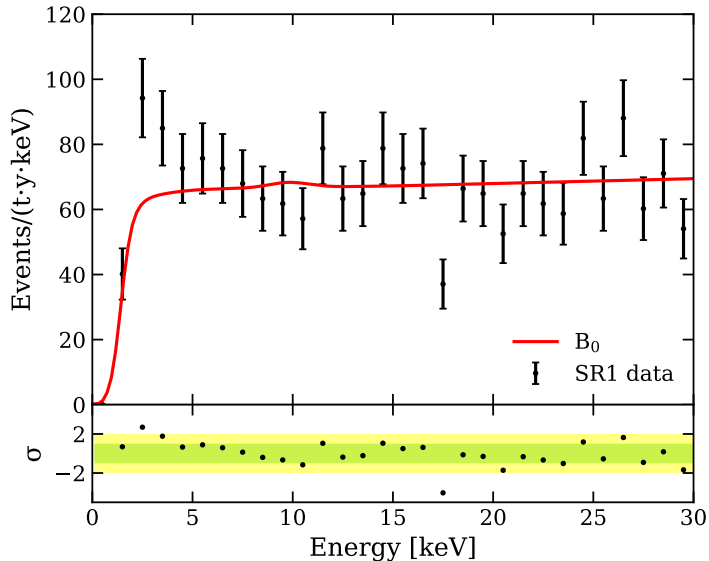


Figure 4.3: Electron recoil events as a function of recoil energy recorded in the XENON1T dark matter detector (black points), and the expected event rate from the background model (red curve). There is an excess in the lower end of the electron recoil energy spectrum. The figure is taken from [6].

amounts of tritium in the detector which have not been accounted for in the background analysis. This explanation has a similar statistical significance as the neutrino magnetic moment explanation [6].

Neutrino magnetic moments can also be probed in nuclear interactions. In particular, one can analyze coherent elastic neutrino-nucleus scattering (CE ν NS), where the momentum exchange is low enough for the nucleus to be treated as a point particle. The scattering cross section due to a neutrino magnetic moment in such a process is proportional to that of elastic neutrino-electron scattering, given in Eq. (4.41). CE ν NS was first observed by the COHERENT collaboration [33], and also recently by the “NCC-1701” detector using antineutrinos from the Dresden-II nuclear reactor in the United States [34]. Very recently, the results from these experiments were used in Ref [35] to set limits on the neutrino magnetic moment. These are $\mu_{\nu_e}^{\text{eff}} < 2.13 \times 10^{-10} \mu_B$ and $\mu_{\nu_\mu}^{\text{eff}} < 18 \times 10^{-10} \mu_B$. Being weaker than the limits from elastic neutrino-electron scattering, these new limits are not in conflict with the interpretation of the XENON1T excess as an enhanced neutrino magnetic moment.

In addition to the limits obtained from terrestrial experiments, one can also use astrophysical and cosmological data to set constraints on neutrino magnetic moments. In the plasma of a star, photons acquire an effective mass, allowing the decay into neutrinos via the magnetic moment interaction. The emitted neutrinos would carry away a large amount of energy from the star. Thus, large neutrino magnetic moments may be in conflict with the standard stellar evolution models. From data on red giants, the limit $\mu_\nu^{\text{eff}} < 4.5 \times 10^{-12} \mu_B$ on a generic neutrino magnetic moment has been obtained [36]. This is in conflict with the magnetic moment interpretation of the XENON1T data. However, the limit can be avoided if the neutrinos are coupled to a light scalar through a Yukawa interaction, thereby obtaining a medium-dependent effective mass. Thus, the decay of plasma photons may become kinematically forbidden. This idea is explored in Refs. [32, 37].

Constraints on the neutrino magnetic moment can be obtained from data on Big-Bang Nucleosynthesis (BBN). In the early universe, weak charged current interactions between electrons, electron neutrinos, and nuclei were in thermal equilibrium. In these reactions, protons are converted into neutrons and vice versa. The formation of nuclei depends on the relative number of neutrons and protons, which in turn depends on the rates of the aforementioned weak interaction processes. Thus, one can discern neutrino properties from data on abundances of light nuclei in the early universe. Limits on Majorana transition magnetic moments on the order of $10^{-10} \mu_B$ have been derived from BBN [38].

Transition magnetic moments between active neutrinos and heavier sterile, right-chiral neutrinos N_R open up the possibility for N_R to be produced in the early universe, which affects BBN. The cosmic microwave background is also affected, through the effective number of relativistic degrees of freedom. These cosmological limits depend on the mass of the sterile neutrino, and its lifetime, which in turn depends on the magnetic moment mediating the decay $N_R \rightarrow \gamma \nu_L$. A detailed analysis can be found in Ref. [32]. Here we only remark that stringent limits are obtained for sterile masses below ~ 100 keV, which may be in conflict with the interpretation of the XENON1T excess as an active-to-sterile transition magnetic moment. Possibilities for avoiding the cosmological limits are also discussed in Ref. [32].

In conclusion, terrestrial experiments are able to set limits on the effective neutrino magnetic moment at the order of $10^{-11} \mu_B$, with more stringent limits coming from astrophysics and cosmology. As shall be seen in the next chapter, the Standard Model predicts neutrino magnetic moments several orders of magnitude smaller than these limits. Thus, experimental evidence of neutrino magnetic moments in current and future detectors would be a clear sign of new physics. If the XENON1T excess persists, it may be such a sign.

Chapter 5

Neutrino Magnetic Moment in the Standard Model

5.1 Dirac Neutrinos

As a first example of a calculation of the magnetic moment of neutrinos, let us consider the Standard Model, extended to include massive neutrinos. In particular, we first consider the case of the three standard flavors having Dirac mass terms.

The leading contributions to the neutrino magnetic moment with Standard Model interactions comes from one-loop electroweak diagrams. We seek the magnetic moment μ_{fi} between the neutrino mass eigenstates ν_i and ν_f , which are related to the flavor eigenstates ν_α by the unitary transformation

$$\nu_\alpha = \sum_{j=1}^3 U_{\alpha j} \nu_j, \quad (5.1)$$

where $U_{\alpha i}$ is the PMNS matrix. We assume that the neutrinos are Dirac fields with left- and right-chiral components, $\nu_j = \nu_{jL} + \nu_{jR}$. The relevant diagrams are shown in Fig. 5.1.

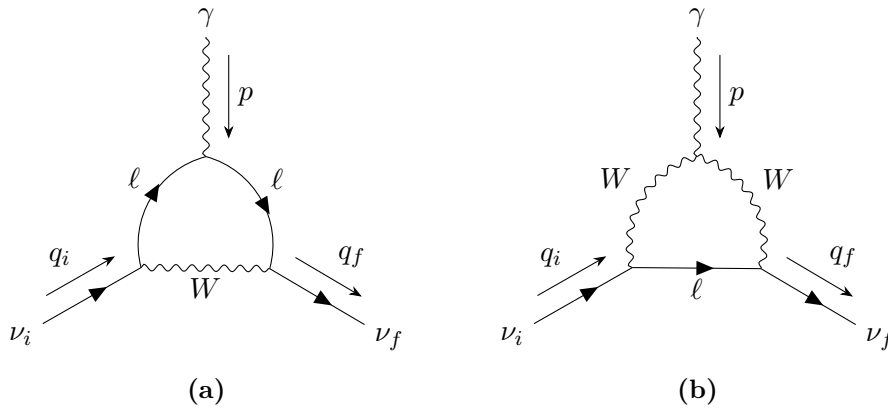


Figure 5.1: Diagrams contributing to the magnetic moment μ_{fi} in the Standard Model with massive Dirac neutrinos. ν_i and ν_f are mass eigenstates, and ℓ is any charged lepton. For Dirac neutrinos, one may have $i = f$ or $i \neq f$, describing diagonal and transition magnetic moments, respectively.

The amplitude $\mathcal{M}^\mu = \mathcal{M}_a^\mu + \mathcal{M}_b^\mu$ is obtained by employing the standard electroweak Feynman rules, which are summarized in Section A.1. Each diagram in Fig. 5.1 can involve either of the charged lepton flavors e, μ, τ in the loop, so the amplitudes include a sum over lepton flavor α . We find

$$\begin{aligned} \mathcal{M}_a^\mu &= -\frac{g^2 e}{2} \sum_{\alpha=e,\mu,\tau} U_{\alpha f}^* U_{\alpha i} \\ &\times \int \frac{d^4 k}{(2\pi)^4} \frac{\bar{u}(q_f) \gamma^\nu P_L (\not{q}_f + \not{k} + m_{\ell_\alpha}) \gamma^\mu (\not{q}_i + \not{k} + m_{\ell_\alpha}) \gamma^\rho P_L u(q_i) (-g_{\nu\rho} + k_\nu k_\rho / m_W^2)}{[(q_f + k)^2 - m_{\ell_\alpha}^2 + i\varepsilon] [(q_i + k)^2 - m_{\ell_\alpha}^2 + i\varepsilon] [k^2 - m_W^2 + i\varepsilon]}, \end{aligned} \quad (5.2)$$

and

$$\begin{aligned} \mathcal{M}_b^\mu &= \frac{g^2 e}{2} \sum_{\alpha=e,\mu,\tau} U_{\alpha f}^* U_{\alpha i} \\ &\times \int \frac{d^4 k}{(2\pi)^4} \left\{ \bar{u}(q_f) \gamma^\nu P_L (\not{k} + m_{\ell_\alpha}) \gamma^\rho P_L u(q_i) \right. \\ &\quad \times \frac{(-g_{\nu\lambda} + (k - q_f)_\nu (k - q_f)_\lambda / m_W^2) (-g_{\kappa\rho} + (k - q_i)_\kappa (k - q_i)_\rho / m_W^2)}{[k^2 - m_{\ell_\alpha}^2 + i\varepsilon] [(k - q_f)^2 - m_W^2 + i\varepsilon] [(k - q_i)^2 - m_W^2 + i\varepsilon]} \\ &\quad \left. \times \left[g^{\mu\lambda} (2q_f - q_i - k)^\kappa + g^{\lambda\kappa} (2k - q_i - q_f)^\mu + g^{\kappa\mu} (2q_i - q_f - k)^\lambda \right] \right\}. \end{aligned} \quad (5.3)$$

Using `Package-X` [25], the form factor $F_M(p^2)$ was projected out of \mathcal{M}^μ and the loop integral performed. Then, using Eq. (4.25), taking the on-shell limit $p^2 \rightarrow 0$ and expanding to first order in the neutrino masses, we obtain

$$\begin{aligned} \mu_{fi} &= \sum_{\alpha=e,\mu,\tau} \left\{ U_{\alpha f}^* U_{\alpha i} - 3eg^2(m_f + m_i) \right. \\ &\quad \left. \times \frac{m_{\ell_\alpha}^6 - 6m_{\ell_\alpha}^4 m_W^2 + 7m_{\ell_\alpha}^2 m_W^4 - 2m_W^6 + 2m_{\ell_\alpha}^4 m_W^2 \log\left(\frac{m_{\ell_\alpha}^2}{m_W^2}\right)}{256m_W^2 (m_W^2 - m_{\ell_\alpha}^2)^3 \pi^2} \right\}. \end{aligned} \quad (5.4)$$

Defining $a_\alpha = m_{\ell_\alpha}^2 / m_W^2$, and writing in terms of the Fermi constant $G_F = \sqrt{2}g^2 / 8m_W^2$, we have

$$\begin{aligned} \mu_{fi} &= \frac{3eG_F}{32\sqrt{2}\pi^2} (m_f + m_i) \sum_{\alpha=e,\mu,\tau} \left[1 + \frac{1}{1 - a_\alpha} - \frac{2a_\alpha}{(1 - a_\alpha)^2} - \frac{2a_\alpha^2 \log a_\alpha}{(1 - a_\alpha)^3} \right] U_{\alpha f}^* U_{\alpha i} \\ &\equiv \frac{3eG_F}{32\sqrt{2}\pi^2} (m_f + m_i) \sum_{\alpha=e,\mu,\tau} f(a_\alpha) U_{\alpha f}^* U_{\alpha i}, \end{aligned} \quad (5.5)$$

where the loop function $f(a_\alpha)$ was written in a form where the limit $a_\alpha \rightarrow 0$ is easily seen. Indeed, since a_α is small,

$$a_\alpha = \frac{m_{\ell_\alpha}^2}{m_W^2} \leq \frac{m_\tau^2}{m_W^2} \approx 4.9 \times 10^{-4}, \quad (5.6)$$

we can approximate $f(a_\alpha) \approx 2$. Then, we can use the unitarity of the PMNS matrix,

$$\sum_{\alpha} U_{\alpha f}^* U_{\alpha i} = \delta_{fi}, \quad (5.7)$$

yielding for the diagonal magnetic moment

$$\mu_{ii} \approx \frac{3eG_F m_i}{8\sqrt{2}\pi^2}, \quad (5.8)$$

which agrees with the literature [39]. Note that the magnetic moment is proportional to the neutrino mass, as expected in Eq. (3.58). Numerically,

$$\mu_{ii} \approx 3.20 \times 10^{-19} \left(\frac{m_i}{1 \text{ eV}} \right) \mu_B, \quad (5.9)$$

which is roughly 8 orders of magnitude lower than the experimental bounds discussed in Section 4.4.

For the transition magnetic moments, i.e. $i \neq f$, the leading order contribution in Eq. (5.5) vanishes because of the unitarity of the PMNS matrix, Eq. (5.7). Thus, the leading order contribution to the transition magnetic moments comes from the 2nd term in the expansion $f(a_\alpha) \approx 2 - a_\alpha$, so

$$\mu_{fi} \approx -\frac{3eG_F}{32\sqrt{2}\pi^2} (m_f + m_i) \sum_{\alpha=e,\mu,\tau} a_\alpha U_{\alpha f}^* U_{\alpha i}, \quad (5.10)$$

which is suppressed by a factor $\sim 10^{-4}$ relative to the diagonal magnetic moment due to the ratio a_α .

5.2 Majorana Neutrinos

If neutrinos are Majorana fermions, there are additional diagrams contributing to the magnetic moment; since the fields ν and $\bar{\nu}$ contain the same operators, there are more allowed contractions with the external states $|\nu_i\rangle$ and $|\nu_f\rangle$. The contributing diagrams in the case of Majorana neutrinos are shown in Fig. 5.2.

The amplitudes of the diagrams in Fig. 5.2 must be evaluated using the Feynman rules for fermion-number-violating interactions, given in Ref. [40]. These rules are summarized in Section A.3. Choosing the direction of fermion flow as indicated by the gray arrows in Fig. 5.2, the diagrams in Fig. 5.2a and Fig. 5.2b are the same diagrams as shown in Fig. 5.1, and yield the amplitudes \mathcal{M}_a and \mathcal{M}_b , respectively. The additional diagrams, Fig. 5.2c and Fig. 5.2d, have lepton number flow antiparallel to the fermion flow. The amplitudes obtained from these diagrams are

$$\begin{aligned} \mathcal{M}_c^\mu &= \frac{g^2 e}{2} \sum_{\alpha=e,\mu,\tau} U_{\alpha i}^* U_{\alpha f} \\ &\times \int \frac{d^4 k}{2\pi^4} \frac{\bar{u}(q_f) \gamma^\nu P_R (\not{q}_f - \not{k} + m_{\ell_\alpha}) \gamma^\mu (\not{q}_i - \not{k} + m_{\ell_\alpha}) \gamma^\rho P_R u(q_i) (-g_{\nu\rho} + k_\nu k_\rho / m_W^2)}{[(q_f - k)^2 - m_{\ell_\alpha}^2 + i\varepsilon] [(q_i - k)^2 - m_{\ell_\alpha}^2 + i\varepsilon] [k^2 - m_W^2 + i\varepsilon]}, \end{aligned} \quad (5.11)$$

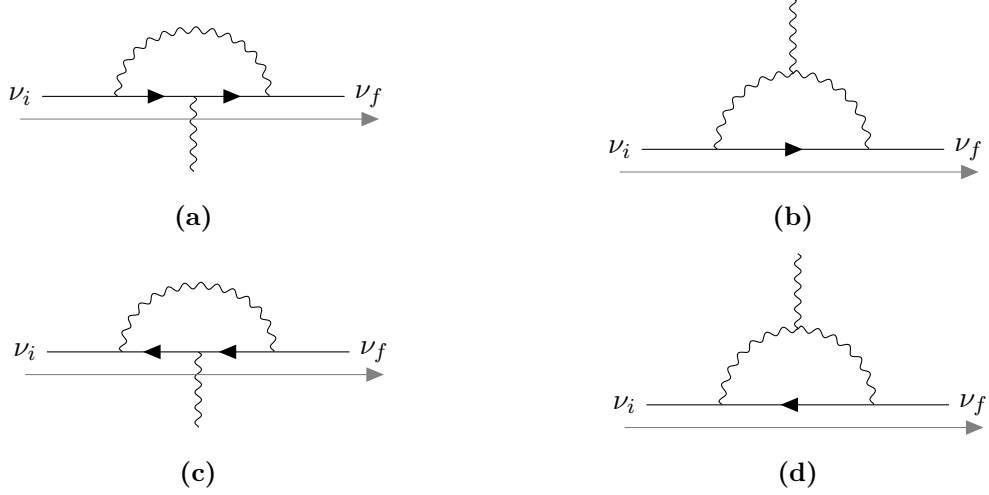


Figure 5.2: Diagrams contributing to the neutrino magnetic moment in the Standard Model with Majorana neutrinos. The gray arrows indicate the chosen fermion flow, which is used to determine the correct amplitude corresponding to the Feynman rules for fermion-number-violating interactions summarized in Section A.3. For Majorana neutrinos, only transition magnetic moments are allowed, so $i \neq f$.

and

$$\begin{aligned}
\mathcal{M}_d^\mu &= -\frac{g^2 e}{2} \sum_{\alpha=e,\mu,\tau} U_{\alpha i}^* U_{\alpha f} \\
&\times \int \frac{d^4 k}{(2\pi)^4} \left\{ \bar{u}(q_f) \gamma^\nu P_R (-\not{k} + m_{\ell_\alpha}) \gamma^\rho P_R u(q_i) \right. \\
&\quad \times \frac{(-g_{\nu\lambda} + (k - q_f)_\nu (k - q_f)_\lambda / m_W^2) (-g_{\kappa\rho} + (k + q_i)_\kappa (k + q_i)_\rho / m_W^2)}{[k^2 - m_{\ell_\alpha}^2 + i\varepsilon] [(k + q_f)^2 - m_W^2 + i\varepsilon] [(k + q_i)^2 - m_W^2 + i\varepsilon]} \\
&\quad \left. \times \left[g^{\mu\lambda} (2q_f - q_i + k)^\kappa + g^{\lambda\kappa} (-2k - q_i - q_f)^\mu + g^{\kappa\mu} (2q_i - q_f + k)^\lambda \right] \right\}. \tag{5.12}
\end{aligned}$$

Adding up the four diagrams and using the same methodology as in the Dirac case, we arrive at

$$\begin{aligned}
\mu_{fi}^M &= \frac{3eG_F}{32\sqrt{2}\pi^2} (m_f + m_i) \sum_{\alpha=e,\mu,\tau} f(a_\alpha) (U_{\alpha f}^* U_{\alpha i} - U_{\alpha i}^* U_{\alpha f}), \\
&= \frac{3ieG_F}{16\sqrt{2}\pi^2} (m_f + m_i) \sum_{\alpha=e,\mu,\tau} f(a_\alpha) \text{Im} (U_{\alpha f}^* U_{\alpha i}). \tag{5.13}
\end{aligned}$$

The Majorana magnetic moment matrix is antisymmetric and imaginary. The expression is larger than the Dirac case, Eq. (5.5), by a factor of 2, but these are not directly comparable due to the PMNS matrix being different [13].

A simpler way to obtain the magnetic moment of Majorana neutrinos is to use the method described in Section 4.2. Using Eq. (4.37), we easily obtain Eq. (5.13) from the Dirac magnetic moment in Eq. (5.5). This illustrates how the magnetic moments of Majorana neutrinos can be calculated with only half the contributing diagrams explicitly evaluated.

As we learned in Section 2.4, massive neutrinos are Majorana particles if a singlet field with a Majorana mass terms is present in the model. Thus, in common models explaining the mass of neutrinos, such as the see-saw mechanism, the relevant formula for the neutrino magnetic moment is Eq. (5.13). The mixing matrix U appearing in Eq. (5.13) assumes three flavors, but in the see-saw mechanism, more singlet neutrinos are present. However, the heavy states are kinematically unreachable by the light states which primarily consist of the three flavors e, μ, τ . Consequently, the phenomenologically interesting transition magnetic moments are between the three light states. The formulas for the neutrino magnetic moment of both Dirac and Majorana neutrinos can be modified to include a general number of singlet neutrinos, see Ref. [13].

A potential scenario is that new physics at a high energy scale produces the mass term

$$\mathcal{L}_{\text{Mass}} = \frac{1}{2} \sum_{\alpha, \beta=e, \mu, \tau} M_{\alpha\beta}^L \overline{\nu_{\alpha L}^c} \nu_{\beta L} + H.c., \quad (5.14)$$

where M^L is a matrix of Majorana masses for the active neutrinos ν_L . As mentioned in Section 2.4, such a mass term is not invariant under $SU(2)_L \times U(1)_Y$, and is therefore forbidden in the Standard Model. The new physics could be for instance the introduction of a Higgs triplet [41] or spontaneous symmetry breaking in a left-right symmetric model [42]. With the mass term Eq. (5.14) the active neutrinos are Majorana particles, and Eq. (5.13) applies. However, the introduction of new particles in the high energy model may give additional contributions to the neutrino magnetic moments, which are not included in the result in Eq. (5.13).

Chapter 6

Fine-Tuning and the Voloshin Mechanism

As we have seen in the calculation of the neutrino magnetic moment in the Standard Model in Chapter 5, the magnetic moment is suppressed due to its proportionality to the small neutrino mass. We shall now see that even in a model which avoids this direct proportionality, a large neutrino magnetic moment requires a large amount of fine-tuning to avoid neutrino masses incompatible with experiment. A solution to this issue due to Voloshin [43], where a new $SU(2)_\nu$ symmetry is introduced, will then be discussed.

6.1 Neutrino Magnetic Moment and Mass

Voloshin considers a theory with a new charged scalar η which couples to neutrinos and the tau lepton. The relevant part of the Lagrangian is [43]

$$\mathcal{L} = f(\chi_\tau \chi_{\nu_e})\eta - f'(\chi_\tau^c \chi_{\nu_e}^c)\eta^* + H.c. , \quad (6.1)$$

where $(\chi_1 \chi_2) = \epsilon_{ab} \chi_1^a \chi_2^b$, ϵ is the antisymmetric symbol, and $a, b = (1, 2)$. Eq. (6.1) is written in two-spinor notation. In four-spinor notation, the same Lagrangian is

$$\mathcal{L} = f \ell_{\tau L}^T \nu_L \eta + f' \overline{\ell_{\tau R}} \overline{N_R^T} \eta^* + H.c. . \quad (6.2)$$

The translation of Eq. (6.1) into the 4-spinor notation is shown in Appendix C. This Lagrangian gives rise to 1-loop diagrams like

$$\text{Diagram 1} + \text{Diagram 2} . \quad (6.3)$$

These diagrams contribute to the neutrino magnetic moment, yielding [43]

$$\mu_\nu = \frac{ef f'}{16\pi^2} \frac{m_\tau}{m_\eta^2} F(m_\tau^2/m_\eta^2), \quad (6.4)$$

where $F(x) = -(1-x)^{-2} \log x - (1-x)^{-1}$. Depending on couplings f , f' and the mass of the scalar m_η , the neutrino magnetic moment can be made large. Note that μ_ν is proportional to m_τ , not m_ν as in the Standard Model. This is because the Lagrangian Eq. (6.2) includes couplings for right-chiral neutrinos, so the chirality flip occurs on the tau lepton line inside the loop. We now see the motivation for the coupling to the tau; It is the heaviest charged lepton.

Since the magnetic moment operator is chirality flipping, removing the photons from the above diagrams gives a diagram which contributes to the neutrino Dirac mass,



$$\text{Diagram (6.5)} \quad (6.5)$$

This diagram leads to the renormalization group equation [43]

$$\frac{dm_\nu(p^2)}{d \log p^2} = \frac{f f'}{16\pi^2} m_\tau, \quad \text{for } p^2 \gg m_\eta^2. \quad (6.6)$$

Combining Eqs. (6.4) and (6.6) gives

$$\frac{dm_\nu(p^2)}{d \log p^2} = \frac{\mu_\nu}{e} \frac{m_\eta^2}{F(m_\tau^2/m_\eta^2)}. \quad (6.7)$$

If we want a large neutrino magnetic moment on the order of $10^{-11} \mu_B$, then

$$\mu_\nu \sim 10^{-11} \mu_B = 10^{-11} \frac{e}{2m_e} \implies \frac{\mu_\nu}{e} \sim 10^{-16} \text{ eV}^{-1}. \quad (6.8)$$

Moreover, η must have a mass $m_\eta \gg m_\tau$ to not be excluded by experimental data. Then, we can use the approximation

$$\begin{aligned} F(x) &\approx -\log x - 1 = \log \frac{1}{x} - 1 \\ \implies F(m_\tau^2/m_\eta^2) &\approx \log(m_\eta^2/m_\tau^2) - 1 \sim \log(10000) - 1 \sim 10. \end{aligned} \quad (6.9)$$

Substituting these numbers back into Eq. (6.7) we obtain

$$\frac{dm_\nu(p^2)}{d \log p^2} \sim \frac{10^{-16} \text{ eV}^{-1} \times 10^{22} \text{ eV}^2}{10} = 10^5 \text{ eV}. \quad (6.10)$$

Integrating from a low energy scale p , where the Standard Model is an effective theory and the neutrino mass is experimentally constrained, to the scale of the UV-complete theory Λ , we

obtain

$$\begin{aligned}
m_\nu(\Lambda^2) - m_\nu(p^2) &= 10^5 \text{ eV} \left(\log \frac{\Lambda^2}{p^2} \right) \\
\implies m_\nu(p^2) &= m_\nu(\Lambda^2) - 10^5 \text{ eV} \left(\log \frac{\Lambda^2}{p^2} \right)
\end{aligned}
\tag{6.11}$$

Therefore $m_\nu(\Lambda^2)$ must be tuned with an accuracy of $10^{-5} \text{ eV} / \log \frac{\Lambda^2}{p^2}$ in order to avoid a neutrino mass of order 10^5 eV . Tuning in this context means that a small change in a parameter leads to unacceptable predictions.

Below the scale of electroweak symmetry breaking, where the fermions are massive and magnetic moments are non-zero, one can make a naïve, model independent argument to illustrate the tuning issue [44]. Introducing new physics to enhance the neutrino magnetic moment means invoking new interactions yielding loop diagrams like Fig. 6.1a. Then, one inevitably obtains diagrams like Fig. 6.1b by just removing the photon line, which make loop contributions to the Dirac mass of the neutrino. By dimensional analysis we write

$$\begin{aligned}
\mu_\nu &\sim \frac{eG}{\Lambda} \\
\delta m_\nu &\sim G\Lambda,
\end{aligned}
\tag{6.12}$$

where e appears because of the coupling to the photon, G is a dimensionless combination of couplings and loop factors coming from new physics, and Λ is the energy scale of the new physics. Thus, we can relate the magnetic moment and the mass contribution by

$$\mu_\nu \sim \frac{e\delta m_\nu}{\Lambda^2} = \frac{2m_e\delta m_\nu}{\Lambda^2} \mu_B.
\tag{6.13}$$

Assuming new physics not far below the electroweak scale, we obtain

$$\frac{\mu_\nu}{\mu_B} \sim 10^{-16} \frac{\delta m_\nu}{\text{eV}},
\tag{6.14}$$

giving $\delta m_\nu \gtrsim 10^5 \text{ eV}$ in order to obtain a neutrino magnetic moment on the order of $10^{-11} \mu_B$. This mass contribution must be tuned against for the neutrino masses to be compatible with data. If neutrino masses are generated only by a Yukawa coupling to the Higgs field, the coupling must be tuned to

$$y^\nu \sim 10^{-12} - 10^{-6},
\tag{6.15}$$

where the negative term is needed to cancel δm_ν , and the small positive term gives the correct order of magnitude for the neutrino mass, $m_\nu \sim 10^{-1} \text{ eV}$.

6.2 The Role of Majorana Mass Terms

The above argument shows that the mass of neutrinos becomes large if one naively introduces a large neutrino magnetic moment. However, if the right-chiral singlet neutrinos have a Majorana mass term, a small active neutrino mass is generated easily via the see-saw mechanism, as described in Section 2.5. In that case, the active neutrino mass is $m_\nu = m_D^2/m_N$, where m_N

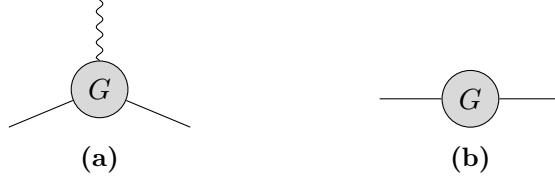


Figure 6.1: a) Generic diagrams contributing to the neutrino magnetic moment. b) Diagrams which appear in theories where the diagrams in (a) are allowed. These diagrams contribute to the neutrino mass. G is a combination of coupling constants and loop factors.

is the mass of the right-chiral singlet neutrino and m_D is the Dirac mass appearing in the operator $m_D \bar{\nu} N$. The observed range of active neutrino masses can be accommodated even if $m_D \sim v = 246 \text{ GeV}$, by letting the unconstrained parameter m_N be large. In that case, $m_N \gtrsim 10 \text{ TeV}$ in order for the relation $m_D/m_N \ll 1$ to hold, and m_N could be taken up to the GUT scale of 10^{16} GeV . With a non-zero Majorana mass for the right-chiral singlet neutrino and the Dirac mass correction associated with $\mu_\nu \sim 10^{11} \mu_B$, the Yukawa coupling is estimated to

$$y^\nu \sim 10^{-12} \sqrt{\frac{m_N}{\text{eV}}} \sim 10^{-6}. \quad (6.16)$$

If m_N is at the conventional see-saw scale of 10^{14} GeV , the tuning issue disappears, since the correction is then many orders of magnitude smaller than the tree-level value. Thus, the see-saw mechanism can alleviate the fine-tuning issue in addition to the smallness issue for the Yukawa coupling.

However, the see-saw scale is far above the range of current experiments sensitive to the process $\nu\gamma \rightarrow N$ in which the neutrino magnetic moment could contribute [32]. When insisting on singlet neutrino masses in the experimentally available range of $m_N \lesssim \text{MeV}$, the see-saw mechanism breaks down, since the assumption $m_D \ll m_N$ does not hold when m_D receives a large loop contribution. Thus, for neutrino magnetic moments that are phenomenologically interesting, the tuning issue must be addressed in some other way.

6.3 Voloshin's Solution to the Tuning Issue

To solve the fine-tuning issue, Voloshin introduces an $\text{SU}(2)_\nu$ symmetry under which ν_L and N_R^c transform as a doublet [43]. We will now see that under such a symmetry, a Dirac mass term is forbidden, while a magnetic moment term is allowed.

Let $\mathcal{N} = (\nu_L, N_R^c)^T$ be the $\text{SU}(2)_\nu$ doublet, and τ^i be the generators of the group, i.e. the

Pauli matrices¹. We can then rewrite the Dirac mass term as [13]

$$\begin{aligned}
\overline{N_R\nu_L} &= \frac{1}{2} \left(\overline{N_R\nu_L} \right)^T + \frac{1}{2} \overline{N_R} C C^\dagger \nu_L \\
&= -\frac{1}{2} \nu_L^T \overline{N_R}^T - \frac{1}{2} \overline{N_R} C^T C^\dagger \nu_L \\
&= -\frac{1}{2} \nu_L^T C^\dagger C \overline{N_R}^T - \frac{1}{2} \left(C \overline{N_R}^T \right)^T C^\dagger \nu_L \\
&= -\frac{1}{2} \nu_L^T C^\dagger N_R^c - \frac{1}{2} N_R^{cT} C^\dagger \nu_L \\
&= -\frac{1}{2} \begin{pmatrix} \nu_L^T & N_R^{cT} \end{pmatrix} C^\dagger \begin{pmatrix} N_R^c \\ \nu_L \end{pmatrix} \\
&= -\frac{1}{2} \mathcal{N}^T C^\dagger \tau^1 \mathcal{N},
\end{aligned} \tag{6.17}$$

where we used $\mathcal{L} = \mathcal{L}^T$, the anticommutation of spinors, and $C^T = -C$. Meanwhile, the magnetic moment operator can be written as

$$\begin{aligned}
\overline{N_R}\sigma_{\mu\nu}\nu_L &= \frac{1}{2} \left(\overline{N_R}\sigma_{\mu\nu}\nu_L \right)^T - \frac{1}{2} \overline{N_R} C^T C^\dagger \sigma_{\mu\nu}\nu_L \\
&= -\frac{1}{2} \nu_L^T \sigma_{\mu\nu}^T \overline{N_R}^T - \frac{1}{2} \left(C \overline{N_R}^T \right)^T C^\dagger \sigma_{\mu\nu}\nu_L \\
&= \frac{1}{2} \nu_L^T C^\dagger \sigma_{\mu\nu} C \overline{N_R}^T - \frac{1}{2} N_R^{cT} C^\dagger \sigma_{\mu\nu}\nu_L \\
&= \frac{1}{2} \nu_L^T C^\dagger \sigma_{\mu\nu} N_R^c - \frac{1}{2} N_R^{cT} C^\dagger \sigma_{\mu\nu}\nu_L \\
&= \frac{1}{2} \begin{pmatrix} \nu_L^T & N_R^{cT} \end{pmatrix} C^\dagger \sigma_{\mu\nu} \begin{pmatrix} N_R^c \\ -\nu_L \end{pmatrix} \\
&= \frac{1}{2} \mathcal{N}^T C^\dagger \sigma_{\mu\nu} i\tau^2 \mathcal{N},
\end{aligned} \tag{6.18}$$

where the property $C^\dagger \sigma_{\mu\nu} C = -\sigma_{\mu\nu}^T$ of the charge conjugation matrix was used. Let us now see how these quantities transform under an infinitesimal $SU(2)_\nu$ transformation. The doublet and its transpose transform according to

$$\begin{aligned}
\mathcal{N} &\rightarrow e^{i\lambda^i \tau^i} \mathcal{N} = \mathcal{N} + i\lambda^i \tau^i \mathcal{N} = \mathcal{N} + \left(i\lambda^1 \tau^1 + i\lambda^2 \tau^2 + i\lambda^3 \tau^3 \right) \mathcal{N} \\
\mathcal{N}^T &\rightarrow \mathcal{N}^T e^{i\lambda^i \tau^{iT}} = \mathcal{N}^T + \mathcal{N}^T i\lambda^i \tau^{iT} = \mathcal{N}^T + \mathcal{N}^T \left(i\lambda^1 \tau^1 - i\lambda^2 \tau^2 + i\lambda^3 \tau^3 \right).
\end{aligned} \tag{6.19}$$

Making use of the anticommutation relation $\{\tau^i, \tau^j\} = 2\delta^{ij} \mathbb{1}$, the $SU(2)_\nu$ content of the Dirac mass term transforms as

$$\begin{aligned}
\mathcal{N}^T \tau^1 \mathcal{N} &\rightarrow \left[\mathcal{N}^T + \mathcal{N}^T \left(i\lambda^1 \tau^1 - i\lambda^2 \tau^2 + i\lambda^3 \tau^3 \right) \right] \tau^1 \left[\mathcal{N} + \left(i\lambda^1 \tau^1 + i\lambda^2 \tau^2 + i\lambda^3 \tau^3 \right) \mathcal{N} \right] \\
&= \mathcal{N}^T \tau^1 \left[1 + \left(i\lambda^1 \tau^1 + i\lambda^2 \tau^2 - i\lambda^3 \tau^3 \right) \right] \left[1 + \left(i\lambda^1 \tau^1 + i\lambda^2 \tau^2 + i\lambda^3 \tau^3 \right) \right] \mathcal{N} \\
&= \mathcal{N}^T \tau^1 \mathcal{N} + \mathcal{N}^T \tau^1 \left(2i\lambda^1 \tau^1 + 2i\lambda^2 \tau^2 \right) \mathcal{N} + \mathcal{O}(\lambda^2),
\end{aligned} \tag{6.20}$$

¹The generators of $SU(2)_\nu$ are named τ^i to differentiate them from the Pauli matrices acting in spinor space.

while the magnetic moment term transforms as

$$\begin{aligned}
\mathcal{N}^T \tau^2 \mathcal{N} &\rightarrow \left[\mathcal{N}^T + \mathcal{N}^T \left(i\lambda^1 \tau^1 - i\lambda^2 \tau^2 + i\lambda^3 \tau^3 \right) \right] \tau^2 \left[\mathcal{N} + \left(i\lambda^1 \tau^1 + i\lambda^2 \tau^2 + i\lambda^3 \tau^3 \right) \mathcal{N} \right] \\
&= \mathcal{N}^T \tau^2 \left[1 - \left(i\lambda^1 \tau^1 + i\lambda^2 \tau^2 + i\lambda^3 \tau^3 \right) \right] \left[1 + \left(i\lambda^1 \tau^1 + i\lambda^2 \tau^2 + i\lambda^3 \tau^3 \right) \right] \mathcal{N} \\
&= \mathcal{N}^T \tau^2 \mathcal{N} + \mathcal{O}(\lambda^2).
\end{aligned} \tag{6.21}$$

Thus, the magnetic moment term is invariant under $SU(2)_\nu$, while the Dirac mass term is not. In the following chapter, we shall see how the $SU(2)_\nu$ symmetry can be implemented in practice in a model with scalar leptoquarks.

Chapter 7

Scalar Leptoquark Model

As we discussed in Chapter 4, the XENON1T experiment reported an excess in electron recoil events that can be interpreted as a signal of a large neutrino magnetic moment. In Ref. [32], it was found that the excess can be accommodated by a transition magnetic moment on the order of $10^{-11}\mu_B$ from ν_μ to a heavier sterile state N_R . In the same paper, a model with a scalar leptoquark was proposed to explain this magnetic moment, while avoiding a large active neutrino mass. In this chapter, we investigate said model.

7.1 The Model

To enhance the neutrino magnetic moment, a new charged particle must be introduced to run in the loop. In Voloshin's model, this was the charged scalar η . If the new particle is a boson, we require a charged fermion to close the loop. One possibility is that the new particle is a leptoquark, which as the name suggests, couples quarks to leptons. Then, the fermion running in the loop is a Standard Model quark. By writing all couplings between quarks and leptons allowed by gauge invariance, one can obtain the possible leptoquark states. These are six scalar and six vector fields with varying couplings to the Standard Model fermions and right-chiral neutrinos. The interested reader is referred to Ref. [45] for a comprehensive review.

In the model proposed in Ref. [32], a scalar leptoquark S_1 coupled to the third generation of quarks is introduced. S_1 has quantum numbers $(\bar{\mathbf{3}}, \mathbf{1}, 1/3)$ under $SU(3)_c \times SU(2)_L \times U(1)_Y$, and contributes to the magnetic moment through diagrams like Fig. 7.1. The neutrino content of the model is one active flavor ν_L , and one sterile flavor N_R . Thus, we consider transition magnetic moments between these.

Since S_1 is an $SU(2)_L$ singlet, only the coupling to the $U(1)_Y$ gauge boson contributes to the electromagnetic interaction after spontaneous symmetry breaking. Ignoring $SU(3)_c$, the covariant derivative is

$$D^\mu S_1 = \left(\partial^\mu + \frac{1}{3} i g' B^\mu \right) S_1, \quad (7.1)$$

which leads to the interaction

$$(D^\mu S_1)^\dagger (D_\mu S_1) \supset \frac{1}{3} i g' B^\mu \left(S_1 \partial_\mu S_1^\dagger - S_1^\dagger \partial_\mu S_1 \right). \quad (7.2)$$

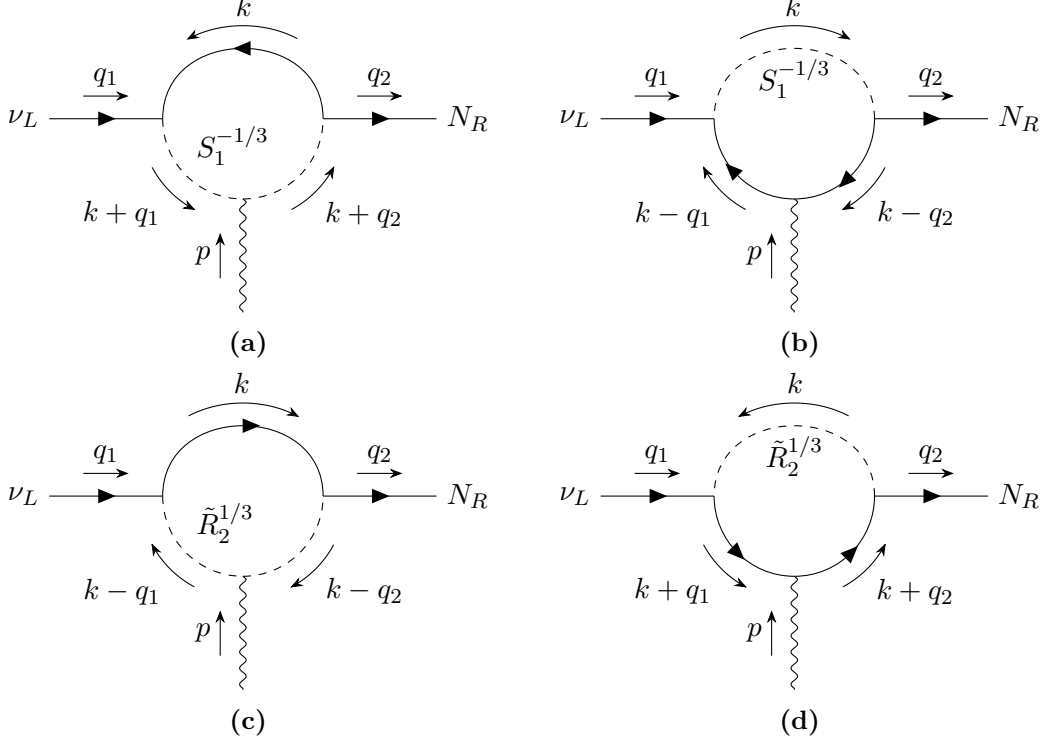


Figure 7.2: Diagrams contributing to the active-to-sterile transition neutrino magnetic moment in the scalar leptoquark model. a) Contributions from the singlet scalar leptoquark S_1 . b) Contributions from the doublet scalar leptoquark \tilde{R}_2 . The fermion line running in the loops is the bottom quark, on which a chirality flip occurs. The superscripts on the leptoquarks indicate electric charge.

ν_L . Eq. (7.6) is written in the quark mass basis; quark mixing in the third generation is small, so it has been ignored. From Eq. (7.6), vertex factors for the S_1 interactions with the Standard Model fermions are extracted. For the neutrino magnetic moment, we need the vertex factors for the interaction of S_1 with the active and sterile neutrinos. These are given in Section A.2.

7.2 Prediction for the Neutrino Magnetic Moment

Let us now calculate the transition magnetic moment $\mu_{N\nu}$. The relevant diagrams are shown in Fig. 7.2a and Fig. 7.2b, and yield the amplitudes

$$\mathcal{M}_a = \frac{1}{3} N_c y_1 y_2 e \int \frac{d^4 k}{(2\pi)^4} \frac{\bar{u}(q_f) P_L (\not{k} + m_b) P_L u(q_i) (q_i^\mu + q_f^\mu + 2k^\mu)}{[k^2 - m_b^2 + i\varepsilon] [(q_i + k)^2 - m_{LQ}^2 + i\varepsilon] [(q_f + k)^2 - m_{LQ}^2 + i\varepsilon]}, \quad (7.7)$$

$$\mathcal{M}_b = \frac{1}{3} N_c y_1 y_2 e \int \frac{d^4 k}{(2\pi)^4} \frac{\bar{u}(q_f) P_L (\not{k} - \not{q}_f + m_b) \gamma^\mu (\not{k} - \not{q}_i + m_b) P_L u(q_i)}{[(k - q_f)^2 - m_b^2 + i\varepsilon] [(k - q_i)^2 - m_b^2 + i\varepsilon] [k^2 - m_{LQ}^2 + i\varepsilon]}. \quad (7.8)$$

Note that since we consider only the transition $\nu_L \gamma \rightarrow N_R$ between chiral fermions, we have to use the formula $\mu_{N\nu} = 2iF_M(0)/(m_f + m_i)$ for the magnetic moment, as explained in Section 4.1.

From the total amplitude $\mathcal{M} = \mathcal{M}_a + \mathcal{M}_b$ we then obtain, to zeroth order in neutrino mass,

$$\begin{aligned}\mu_{N\nu} &= \frac{ey_1y_2m_b}{16\pi^2m_{LQ}^2} \left(-\frac{1}{a-1} + \frac{\log a}{(a-1)^2} \right) \\ &= \frac{y_1y_2m_b m_e}{8\pi^2m_{LQ}^2} \mu_B \left(-\frac{1}{a-1} + \frac{\log a}{(a-1)^2} \right)\end{aligned}\tag{7.9}$$

where $a = m_b^2/m_{LQ}^2$. The leptoquark mass is experimentally constrained to be at least $\mathcal{O}(\text{TeV})$ [10]. With $m_{LQ} = 1 \text{ TeV}$ and $y_1y_2 = 0.1$, we find

$$|\mu_{N\nu}| \approx 3 \times 10^{-11} \mu_B.\tag{7.10}$$

Eq. (7.9) disagrees with Ref. [32] by a factor of 2. The authors of Ref. [32] used formulae from Ref. [45] to calculate the magnetic moment [46]. Said formulae apply for the process $\ell \rightarrow \gamma\ell'$, where ℓ and ℓ' are charged leptons. Here, the external fermions are neutral, so the formulae must be modified. To cross-check the result, the magnetic moment was also calculated using the formulae in Ref. [47]. There, general formulae for the process $f_1 \rightarrow \gamma f_2$, where $f_{1,2}$ are fermions of a general charge Q_f , are given at one-loop order for a Yukawa interaction. Using $Q_f = -1$ reproduces the formula in Ref. [45]. Meanwhile, adapting the formulae to the neutrino case by letting $Q_f = 0$ results in a relative factor of 1/2 when taking the limit $a \rightarrow 0$, giving the magnetic moment in Eq. (7.9).

A sizable neutrino magnetic moment can thus be produced when introducing the scalar leptoquark S_1 . As expected, however, the neutrino mass must be fine-tuned in order to cancel the loop induced δm_D from the diagram in Fig. 7.3a, while simultaneously giving $m_\nu \sim 10^{-1} \text{ eV}$. To avoid this issue, the Voloshin mechanism is implemented by adding another leptoquark \tilde{R}_2 to the model, which transforms according to $(\mathbf{3}, \mathbf{2}, 1/6)$ under the Standard Model gauge group. This leptoquark is a $SU(2)_L$ doublet, $\tilde{R}_2 = (\tilde{R}_2^{2/3}, \tilde{R}_2^{-1/3})$, with superscripts denoting electric charge. Under the Voloshin symmetry $SU(2)_\nu$, (ν_L^c, N_R) and $(\tilde{R}_2^{-1/3}, S_1^\dagger)$ transform as doublets. The interaction Lagrangian of \tilde{R}_2 with the Standard Model fermions is

$$\begin{aligned}\mathcal{L} \supset & -y_1 \left(\tilde{R}_2^\dagger \bar{b}_R^c L_{\alpha L}^c \right) + y_2 \overline{Q_{3L}} N_R \tilde{R}_2 + H.c. \\ & = -y_1 \tilde{R}_2^{2/3 \dagger} \bar{b}_R^c \ell_L^c + y_1 \tilde{R}_2^{-1/3 \dagger} \bar{b}_R^c \nu_L^c + y_2 \bar{t}_L N_R \tilde{R}_2^{2/3} + y_2 \bar{b}_L N_R \tilde{R}_2^{-1/3} + H.c.,\end{aligned}\tag{7.11}$$

where in the second line the $SU(2)_L$ doublets were expanded. The vertex factors for the interactions of \tilde{R}_2 are given in Section A.2.

The additional diagrams contributing to the neutrino magnetic moment at one-loop order are shown in Fig. 7.2c and Fig. 7.2d, and give the amplitudes

$$\mathcal{M}_c = \frac{1}{3} N_c y_1 y_2 e \int \frac{d^4 k}{(2\pi)^4} \frac{\bar{u}(q_f) P_L (\not{k} + m_b) P_L u(q_i) (q_i^\mu + q_f^\mu - 2k^\mu)}{[k^2 - m_b^2 + i\varepsilon] [(k - q_i)^2 - m_{LQ}^2 + i\varepsilon] [(k - q_f)^2 - m_{LQ}^2 + i\varepsilon]},\tag{7.12}$$

$$\mathcal{M}_d = -\frac{1}{3} N_c y_1 y_2 e \int \frac{d^4 k}{(2\pi)^4} \frac{\bar{u}(q_f) P_L (\not{k} + \not{q}_f + m_b) \gamma^\mu (\not{k} + \not{q}_i + m_b) P_L u(q_i)}{[(k + q_f)^2 - m_b^2 + i\varepsilon] [(k + q_i)^2 - m_b^2 + i\varepsilon] [k^2 - m_{LQ}^2 + i\varepsilon]}.\tag{7.13}$$

Note that since S_1 and \tilde{R}_2 are in the same $SU(2)_\nu$ doublet, they have the same mass, which we

denote by m_{LQ} .

Adding \mathcal{M}_c and \mathcal{M}_d to the total amplitude \mathcal{M} before calculating the neutrino magnetic moment gives an extra factor of 2 in the result relative to Eq. (7.9). Meanwhile, the radiative mass correction has the additional diagram shown in Fig. 7.3. The diagrams give the amplitudes

$$\mathcal{M}_{a,b}^{\text{Mass}} = \mp N_c y_1 y_2 \int \frac{d^4 k}{(2\pi)^4} \frac{\bar{u}(q_f) P_L (\not{k} + m_b) P_L u(q_i)}{[(q_i \pm k)^2 - m_{LQ}^2 + i\varepsilon][k^2 - m_b^2 + i\varepsilon]}. \quad (7.14)$$

The relative sign is reversed in the case of the magnetic moment amplitudes, due to the opposite signs in the photon couplings. Thus, the mass diagrams cancel, while the magnetic moment diagrams do not.

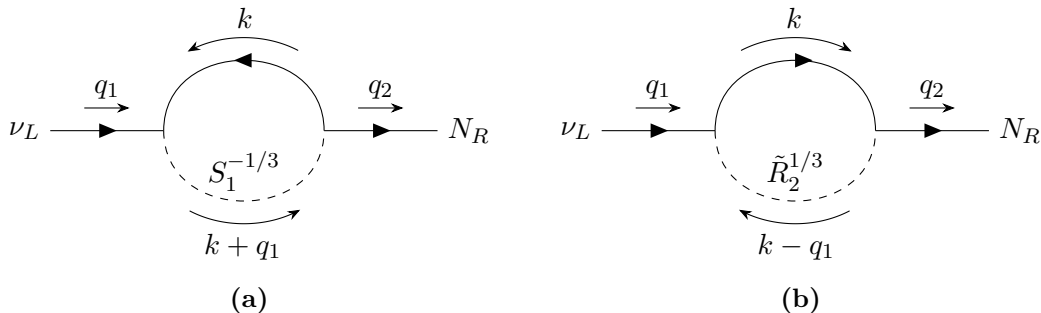


Figure 7.3: Diagrams contributing to the neutrino mass at one-loop order in the scalar leptoquark model. These diagrams are obtained from the ones in Fig. 7.2 by removing the external photon line. Since S_1^\dagger and $\tilde{R}_2^{-1/3}$ form a doublet under the new global $SU(2)_\nu$ symmetry, they have the same masses and Yukawa couplings to fermions, and the diagrams cancel.

The $SU(2)_\nu$ symmetry is not exact. As stated in Ref. [32], the symmetry is explicitly broken by the charged lepton Yukawa couplings, electroweak radiative corrections, and the Majorana mass term for N_R . However, the symmetry breaking from these sources is small, so excessive fine-tuning of the neutrino mass is still avoided.

In addition to the symmetry breaking sources already mentioned, the interaction Lagrangians Eq. (7.6) and Eq. (7.11) contain couplings to the top quark which break $SU(2)_\nu$, a source of symmetry breaking which was not pointed out in Ref. [32]. These terms are required by electroweak gauge invariance. The top quark couples to N_R , but not to ν_L , so contributions to the neutrino mass arise at two-loop level, as shown in Fig. 7.4. Note that there is a chirality flip on the internal bottom quark line in both diagrams. Thus, a rough estimate of the neutrino mass contribution from the first diagram in Fig. 7.4 is

$$\delta m_D \sim \frac{y_1 y_2^3 m_b}{(16\pi^2)^2} \sim 10^3 \text{ eV}, \quad (7.15)$$

using the chosen values for the couplings. This is still around three orders of magnitude below the estimated contribution in a model without the Voloshin mechanism. To obtain the estimate from the second diagram in Fig. 7.4, one must exchange $(y_1 y_2)$ for the $SU(2)_L$ gauge coupling g^2 , which does not change the conclusion. Thus, a Dirac mass is still present and must be dealt with to obtain acceptable active neutrino masses. In Section 7.4, we will explore how the desired neutrino mass spectrum can be achieved.

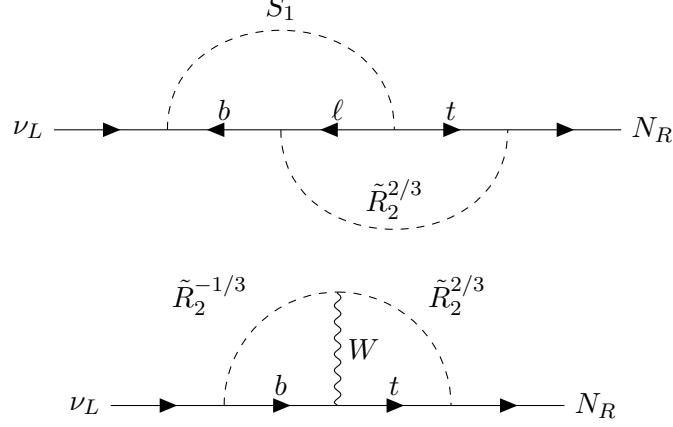


Figure 7.4: Contributions to the Dirac mass of the Neutrinos coming from the $SU(2)_\nu$ breaking top quark interaction terms in the scalar leptoquark model. Since these diagrams arise at two-loop order, the contributions to the neutrino mass are smaller than the one-loop diagram Fig. 7.3a which would contribute in the absence of the $SU(2)_\nu$ symmetry.

It should be noted that the scalar leptoquark model described here can explain B -meson anomalies as well as a large neutrino magnetic moment [32], making it more compelling. In Chapter 8, these flavor physics anomalies will be described in more detail as we propose a vector leptoquark model for a large neutrino magnetic moment which explain the B -meson anomalies as well.

7.3 More Neutrino Flavors

So far we have focused on a single active neutrino flavor, assumed to be the muon neutrino. A straightforward extension of the model is to include the other active flavors. Considering only the singlet S_1 for simplicity, the leptoquark-neutrino interaction term is modified to

$$\begin{aligned}
\mathcal{L} \supset & -y_2 \sum_{\alpha=e,\mu,\tau} \bar{b}_L^c \nu_{\alpha L} S_1^\dagger + H.c. \\
& = -y_2 \sum_{\alpha=e,\mu,\tau} \sum_{i=1}^4 U_{\alpha k} \bar{b}^c P_L \nu_k S_1^\dagger + H.c. ,
\end{aligned} \tag{7.16}$$

where in the second line, we switched to the mass basis. Since the model now contains four neutrino flavors — three active and one sterile — there are four mass eigenstates. The interaction in Eq. (7.16) permits magnetic moment transitions $\nu_i \gamma \rightarrow \nu_f$. The diagrams are the same as Fig. 7.2a and Fig. 7.2b, exchanging $\nu_L \rightarrow \nu_i$ and $N_R \rightarrow \nu_f$. The amplitudes are

$$\mathcal{M}_e = -\frac{1}{3} N_c y_2^2 e \int \frac{d^4 k}{(2\pi)^4} \frac{\bar{u}(q_f) P_R (\not{k} + m_b) P_L u(q_i) (q_i^\mu + q_f^\mu + 2k^\mu)}{[k^2 - m_b^2 + i\varepsilon] [(q_i + k)^2 - m_{LQ}^2 + i\varepsilon] [(q_f + k)^2 - m_{LQ}^2 + i\varepsilon]}, \tag{7.17}$$

$$\mathcal{M}_f = -\frac{1}{3} N_c y_2^2 e \int \frac{d^4 k}{(2\pi)^4} \frac{\bar{u}(q_f) P_R (\not{k} - \not{q}_f + m_b) \gamma^\mu (\not{k} - \not{q}_i + m_b) P_L u(q_i)}{[(k - q_f)^2 - m_b^2 + i\varepsilon] [(k - q_i)^2 - m_b^2 + i\varepsilon] [k^2 - m_{LQ}^2 + i\varepsilon]}, \tag{7.18}$$

which give, to first order in neutrino mass, the magnetic moment

$$\mu_{fi} = \frac{ey_2^2(m_f + m_i)}{128\pi^2 m_{LQ}^2} \left[-\frac{1}{1-a} + \frac{2}{(1-a)^2} + \frac{2a \log a}{(1-a)^3} \right] \sum_{\alpha, \beta=e, \mu, \tau} (U_{f\beta} U_{i\alpha}^* - U_{i\beta} U_{f\alpha}^*), \quad (7.19)$$

where we have assumed the massive neutrinos are of Majorana type due to the presence of the heavier N_R , and used Eq. (4.37) to obtain the magnetic moment from two of the four allowed diagrams. The magnetic moment is proportional to the neutrino mass, as in the Standard Model case. This is expected, since the leptoquark interaction Eq. (7.16) only contains the left-chiral part of the neutrino, and the chirality flip has to occur at an external line. Thus, a large neutrino magnetic moment between the light states is not possible in this model. However, we have an opportunity to investigate how the mass proportionality arises in the evaluation of the loop integrals.

Let us compare \mathcal{M}_a in Eq. (7.7) and \mathcal{M}_e in Eq. (7.17). Their spinor structures only differ by the leftmost chirality projector, which is P_L in \mathcal{M}_a and P_R in \mathcal{M}_e . The denominators are identical. As in the calculation of the anomalous magnetic moment of a charged lepton, we use Feynman parametrization to rewrite the denominator and shift the integration variable k^μ such that

$$\frac{1}{ABC} \rightarrow 2 \int_0^1 dx dy dz \delta(x+y+z-1) \frac{1}{(k^2 - \Delta)^3}, \quad (7.20)$$

where

$$\begin{aligned} A &= k^2 - m_b^2 + i\varepsilon, \\ B &= (q_i + k)^2 - m_{LQ}^2 + i\varepsilon, \\ C &= (q_f + k)^2 - m_{LQ}^2 + i\varepsilon, \\ \Delta &= xm_b^2 + y(y-1)m_i^2 + z(z-1)m_f^2 + (y+z)m_{LQ}^2 + 2yzq_i q_f, \end{aligned} \quad (7.21)$$

and k^μ was shifted by

$$k^\mu \rightarrow k^\mu - yq_i^\mu + zq_f^\mu. \quad (7.22)$$

We now turn to the numerators, considering first that of \mathcal{M}_e . Since γ_5 and γ^μ anticommute and $P_L P_R = 0$, the m_b term vanishes. Shifting k^μ according to Eq. (7.22) gives

$$\begin{aligned} \mathcal{M}_e &\propto \bar{u}(q_f) P_R \not{k} (q_i^\mu + q_f^\mu + 2k^\mu) u(q_i) \\ &\rightarrow \bar{u}(q_f) P_R \left(\not{k} - y\not{q}_i + z\not{q}_f \right) \left((1-2y)q_i^\mu + (1+2z)q_f^\mu + 2k^\mu \right) u(q_i). \end{aligned} \quad (7.23)$$

Now, distributing the chirality projector and utilizing the momentum space Dirac equation, we obtain

$$\mathcal{M}_e \propto \bar{u}(q_f) (P_R \not{k} - ym_i P_R + zm_f P_L) \left((1-2y)q_i^\mu + (1+2z)q_f^\mu + 2k^\mu \right) u(q_i), \quad (7.24)$$

and the proportionality to the neutrino masses becomes apparent. Meanwhile, in the numerator of \mathcal{M}_a only the m_b term survives. There is no \not{k} which brings $\not{q}_{i,f}$ upon shifting the integration variable, and thus the amplitude is proportional to m_b instead of the neutrino masses. Again, this is traced back to the fact that the interaction Lagrangian includes couplings to a right-chiral neutrino.

7.4 Neutrino Mass Scenarios

So far, we have assumed a neutrino sector containing the fields ν_L and N_R , and the Voloshin mechanism has been employed to avoid a large loop contribution to the neutrino mass. However, the specifics of the neutrino mass terms have not been discussed. The desired mass spectrum is one light state of the order 0.1 eV, and one heavier state of the order 100 keV. In the limit of exact $SU(2)_\nu$ symmetry the Dirac mass term is forbidden, but as we saw in Section 7.2 the symmetry is explicitly broken, giving $\delta m_D \sim \text{keV}$. Thus, we still need some tuning unless the correct mass scale is generated by some other mechanism. For example, the ordinary see-saw formula requires $m_N \sim 10 \text{ MeV}$ to generate the correct active mass without tuning, which is infeasible for explaining the excess in recoil event from $\lesssim \text{MeV}$ solar neutrinos. In this section we explore further options for generating the desired neutrino masses.

With the goal of more flexibility in neutrino mass generation, we add a chiral singlet fermion F_L to the model. Let us assume the following mass Lagrangian:

$$\mathcal{L}_{\text{mass}} = -m_D \bar{\nu}_L N_R - m_{NF} \bar{F}_L N_R - \frac{1}{2} m_F \bar{F}_L^c F_L + H.c., \quad (7.25)$$

in which the new fermion has a Majorana mass term while the other two fields only appear in Dirac mass terms. Defining the array of left-chiral fields

$$\Psi_L = \begin{pmatrix} \nu_L & N_R^c & F_L \end{pmatrix}^T, \quad (7.26)$$

the mass Lagrangian is written as

$$\mathcal{L}_{\text{mass}} = \frac{1}{2} \Psi_L^T C^\dagger \mathcal{M} \Psi_L, \quad (7.27)$$

where \mathcal{M} is the 3×3 mass matrix

$$\mathcal{M} = \begin{pmatrix} 0 & m_D & 0 \\ m_D & 0 & m_{NF} \\ 0 & m_{NF} & m_F \end{pmatrix}. \quad (7.28)$$

To diagonalize \mathcal{M} and obtain the mass eigenvalues, we use the technique shown in Ref. [48]. We define the matrices

$$M_a = \begin{pmatrix} m_D \\ 0 \end{pmatrix}, \quad M_b = \begin{pmatrix} 0 & m_{NF} \\ m_{NF} & m_F \end{pmatrix}, \quad (7.29)$$

so that the mass matrix can be written as

$$\mathcal{M} = \begin{pmatrix} 0 & M_a^T \\ M_a & M_b \end{pmatrix}. \quad (7.30)$$

Note that the structure of M_b and the block structure of \mathcal{M} are identical to the combined Dirac-Majorana mass matrix in Eq. (2.110), so the same formalism can be employed.

7.4.1 Double See-Saw

Let us now assume

$$m_D, m_{NF} \ll m_F, \quad m_D \ll \frac{m_{NF}^2}{m_F}. \quad (7.31)$$

The condition $m_{NF} \ll m_F$ gives see-saw eigenvalues for M_b . That is, the eigenvalues of M_b are approximately m_F and m_{NF}^2/m_F . By assumption, both of these are much larger than m_D . We can therefore use the results of the see-saw mechanism with $3+n$ neutrinos. Block-diagonalizing \mathcal{M} gives

$$\mathcal{W}^T \mathcal{M} \mathcal{W} \approx \begin{pmatrix} m_1 & 0 \\ 0 & M_2 \end{pmatrix}, \quad (7.32)$$

where m_1 and the eigenvalues of M_2 are the neutrino masses. Carrying over the results in Section 2.5, we have

$$\begin{aligned} m_1 &\approx -M_a^T M_b^{-1} M_a \\ &= - \begin{pmatrix} m_D & 0 \end{pmatrix} \begin{pmatrix} -\frac{m_F}{m_{NF}^2} & \frac{1}{m_{NF}} \\ \frac{1}{m_{NF}} & 0 \end{pmatrix} \begin{pmatrix} m_D \\ 0 \end{pmatrix} \\ &= \frac{m_D^2 m_F}{m_{NF}^2}. \end{aligned} \quad (7.33)$$

Thus we have the mass spectrum

$$\begin{aligned} m_1 &= \frac{m_D^2 m_F}{m_{NF}^2} & m_2 &= \frac{m_{NF}^2}{m_F} & m_3 &= m_F. \\ &= \frac{m_D^2}{m_2}, & &= \frac{m_{NF}^2}{m_3}, & & \end{aligned} \quad (7.34)$$

As two of the masses have a see-saw formula, this is called the double see-saw mechanism. The masses m_1 and m_2 are related by the exact same equation as in the conventional see-saw case, so no new parameter space is opened up. Invoking Occam's razor, this scenario is disfavored, since the introduction of F_L provides no benefit.

7.4.2 Inverse See-Saw

We now turn to the scenario

$$m_F \ll m_D \ll m_{NF}, \quad (7.35)$$

which is called the inverse see-saw. m_F is required to be small, but since lepton number is conserved in the limit $m_F \rightarrow 0$, this scenario is natural in the 't Hooft sense. In this context, a small valued parameter is natural if a symmetry is restored when the parameter goes to zero [49]. The mass matrix still has the structure of Eq. (7.28), and we define the same matrices M_a and M_b as in Eq. (7.29). The eigenvalues of M_b are

$$m_{2,3} = \frac{1}{2} \left(m_F \pm \sqrt{m_F^2 + 4m_{NF}^2} \right), \quad (7.36)$$

which give the two heavier masses. Expanding to first order in the small ratio m_F/m_{NF} and redefining the fields with unphysical phase shifts to make the masses positive, we have

$$m_{2,3} \approx m_{NF} \pm \frac{1}{2}m_F. \quad (7.37)$$

The masses are nearly degenerate. Note that the mass eigenvalues $m_{2,3}$ are much larger than m_D , by the assumption Eq. (7.35). Thus, we can proceed with diagonalization using the same method as for the double see-saw scenario, obtaining

$$m_1 = \frac{m_D^2 m_F}{m_{NF}^2}. \quad (7.38)$$

Our requirement for m_2 fixes $m_{NF} \sim 10^5$ eV. Then, to achieve $m_1 \sim 10^{-1}$ eV while satisfying Eq. (7.35), we take $m_D \sim 10^4$ eV and $m_F \sim 10$ eV. The correction $\delta m_D \sim 10^3$ eV is therefore not an issue. The Dirac mass is one order of magnitude below the electron mass. While this means the neutrino Yukawa coupling is small ($\mathcal{O}(10^{-7})$), it is still several orders of magnitude larger than it would be without invoking a see-saw mechanism.

In the limit $m_F \rightarrow 0$, the two heavier states combine to form a Dirac spinor, and the light state becomes massless. Defining the small ratio $R = m_D/m_{NF}$, the mixing matrix is approximated by

$$\mathcal{W} \approx \begin{pmatrix} -1 & \frac{R}{\sqrt{2}} & \frac{R}{\sqrt{2}} \\ 0 & -\frac{1}{\sqrt{2}} & \frac{1}{\sqrt{2}} \\ R & \frac{1}{\sqrt{2}} & \frac{1}{\sqrt{2}} \end{pmatrix}, \quad \mathcal{W}^T \mathcal{W} = \mathbb{1} + \mathcal{O}(R^2), \quad (7.39)$$

Parameterizing the mixing matrix in the standard way, we can extract the three Euler mixing angles. There is maximal mixing between the two sterile states, with $\tan \theta_{NF} = 1/\sqrt{2}$. The active-sterile mixing is $\tan \theta_{\nu S} = \pm R/\sqrt{2}$, with $S = F, N$. With the numbers assumed above, $|\tan \theta_{\nu S}| \sim 10^{-1}$. This is probably excluded by experimental limits, but further analysis is needed to draw a definite conclusion [50, 51]. Thus, we avoid tuning at the cost of large active-sterile mixing.

In conclusion, the correct neutrino mass spectrum can be obtained without fine-tuning in the scalar leptoquark model by invoking the global $SU(2)_\nu$ symmetry together with the inverse see-saw mechanism.

Chapter 8

Vector Leptoquark Model

8.1 The Model

For a model to generate neutrino magnetic moments at one-loop, it must contain couplings between the neutrinos and charged particles, which run in the loop and couple to the external photon. There are two generic possibilities: the loop contains a vector boson, or a scalar boson. We have now seen these cases in action; in the previous chapter, we looked at a model with a charged scalar, in the form of a leptoquark, coupling to the neutrinos. Meanwhile, in the Standard Model, the W bosons, which are charged vectors, run in the loop. In that case the neutrino magnetic moment is heavily suppressed by the neutrino mass. In this chapter, we explore the possibility of a new charged vector particle, in the form of a leptoquark, producing a large neutrino magnetic moment. We will also explore the possibility of simultaneously explaining flavor physics anomalies.

To generate a sizable neutrino magnetic moment, we need the vector leptoquark to couple both to left- and right-chiral neutrinos. There are two options [45]: The $SU(2)_L$ singlet $U_1^\mu \sim (\mathbf{3}, \mathbf{1}, 2/3)$, and the doublet $\tilde{V}_2^\mu \sim (\bar{\mathbf{3}}, \mathbf{2}, -1/6)$, where the brackets signify quantum numbers under the Standard Model gauge group. Here, we focus on the singlet U_1^μ , which has been studied in the context of B -meson anomalies and muon $g - 2$ [52–55]. With a single right-chiral neutrino N_R , U_1^μ couples to leptons and quarks through the Lagrangian

$$\mathcal{L} \supset U_1^\mu \left(x_L^{i\alpha} \overline{Q_{iL}} \gamma_\mu L_{\alpha L} + x_R^{i\alpha} \overline{d_{iR}} \gamma_\mu \ell_{\alpha R} + x_R^{iN} \overline{u_{iR}} \gamma_\mu N_R \right), \quad (8.1)$$

where Q_{iL} are the $SU(2)_L$ quark doublets, u_i are the up-type quarks (u, c, t), d_i are the down-type quarks (d, s, b), α is the lepton flavor index $\alpha \in \{e, \mu, \tau\}$, and $x_{L,R}^{i\alpha}$ are dimensionless couplings. Thus, every quark generation is coupled to every lepton flavor with varying coupling strengths. The couplings to first generation quarks and leptons are strongly constrained by atomic parity violation and μ - e conversion on nuclei [45]. Thus, we let $x_{L,R}^{1\alpha} = 0$ for all α , and $x_{L,R}^{ie} = 0$ for all i . Therefore, the model cannot produce neutrino magnetic moments involving the electron neutrino. However, we can obtain a transition magnetic moment $\mu_{N\nu_\mu}$, to explain the XENON1T excess as interpreted in Ref. [32].

Whereas the scalar leptoquarks in Eq. (7.6) and Eq. (7.11) couple the right-chiral neutrino to the down-type quarks, we see from Eq. (8.2) that the vector U_1^μ couples N_R to the up-type quarks.

Assuming the couplings are not separated by several orders of magnitude, the dominating contributions will be those with the top quark running in the loop, giving amplitudes enhanced by its large mass.

Eq. (8.2) is written in the weak basis, which coincides with the neutrino flavor basis. Expanding the $SU(2)_L$ doublets, and writing the quark fields in the flavor/mass basis, we receive factors of the unitary quark transformation matrices $V_{L,R}^{u,d}$. Multiplying by $V_L^d V_L^{d\dagger} = 1$ and absorbing the remaining transformation matrices into the coupling matrices, we can write

$$\mathcal{L} \supset U_1^\mu \left[V_{u_i d_j}^{\text{CKM}} x_L^{j\alpha} \overline{u_{iL}} \gamma_\mu \nu_{\alpha L} + x_L^{i\alpha} \overline{d_{iL}} \gamma_\mu \ell_{\alpha L} + x_R^{i\alpha} \overline{d_{iR}} \gamma_\mu \ell_{\alpha R} + x_R^{iN} \overline{u_{iR}} \gamma_\mu N_R \right]. \quad (8.2)$$

With the goal of obtaining the $\nu_\mu \rightarrow N_R$ transition magnetic moment, we keep the neutrinos in the flavor basis. Our coupling flavor structure then coincides with that of Ref. [55].

The kinetic terms of U_1^μ and its interactions with the Standard Model gauge bosons are governed by the Lagrangian [45]

$$\mathcal{L} \supset -\frac{1}{2} U_{1\mu\nu}^\dagger U_1^{\mu\nu} + m_{U_1}^2 U_{1\mu}^\dagger U_1^\mu + ig' \kappa_Y \frac{2}{3} U_{1\mu}^\dagger U_\nu B^{\mu\nu} + ig_s \kappa_s U_{1\mu}^\dagger \frac{\lambda^A}{2} U_\nu G_A^{\mu\nu}, \quad (8.3)$$

where m_{U_1} is the mass of the leptoquark, $U_1^{\mu\nu} = D^\mu U_1^\nu - D^\nu U_1^\mu$ is the leptoquark field strength tensor, and $D^\mu = \partial^\mu + ig' \frac{2}{3} B^\mu + ig_s \frac{\lambda^A}{2} G_A^\mu$ is the covariant derivative. B^μ and G_A^μ are the hypercharge gauge boson field and the gluon fields, respectively, with $B^{\mu\nu}$ and $G_A^{\mu\nu}$ the corresponding field strength tensors. κ_Y and κ_s are dimensionless parameters. Setting $\kappa_{Y,s} = 0$ gives a minimal coupling. We take $\kappa_{Y,s} = 1$, obtaining a Yang-Mills coupling analogous to the $WW\gamma$ coupling in the Standard Model. For completeness, the couplings between U_1^μ and the gluons were included in Eq. (8.3), but they are not relevant to our discussion.

After electroweak symmetry breaking, Eq. (8.3) contains the couplings between the leptoquark and the photon. To calculate the neutrino magnetic moment, we extract the terms with two leptoquarks and one photon, which are

$$\mathcal{L} \supset \frac{2}{3} ie \left[\left(\partial^\mu U_1^\nu - \partial^\nu U_1^\mu \right) A_\mu U_{1\nu}^\dagger - \left(\partial^\mu U_1^{\nu\dagger} - \partial^\nu U_1^{\mu\dagger} \right) A_\mu U_{1\nu} + \left(U_1^{\mu\dagger} U_1^\nu - U_1^{\nu\dagger} U_1^\mu \right) \partial_\mu A_\nu \right]. \quad (8.4)$$

8.2 Prediction for the Neutrino Magnetic Moment

In Eq. (8.2) and Eq. (8.4) we have all the necessary ingredients to calculate the transition magnetic moment $\mu_{N\nu_\alpha}$. The diagrams contributing at one-loop are similar to those in the Standard Model calculation of Chapter 5, but are shown in Fig. 8.1 for convenience.

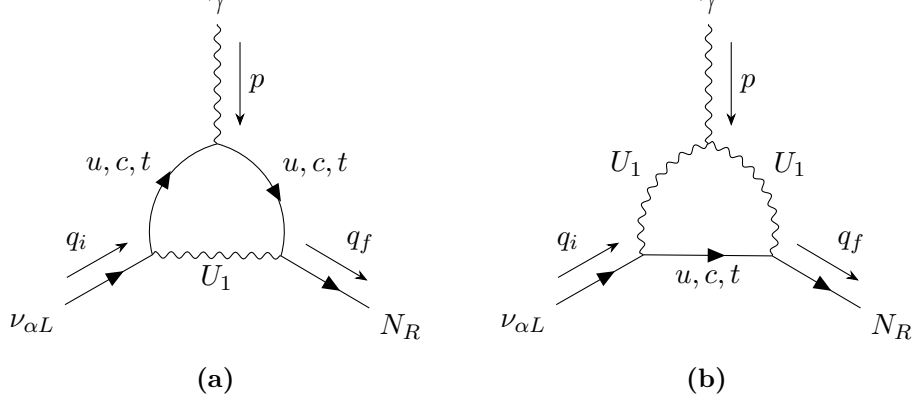


Figure 8.1: Diagrams involving the vector leptoquark U_1^μ contributing to the transition magnetic moment $\mu_{N\nu_\alpha}$. The interaction Lagrangian Eq. (8.2) allows any up-type quark to run in the loop. Since the internal quark line contains a chirality flip, the magnetic moment is proportional to the quark mass.

The amplitudes obtained from Fig. 8.1a and Fig. 8.1b respectively are

$$\mathcal{M}_a^\mu = \frac{2}{3}eN_c \sum_{i,j=1,2,3} V_{u_i d_j}^{\text{CKM}} x_L^{j\alpha} (x_R^{iN})^* \quad (8.5)$$

$$\begin{aligned} & \times \int \frac{d^4 k}{(2\pi)^4} \frac{\bar{u}(q_f) \gamma^\nu P_R (\not{k} + m_{u_i}) \gamma^\rho P_L u(q_i)}{[k^2 - m_{u_i}^2 + i\varepsilon] [(q_f - k)^2 - m_{U_1}^2 + i\varepsilon] [(q_i - k)^2 - m_{U_1}^2 + i\varepsilon]} \\ & \times \left(-g_{\nu\lambda} + \frac{(q_f - k)_\nu (q_f - k)_\lambda}{m_{U_1}^2} \right) \left(-g_{\rho\kappa} + \frac{(q_i - k)_\rho (q_i - k)_\kappa}{m_{U_1}^2} \right) \\ & \times [g^{\mu\kappa} (k + q_f - 2q_i)^\lambda + g^{\kappa\lambda} (q_i + q_f - 2k)^\mu + g^{\mu\lambda} (k + q_i - 2q_f)^\kappa], \end{aligned} \quad (8.6)$$

$$\begin{aligned} \mathcal{M}_b^\mu &= \frac{2}{3}eN_c \sum_{i,j=1,2,3} V_{u_i d_j}^{\text{CKM}} x_L^{j\alpha} (x_R^{iN})^* \\ & \times \int \frac{d^4 k}{(2\pi)^4} \frac{\bar{u}(q_f) \gamma^\nu P_R (\not{q}_f - \not{k} + m_{u_i}) \gamma^\mu (\not{q}_i - \not{k} + m_{u_i}) \gamma^\rho P_L u(q_i) (-g_{\nu\rho} + k_\nu k_\rho / m_{U_1}^2)}{[k^2 - m_{U_1}^2 + i\varepsilon] [(q_f - k)^2 - m_{u_i}^2 + i\varepsilon] [(q_i - k)^2 - m_{u_i}^2 + i\varepsilon]}, \end{aligned} \quad (8.7)$$

where m_{u_i} is the mass of the quark running in the loop. Extracting the magnetic moment using Eq. (4.30) yields

$$\begin{aligned} \mu_{N\nu_\alpha} &= \frac{eN_c}{24\pi^2 m_{U_1}} \sum_{i,j=1,2,3} V_{u_i d_j}^{\text{CKM}} x_L^{j\alpha} (x_R^{iN})^* \times a_{u_i} \left(1 - \frac{3}{a_{u_i}^2 - 1} + \frac{3a_{u_i}^2 \log a_{u_i}^2}{(a_{u_i}^2 - 1)^2} \right) \\ &\equiv \frac{eN_c}{24\pi^2 m_{U_1}} \sum_{i,j=1,2,3} V_{u_i d_j}^{\text{CKM}} x_L^{j\alpha} (x_R^{iN})^* f(a_{u_i}), \end{aligned} \quad (8.8)$$

where $a_{u_i} \equiv m_{u_i}/m_{U_1}$. This is the general transition magnetic moment for a neutrino of flavor α to the sterile neutrino, with contributions from all three up-type quarks. The result was cross-checked with the formulae in Ref. [47].

As already mentioned, we assume the couplings to the first generation of leptons are zero. Thus, $\mu_{N\nu_e} = 0$. Here we focus on $\mu_{N\nu_\mu}$. The three terms in Eq. (8.8) each receive a numerical factor from the loop function $f(a_{u_i})$, which depends on the mass of the vector leptoquark. With

certain model assumptions, the CMS collaboration has constrained the vector leptoquark mass to above 1530 GeV [56]. For numerical calculations, we here take $m_{U_1} = 2$ TeV. Then, the loop function takes the values

$$\begin{aligned} f(a_u) &\approx 4.6 \times 10^{-6}, \\ f(a_c) &\approx 2.5 \times 10^{-3}, \\ f(a_t) &\approx 0.34. \end{aligned} \tag{8.9}$$

Clearly, the contribution from the top quark dominates. This corresponds to the $i = 3$ term in Eq. (8.8), which gives

$$\mu_{N\nu_\mu} \approx \frac{N_c m_e \mu_B}{12\pi^2 m_{U_1}} \left(V_{ts}^{\text{CKM}} x_L^{2\mu} + V_{tb}^{\text{CKM}} x_L^{3\mu} \right) (x_R^{3N})^* f(a_t), \tag{8.10}$$

where the magnetic moment has been written in terms of the Bohr magneton μ_B . Using global fits for the CKM matrix elements [10] and choosing the couplings $x_L^{\mu 2} = -x_L^{\mu 3} = 0.05$, $x_R^{3N} = 0.5$, we obtain the numerical result

$$|\mu_{N\nu_\mu}| \approx 5.7 \times 10^{-11} \mu_B, \tag{8.11}$$

which means that the model can accommodate the desired value $\sim 10^{-11} \mu_B$ with small coupling constants.

The coupling to the third generation of quarks gives the largest contribution because of the magnitude of V_{tb}^{CKM} . Interestingly, setting $x_L^{\mu 3} = 0$ such that $\mu_{N\nu_\mu}$ is proportional to the off-diagonal CKM element V_{ts}^{CKM} , we still find $\mu_{N\nu_\mu} \approx 3.1 \times 10^{-11} \mu_B$ with $x_L^{\mu 2} = x_R^{3N} = 0.6$. Thus, the model can explain the XENON1T excess in a large region of parameter space. However, these coupling values are not suitable to explain flavor physics anomalies, as we shall see in the next section.

Doing a similar calculation with the charm quark running in the loop, corresponding to the $i = 2$ term in Eq. (8.8), gives a contribution of $1.6 \times 10^{-11} \mu_B$ even when all the relevant couplings are set to 1. If $x_R^{2N} \approx x_R^{3N}$, such that a large hierarchy does not weigh up for the difference between the top quark contribution and charm quark contribution to $\mu_{N\nu_\mu}$, we can neglect the latter.

8.3 Flavor Physics Anomalies

In the Standard Model, the gauge interactions act identically on the three generations of leptons. This accidental symmetry is called lepton flavor universality (LFU), and is only broken by the Yukawa interactions. That is, the only property differentiating the three generations is the mass of the particles. A violation of LFU would be a clear indication of new physics, thus motivating experimental searches for such phenomena. In particular, experimental data on decays of B mesons show deviations from the Standard Model predictions, which may be signs of new physics.

The vector leptoquark U_1^μ can be used to explain such LFU violations. The authors of Ref. [55] propose the coupling structure

$$x_L^{2\mu}, x_L^{3\mu}, x_R^{3\tau}, x_R^{2N} \neq 0, \tag{8.12}$$

which we shall now explore in the context of observed flavor anomalies.

The $R(D^{(*)})$ Anomaly

In the Belle [57–60], BaBar [61, 62], and LHCb [63–65] collaborations, LFU has been tested in the charged current transition $b \rightarrow c\ell\nu$, the observables being the ratio of branching fractions

$$R(D^{(*)}) = \frac{\text{Br}(B \rightarrow D^{(*)}\tau\bar{\nu}_\tau)}{\text{Br}(B \rightarrow D^{(*)}\ell_\alpha\bar{\nu}_\alpha)}, \quad (8.13)$$

where $\alpha = e, \mu$, and B and $D^{(*)}$ are non-strange beauty mesons and charmed mesons, respectively, the asterisk referring to an excited state. The world averages of measurements, and the corresponding Standard Model predictions are [66] (Spring 2021 update [67])

$$\begin{aligned} R(D)_{\text{exp}} &= 0.339 \pm 0.030, & R(D^*)_{\text{exp}} &= 0.295 \pm 0.014, \\ R(D)_{\text{SM}} &= 0.299 \pm 0.003, & R(D^*)_{\text{SM}} &= 0.252 \pm 0.005, \end{aligned} \quad (8.14)$$

The measurements exceed the Standard Model prediction at a combined significance of 3.4σ .

Introducing the U_1 leptoquark with the interactions in Eq. (8.2), the $b \rightarrow c\ell\nu$ transition receives the extra contribution from $b \rightarrow c\tau N_R$ shown in Fig. 8.2. With the goal of comparing the model predictions to the experimental values, we now calculate the quantity

$$\frac{R(D^{(*)})_{\text{exp}}}{R(D^{(*)})_{\text{SM}}} - 1 = \frac{\text{Br}(B \rightarrow D^{(*)}\tau\bar{\nu})_{\text{total}}}{\text{Br}(B \rightarrow D^{(*)}\tau\bar{\nu})_{\text{SM}}} - 1. \quad (8.15)$$

The branching ratio is defined as $\text{Br}(A \rightarrow B) = \Gamma_{A \rightarrow B} / \sum \Gamma$, where $\Gamma_{A \rightarrow B}$ is the decay rate of the process and $\sum \Gamma$ is the total decay rate. Thus, we can write

$$\frac{R(D^{(*)})_{\text{exp}}}{R(D^{(*)})_{\text{SM}}} - 1 = \frac{(\Gamma_{B \rightarrow D^{(*)}\tau\bar{\nu}_\tau} + \Gamma_{B \rightarrow D^{(*)}\tau\bar{N}_R}) / (\sum \Gamma_{\text{SM}} + \Gamma_{B \rightarrow D^{(*)}\tau\bar{N}_R})}{\Gamma_{B \rightarrow D^{(*)}\tau\bar{\nu}_\tau} / \sum \Gamma_{\text{SM}}} - 1. \quad (8.16)$$

Assuming the new physics gives a small contribution to the decay rate relative to the total Standard Model decay rate, this reduces to

$$\frac{R(D^{(*)})_{\text{exp}}}{R(D^{(*)})_{\text{SM}}} - 1 \approx \frac{\Gamma_{B \rightarrow D^{(*)}\tau\bar{N}_R}}{\Gamma_{B \rightarrow D^{(*)}\tau\bar{\nu}_\tau}}. \quad (8.17)$$

Since we are calculating a ratio of decay rates, complications due to the hadronic structure cancel out, and we can work at the quark level. Further, since the neutrino masses are many orders of magnitude smaller than the quark masses, the difference in phase space is negligible. Thus, the ratio only depends on the squared unpolarized amplitudes,

$$\frac{R(D^{(*)})_{\text{exp}}}{R(D^{(*)})_{\text{SM}}} - 1 \approx \frac{|\mathcal{M}_{b \rightarrow c\tau\bar{N}_R}|_{\text{unpol.}}^2}{|\mathcal{M}_{b \rightarrow c\tau\bar{\nu}_\tau}|_{\text{unpol.}}^2}. \quad (8.18)$$

Using the Feynman rules of the Standard Electroweak theory and the vector leptoquark model shown in Appendix A, one can straightforwardly write the amplitudes for the processes

$$b(p_1, s_1) \rightarrow c(p_2, s_2) + \tau(p_3, s_3) + \bar{\nu}(p_4, s_4), \quad (8.19)$$

where the quantities in the brackets are the momenta and spins of the external particles, and ν

denotes either ν_τ or N_R . We obtain

$$\begin{aligned}\mathcal{M}_{b \rightarrow c\tau\bar{\nu}_\tau} &= -i\frac{g^2}{2}V_{cb}^{\text{CKM}} [\bar{u}_{s_3}(p_3)\gamma_\mu P_L v_{s_4}(p_4)] \frac{-g^{\mu\nu} + q^\mu q^\nu/m_W^2}{q^2 - m_W^2} [\bar{u}_{s_2}(p_2)\gamma_\nu P_L u_{s_1}(p_1)] \\ &\approx -i\frac{g^2}{2m_W^2}V_{cb}^{\text{CKM}} [\bar{u}_{s_3}(p_3)\gamma^\mu P_L v_{s_4}(p_4)] [\bar{u}_{s_2}(p_2)\gamma_\mu P_L u_{s_1}(p_1)],\end{aligned}\quad (8.20)$$

$$\begin{aligned}\mathcal{M}_{b \rightarrow c\tau\bar{N}_R} &= -ix_R^{2N}(x_R^{3\tau})^* [\bar{u}_{s_3}(p_3)\gamma_\mu P_R v_{s_4}(p_4)] \frac{-g^{\mu\nu} + q^\mu q^\nu/m_{U_1}^2}{q^2 - m_{U_1}^2} [\bar{u}_{s_2}(p_2)\gamma_\nu P_R u_{s_1}(p_1)] \\ &\approx -i\frac{x_R^{2N}(x_R^{3\tau})^*}{m_{U_1}^2} [\bar{u}_{s_3}(p_3)\gamma^\mu P_R v_{s_4}(p_4)] [\bar{u}_{s_2}(p_2)\gamma_\mu P_R u_{s_1}(p_1)],\end{aligned}\quad (8.21)$$

where $q = p_2 - p_1 = p_3 + p_4$. The process has the characteristic energy scale $m_c, m_b \sim \mathcal{O}(1 \text{ GeV})$, so we have taken the limits $q^2/m_W^2 \rightarrow 0$ and $q^2/m_{U_1}^2 \rightarrow 0$. To find the squared amplitudes, we average over initial spin and sum over final spins,

$$|\mathcal{M}|_{\text{unpol.}}^2 = \frac{1}{2} \sum_{s_1, s_2, s_3, s_4} \mathcal{M}^* \mathcal{M}. \quad (8.22)$$

Using energy projection operators to eliminate spin sums as described in Eq. (B.12), the Standard Model process yields

$$|\mathcal{M}_{b \rightarrow c\tau\bar{\nu}_\tau}|_{\text{unpol.}}^2 = \frac{g^4}{8m_W^4} |V_{cb}^{\text{CKM}}|^2 A_{\mu\nu} B^{\mu\nu}, \quad (8.23)$$

where

$$\begin{aligned}A^{\mu\nu} &= \frac{1}{16m_\tau m_{\nu_\tau}} \text{tr} [(p_3' + m_\tau) \gamma^\mu (1 - \gamma_5) (p_4 - m_{\nu_\tau}) (1 + \gamma_5) \gamma^\nu] \\ &= \frac{1}{2m_\tau m_{\nu_\tau}} \left(p_3^\nu p_4^\mu + p_3^\mu p_4^\nu - p_3 p_4 g^{\mu\nu} - i\epsilon^{\mu\nu\lambda\rho} p_{3\lambda} p_{4\rho} \right),\end{aligned}\quad (8.24)$$

$$\begin{aligned}B^{\mu\nu} &= \frac{1}{16m_c m_b} \text{tr} [(p_2' + m_c) \gamma^\mu (1 - \gamma_5) (p_1 + m_b) (1 + \gamma_5) \gamma^\nu] \\ &= \frac{1}{2m_c m_b} \left(p_1^\nu p_2^\mu + p_1^\mu p_2^\nu - p_1 p_2 g^{\mu\nu} + i\epsilon^{\mu\nu\lambda\rho} p_{1\lambda} p_{2\rho} \right).\end{aligned}\quad (8.25)$$

The traces of products of gamma matrices were evaluated using the relations in Eq. (B.5). Contracting, we obtain

$$|\mathcal{M}_{b \rightarrow c\tau\bar{\nu}_\tau}|_{\text{unpol.}}^2 = \frac{g^4}{8m_W^4} |V_{cb}^{\text{CKM}}|^2 \frac{(p_1 p_3)(p_2 p_4)}{m_b m_c m_\tau m_{\nu_\tau}}. \quad (8.26)$$

Meanwhile, the leptoquark diagram gives

$$|\mathcal{M}_{b \rightarrow c\tau\bar{N}_R}|_{\text{unpol.}}^2 = \frac{|x_R^{2N} x_R^{3\tau}|^2}{2m_{U_1}^4} C_{\mu\nu} D^{\mu\nu}, \quad (8.27)$$

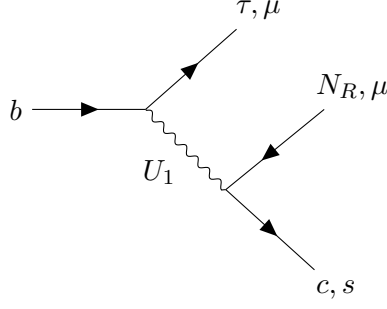


Figure 8.2: Tree-level diagrams contributing to the flavor observables $R(K^{(*)})$ and $R(D^{(*)})$ in the model with a vector leptoquark U_1^μ and a sterile neutrino N_R .

where

$$\begin{aligned} C^{\mu\nu} &= \frac{1}{16m_c m_{N_R}} \text{tr} [(\not{p}_2 + m_c) \gamma^\mu (1 + \gamma_5) (\not{p}_4 - m_{N_R}) (1 - \gamma_5) \gamma^\nu] \\ &= \frac{1}{2m_c m_{N_R}} \left(p_2^\nu p_4^\mu + p_2^\mu p_4^\nu - p_2 p_4 g^{\mu\nu} - i\epsilon^{\mu\nu\lambda\rho} p_{3\lambda} p_{4\rho} \right), \end{aligned} \quad (8.28)$$

$$\begin{aligned} D^{\mu\nu} &= \frac{1}{16m_b m_\tau} \text{tr} [(\not{p}_3 + m_\tau) \gamma^\mu (1 + \gamma_5) (\not{p}_1 + m_b) (1 - \gamma_5) \gamma^\nu] \\ &= \frac{1}{2m_b m_\tau} \left(p_1^\nu p_3^\mu + p_1^\mu p_3^\nu - p_1 p_3 g^{\mu\nu} - i\epsilon^{\mu\nu\lambda\rho} p_{1\lambda} p_{3\rho} \right), \end{aligned} \quad (8.29)$$

which gives the unpolarized squared amplitude

$$|\mathcal{M}_{b \rightarrow c\tau\bar{N}_R}|_{\text{unpol.}}^2 = \frac{|x_R^{2N} x_R^{3\tau}|^2}{2m_{U_1}^4} \frac{(p_1 p_3)(p_2 p_4)}{m_b m_c m_\tau m_{N_R}}. \quad (8.30)$$

Taking the limit $m_{\nu_\tau} = m_{N_R} \rightarrow 0$ and inserting Eq. (8.26) and Eq. (8.30) into Eq. (8.18), we arrive at

$$\frac{R(D^{(*)})_{\text{exp}}}{R(D^{(*)})_{\text{SM}}} - 1 = \frac{|x_R^{2N} x_R^{3\tau}|^2}{m_{U_1}^4} \frac{v^4}{4|V_{cb}^{\text{CKM}}|^2}, \quad (8.31)$$

where the relation $m_W = vg/2$ was used.

Since $R(D)$ and $R(D^*)$ are both given by Eq. (8.31), we use the average of the ratios $R(D)_{\text{exp}}/R(D)_{\text{SM}}$ and $R(D^*)_{\text{exp}}/R(D^*)_{\text{SM}}$, weighted by their uncertainties given in Eq. (8.14). Doing so gives the requirement

$$\frac{|x_R^{2N} x_R^{3\tau}|^2}{m_{U_1}^4} \frac{v^4}{4|V_{cb}^{\text{CKM}}|^2} = 0.159 \pm 0.065, \quad (8.32)$$

corresponding to

$$|x_R^{2N} x_R^{3\tau}|^2 = 4.57 \quad (8.33)$$

at the central value, which falls within the 1σ region for both $R(D)$ and $R(D^*)$.

The $R(K^{(*)})$ Anomaly

Another flavor observable is the ratio

$$R(K^{(*)}) = \frac{\text{Br}(B \rightarrow K^{(*)}\mu^+\mu^-)}{\text{Br}(B \rightarrow K^{(*)}e^+e^-)}, \quad (8.34)$$

where $K^{(*)}$ are the K -mesons possessing non-zero strangeness. The decays in Eq. (8.34) come from the neutral current transition $b \rightarrow s\ell^+\ell^-$. Since there are no tree-level flavor changing neutral currents in the Standard Model, the transition happens at the one-loop level. Because of the small mass of e and μ in comparison to the b quark mass, the Standard Model predicts these ratios to be close to unity [68]. Recently, the LHCb collaboration published the experimental value [69]

$$R(K)_{\text{exp}} = 0.846_{-0.041}^{+0.044}, \quad (8.35)$$

which is a 3.1σ deviation from the Standard Model. LHCb has also performed the most accurate measurement of $R(K^*)$ [70],

$$R(K^*)_{\text{exp}} = 0.69_{-0.09}^{+0.12}. \quad (8.36)$$

This value deviates from the Standard model at 2.4σ . Both the experimental values correspond to a dilepton invariant mass squared between 1.1 GeV^2 and 6.0 GeV^2 .

On the theoretical side, the $b \rightarrow s\ell^+\ell^-$ transitions can be treated in a model-independent way by using effective field theory. In this framework one constructs an effective Lagrangian by integrating out the heavy degrees of freedom and adding up the possible relevant operators of a given mass dimension. Such a Lagrangian encodes the low-energy behavior of the Standard Model and potential new physics (NP), and can be written accordingly as

$$\mathcal{L}_{\text{eff}} = \mathcal{L}_{\text{eff}}^{\text{SM}} + \mathcal{L}_{\text{eff}}^{\text{NP}}. \quad (8.37)$$

Relevant to $R(K^{(*)})$ are the dimension 6 operators containing b , s and two charged leptons ℓ . As will be explained shortly, the operators of interest here are

$$\mathcal{L}_{\text{eff}}^{\text{NP}} \supset \frac{4G_F}{\sqrt{2}} V_{tb}^{\text{CKM}} V_{ts}^{\text{CKM}*} \frac{\alpha}{4\pi} \left(C_9^{bs\mu\mu} O_9^{bs\mu\mu} + C_{10}^{bs\mu\mu} O_{10}^{bs\mu\mu} \right) + H.c., \quad (8.38)$$

where

$$O_9^{bs\mu\mu} = (\bar{s}\gamma_\mu P_L b) (\bar{\mu}\gamma^\mu \mu), \quad O_{10}^{bs\mu\mu} = (\bar{s}\gamma_\mu P_L b) (\bar{\mu}\gamma^\mu \gamma_5 \mu), \quad (8.39)$$

and $C_{9,10}$ are the so-called Wilson coefficients. The subscripts on the operators and coefficients come from the naming convention commonly adopted in the literature.

Having integrated out new heavy fields, the effect of new physics can be encoded in the Wilson coefficients, allowing a model-independent analysis. A recent such analysis, based on data on rare B decays, can be found in Ref. [71]. In a combined fit to rare B decay data, it was found that the scenario

$$C_9^{bs\mu\mu} = -C_{10}^{bs\mu\mu} = -0.39 \pm 0.07 \quad (8.40)$$

is preferred over the Standard Model.

To connect to the leptoquark model, consider the diagrams in Fig. 8.2. The amplitude corre-

sponding to the process $b \rightarrow s\mu^+\mu^-$ is

$$\mathcal{M}_{b \rightarrow s\mu^+\mu^-} = -ix_L^{2\mu}(x_L^{3\mu})^* [\bar{u}_s \gamma_\mu P_L v_\mu] \frac{-g^{\mu\nu} + p^\mu p^\nu / m_{U_1}^2}{p^2 - m_{U_1}^2} [\bar{u}_\mu \gamma_\nu P_L u_b], \quad (8.41)$$

where the subscripts on the spinors indicate the corresponding particle, and p^μ is the momentum of the intermediate U_1^μ . To match with the effective theory in Eq. (8.38), we take the limit $p^2/m_{U_1}^2 \rightarrow 0$, giving

$$\mathcal{M}_{b \rightarrow s\mu^+\mu^-} \approx -i \frac{x_L^{2\mu}(x_L^{3\mu})^*}{m_{U_1}^2} [\bar{u}_s \gamma^\mu P_L v_\mu] [\bar{u}_\mu \gamma_\mu P_L u_b]. \quad (8.42)$$

Using the appropriate Fierz identity [3, p. 66] to rearrange the spinors, and expanding the rightmost chirality projector, the approximate amplitude can be rewritten as

$$\begin{aligned} \mathcal{M}_{b \rightarrow s\mu^+\mu^-} \approx & -i \frac{x_L^{2\mu}(x_L^{3\mu})^*}{2m_{U_1}^2} [\bar{u}_s \gamma^\mu P_L u_b] [\bar{u}_\mu \gamma_\mu v_\mu] \\ & + i \frac{x_L^{2\mu}(x_L^{3\mu})^*}{2m_{U_1}^2} [\bar{u}_s \gamma^\mu P_L u_b] [\bar{u}_\mu \gamma_\nu \gamma_5 v_\mu]. \end{aligned} \quad (8.43)$$

As is evident from the operators in Eq. (8.39), this matches the effective description if

$$C_9^{bs\mu\mu} = -C_{10}^{bs\mu\mu} = -\frac{\pi v^2}{\alpha V_{tb}^{\text{CKM}} V_{ts}^{\text{CKM}*}} \frac{x_L^{2\mu}(x_L^{3\mu})^*}{m_{U_1}^2}, \quad (8.44)$$

where v is the Higgs vev, and we used the relation $G_F = (\sqrt{2}v^2)^{-1}$. Thus, with the same coupling structure needed to produce the transition magnetic moment in Eq. (8.10), the model also contributes to $R(K^{(*)})$. The relation $C_9^{bs\mu\mu} = -C_{10}^{bs\mu\mu}$ arises since the contributing term in the interaction Lagrangian Eq. (8.2) is a current of left-chiral muons. Note that the negative sign in Eq. (8.44) is cancelled by the sign of V_{ts}^{CKM} . Thus, assuming real couplings, we require $x_L^{3\mu}$ and $x_L^{2\mu}$ to have opposite signs in order to fit the data. To reach the central fit value in Eq. (8.40), the requirement is

$$x_L^{2\mu} x_L^{3\mu} = -2.38 \times 10^{-3}. \quad (8.45)$$

From Eq. (8.31) and Eq. (8.44), we see that it is possible to explain both the $R(D^{(*)})$ and $R(K^{(*)})$ anomalies in the model given in Eq. (8.2), given the couplings in Eq. (8.12). With these couplings, a transition magnetic moment $\mu_{N\nu_\mu}$ is induced at one-loop order with a charm quark running in the loop. To explain the flavor anomalies, the authors of Ref. [55] take $x_R^{3\tau} x_R^{2N} \sim \mathcal{O}(1)$ and $x_L^{2\mu}, x_L^{3\mu} \ll 1$. As discussed in Section 8.2, this is not sufficient to explain the XENON1T excess.

To obtain a large $\mu_{N\nu_\mu}$, we extend the model to include a non-zero x_R^{3N} , allowing the top quark to run in the loops. As pointed out in Ref. [55], this does not alter the flavor anomaly contributions. Then, the formula for the neutrino magnetic moment is Eq. (8.10). The observables $\mu_{N\nu_\mu}$ and $R(K^{(*)})$ both depend on $x_L^{2\mu}$ and $x_L^{3\mu}$, so we seek a region of parameter space which can accommodate them simultaneously. Meanwhile, $R(D^{(*)})$ does not share parameters with the leading contribution to the neutrino magnetic moment, so we adjust the couplings $x_R^{3\tau}$ and x_R^{2N} assuming they do not affect $\mu_{N\nu_\mu}$.

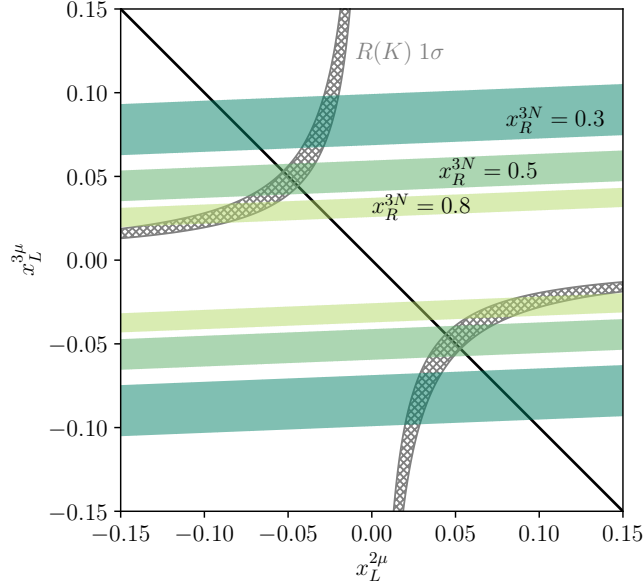


Figure 8.3: Preferred parameter regions in the $x_L^{2\mu} - x_L^{3\mu}$ plane. The gray hatched region is the 1σ region for the Wilson coefficients $C_9^{bs\mu\mu} = -C_{10}^{bs\mu\mu}$ which explain the $R(K^{(*)})$ anomalies. The green areas are regions where $|\mu_{N\nu_\mu}|$ lies between $4.5 \times 10^{-11} \mu_B$ and $6.5 \times 10^{-11} \mu_B$, for three different values of x_R^{3N} . The black line is $x_L^{3\mu} = -x_L^{2\mu}$, showing where these couplings have the same magnitude. Overlapping regions correspond to parameters which can explain the $R(K^{(*)})$ anomalies and the XENON1T excess simultaneously.

For the remaining parameters, we fix $x_L^{2\mu}$ and $x_L^{3\mu}$ such that Eq. (8.44) gives Wilson coefficients in the favored region, and then adjust x_R^{3N} to obtain the desired $\mu_{N\nu_\mu}$. This is illustrated in Fig. 8.3. The 1σ region for $C_9^{bs\mu\mu} = -C_{10}^{bs\mu\mu}$ is obtained by inserting the values in Eq. (8.40) into Eq. (8.44) and solving for $x_L^{3\mu}$. This gives $x_L^{3\mu} \propto -1/x_L^{2\mu}$, resulting in the two symmetric, hatched regions.

Also shown in Fig. 8.3 are parameter regions which give $|\mu_{N\nu_\mu}|$ between $4.5 \times 10^{-11} \mu_B$ and $6.5 \times 10^{-11} \mu_B$. There is a small dependence of the neutrino magnetic moment on $x_L^{2\mu}$, which comes from quark mixing. This alters the preferred parameter regions slightly, giving them a small slope. The magnetic moment depends linearly on the couplings, so taking the absolute value results in two distinct regions for each choice of x_R^{3N} . It is clear from Fig. 8.3 that overlapping parameter regions for the two observables can be found while keeping all couplings small.

To ensure the validity of the model, the authors of Ref. [55] calculated limits on the couplings coming from constraints from other observables. These are observables related to tree-level processes of beauty, charmed, and strange mesons. The addition of $x_R^{3N} \neq 0$ in the model does not contribute at tree-level, and there are no analogous constraints involving the top quark since

it does not form bound states. To summarize, the most stringent constraints given are [55]

$$\text{Br}(B_c \rightarrow \mu N) \implies |x_L^{3\mu} x_R^{2N}| \lesssim 0.23, \quad (8.46)$$

$$\text{Br}(D_s \rightarrow \mu\nu/N) \implies |x_L^{2\mu} x_R^{2N}| \lesssim 0.17 \left(\frac{m_{U_1}}{1 \text{ TeV}} \right)^2, \quad (8.47)$$

$$\text{Br}(B_s \rightarrow \tau\mu) \implies |(x_L^{2\mu})^* x_R^{3\tau}| < 8.8 \times 10^{-3} \left(\frac{m_{U_1}}{1 \text{ TeV}} \right)^2. \quad (8.48)$$

To reach the benchmark point $x_L^{2\mu} = -x_L^{3\mu} \approx 0.05$ with $m_{U_1} = 2 \text{ TeV}$, the constraints give $x_R^{3\tau} \lesssim 0.70$, $x_R^{2N} \lesssim 4.6$, which still gives room to satisfy Eq. (8.32).

Looking at Fig. 8.3, there are large overlapping regions for $R(K^{(*)})$ and $|\mu_{N\nu_\mu}|$ when increasing $x_L^{2\mu}$, since the curve for $C_9^{bs\mu\mu} = -C_{10}^{bs\mu\mu}$ flattens out and matches the slope of the preferred $|\mu_{N\nu_\mu}|$ region. However, the stringent limit from $\text{Br}(B_s \rightarrow \tau\mu)$ then requires one to reduce $x_R^{3\tau}$ and thus increase of x_R^{2N} to explain the $R(D^{(*)})$ anomaly.

In summary, choosing an appropriate point in parameter space, the model can explain the $R(D^{(*)})$ and $R(K^{(*)})$ anomalies together with a large $|\mu_{N\nu_\mu}|$, while satisfying constraints and keeping the couplings small. As a concrete example, the point

$$\left(x_L^{2\mu}, x_L^{3\mu}, x_R^{3\tau}, x_R^{2N}, x_R^{3N} \right) \approx \left(0.05, -0.05, 0.7, 3.0, 0.5 \right) \quad (8.49)$$

gives the desired outcome. The charm contribution to $|\mu_{N\nu_\mu}|$ is in this case more than an order of magnitude lower than the top contribution.

As usual, when removing the photon line from either diagram in Fig. 8.1, we obtain a diagram contributing to the Dirac neutrino mass. The authors of Ref. [55] estimate a contribution proportional to the charm quark mass. Here, since we allow the top quark to run in the loop, the dominant contribution is

$$\delta m_D \sim \frac{1}{16\pi^2} x_R^{3N} m_t \left(x_L^{3\mu} V_{tb} + x_L^{2\mu} V_{ts} \right), \quad (8.50)$$

which gives $\delta m_D \sim 1 \text{ MeV}$ with the couplings needed to fit the data and avoid constraints. With only a Dirac term contributing to the neutrino mass, this means the neutrino Yukawa coupling must be tuned with an accuracy of one part in 10^7 . The authors of Ref. [55] invoke the inverse see-saw mechanism to obtain acceptable active neutrino masses. Here, requiring active-sterile mixing to be

$$\tan \theta_{\nu N} \sim \frac{m_D}{m_R} \lesssim 10^{-2}, \quad (8.51)$$

the inverse see-saw scenario would lead to a heavy mass eigenstate with $m_N \sim 100 \text{ MeV}$, which ruins the explanation of XENON1T data. Thus, fine-tuning of the neutrino Yukawa coupling is necessary.

Chapter 9

Conclusions and Outlook

Motivated by recent experimental results, this thesis has discussed magnetic moments of neutrinos in and beyond the Standard Model. In 2020, the XENON1T experiment reported an excess in electron recoil events at recoil energies around 2–3 keV. This excess can be interpreted as the consequence of a neutrino magnetic moment on the order $10^{-11}\mu_B$, many orders of magnitude above the Standard Model prediction.

To facilitate a clear discussion, the theoretical background necessary for discussing neutrino magnetic moments was given. This included an introduction to neutrino physics in the Standard Model, and some extensions of the standard theory to account for neutrino masses. A thorough introduction to magnetic moments was given, where we connected the classical picture to the quantum mechanical one. We saw that in the framework of quantum field theory, the magnetic moment can be generalized to a coupling constant in an effective Lagrangian, including transition interactions between different particle states. The identification of the magnetic moment in this way was justified by taking the non-relativistic limit and connecting back to the classical concept.

Since neutrinos are electrically neutral, their magnetic moments arise only at loop-level in quantum field theory. To allow the systematical calculation of neutrino magnetic moments in any given model, the electromagnetic vertex function for neutrinos was decomposed into form factors, and we identified the neutrino magnetic moment as one of these form factors. Using this description, magnetic moments can be extracted from amplitudes by means of projection operators, allowing us to avoid calculating entire loop integrals. The methodology was adapted to the specific case of a transition magnetic moment from an active neutrino to a heavier singlet state, connecting our discussion to other works which consider this scenario. We saw how the magnetic moments of Dirac and Majorana neutrinos differ; for Majorana neutrinos the magnetic moment is antisymmetric in the space of neutrino states, thereby only allowing transition magnetic moments. Magnetic moments of Majorana neutrinos can be treated using established Feynman rules for fermion-number violating processes, or they can be extracted from the corresponding Dirac magnetic moments.

Like mass operators, the magnetic moment operator flips chirality. Since the Standard Model neutrinos are left-chiral, a non-zero neutrino magnetic moment requires right-chiral neutrinos in some form. Thus, the discussion of neutrino magnetic moment is closely connected to neutrino mass generation. In the most straight-forward extension of the Standard model, neutrino masses

are generated by Yukawa couplings to the Higgs vev, and the neutrino fields take the form $\nu = \nu_L + \nu_R$. In that case, magnetic moment interactions are transitions between the two chiral components, exactly like in the case of the magnetic moment of charged leptons. If neutrinos are Majorana particles, their chiral decomposition is $\nu = \nu_L + \nu_L^c$, with transition magnetic moments between chiral components of different states. In both these scenarios, the neutrino magnetic moments were calculated assuming the standard electroweak interactions. Using the projection technique, we arrived at magnetic moments which agree with the literature. These results show that the electroweak interactions give neutrino magnetic moments proportional to the neutrino masses. This was understood from the structure of the electroweak interactions; They act only on left-chiral states, so the necessary chirality flip must occur on an external neutrino line, leading to a mass insertion.

To generate large neutrino magnetic moments, one must introduce non-standard interactions in which the right-chiral neutrinos participate. Then, the chirality flip can happen inside the loop and one avoids the proportionality to the neutrino mass. However, a model building challenge arises in such models; the diagrams which generate neutrino magnetic moments also give loop corrections to the neutrino mass when the external photon line is removed. The loop diagrams act as Dirac mass operators, and the resulting corrections give unacceptably large neutrino masses if the magnetic moments are to be large enough to be detected by current experiments. Therefore, the tree-level neutrino mass must be tuned to compensate the large correction. Using a rough, model-independent estimate we found that the neutrino Yukawa coupling must be tuned to an accuracy of one part per million.

It is desirable to avoid fine-tuning of the parameters in a theory. Therefore, we discussed the Voloshin mechanism as a solution to the tuning issue. In this scenario, the left- and right-chiral neutrinos constitute a doublet under a new global $SU(2)$ symmetry, which forbids the Dirac mass operator while allowing the magnetic moment operator. We saw how this symmetry mechanism can be implemented in a specific theory when we considered a recently proposed model with scalar leptoquarks coupled to the third generation quarks [32]. In this model, transition magnetic moments occur between the muon neutrino and a sterile, right-chiral state N_R of mass lower than 1 MeV, which is a kinematically possible process for solar neutrinos. The transition magnetic moment $\mu_{N\nu_\mu}$ was calculated, our results disagreeing with Ref. [32] by a factor of 2. We saw how the Voloshin mechanism is implemented by the introduction of a second scalar leptoquark, with the two leptoquarks together transforming as a doublet under the new $SU(2)$ symmetry. This symmetry requires equal leptoquark couplings and masses, leading to the cancellation of the 1-loop mass diagrams. In the context of the scalar leptoquark model, the generation of the correct neutrino masses was also discussed. The Voloshin mechanism mitigates the fine-tuning issue, and we found that the inverse see-saw mechanism is suitable to obtain the desired masses, albeit with a large active-sterile mixing angle.

A model with vector leptoquarks was proposed to produce the active-to-sterile magnetic moment $\mu_{N\nu_\mu}$ large enough to explain the XENON1T anomaly. An $SU(2)_L$ singlet vector which couples to standard model leptons and quarks can run in one-loop diagrams to produce neutrino magnetic moments. Through the vector leptoquark, the neutrinos couple to the up-type quarks. Because of the vector structure of the couplings, left-chiral fields are coupled to other left-chiral fields, and likewise for the right-chiral fields. For the diagrams producing neutrino magnetic moments, this implies that the chirality flip occurs by a quark mass insertion, allowing the

neutrino magnetic moment to be enhanced by the top quark mass. We assumed a non-Abelian coupling between the vector leptoquark and the Standard Model gauge bosons.

Couplings between the vector leptoquark and the first generation leptons and quarks is strongly constrained by experiment, so magnetic moments involving ν_e are not feasible in this model. However, a large transition magnetic moment from ν_μ to N_R can be achieved by choosing the appropriate coupling structure. In particular, we imposed non-zero left-chiral couplings between the muon family and the second and third quark generations, and a non-zero coupling between the sterile neutrino and the top quark. We found that due to CKM mixing, the XENON1T excess can be accommodated in a large region of parameter space with a 2 TeV leptoquark.

Further, the implications of the vector leptoquark model on lepton flavor anomalies were explored. With the same couplings structure as required to produce a large $\mu_{N\nu_\mu}$, the model also contributes at tree-level to the ratios $R(K^{(*)})$, which quantify lepton flavor violation in the semileptonic $B \rightarrow K^{(*)}\ell^+\ell^-$ decays. With two more non-zero parameters, in particular the couplings between the right-chiral tau lepton and the bottom quark, and the right-chiral charm quark and the sterile neutrino, the model also contributes to the ratio $R(D^{(*)})$. This ratio describes lepton flavor universality violation in the decays $B \rightarrow D^{(*)}\ell\bar{\nu}$. Measurements of $R(K^{(*)})$ and $R(D^{(*)})$ show deviations in both variables with respect to the Standard Model. The contributions to these observables from the vector leptoquark were explicitly calculated, and using the most recent experimental results, an analysis of the parameter space to accommodate both flavor observables and a large neutrino magnetic moment was performed. While satisfying bounds from other flavor physics observables, we found overlapping regions for $\mu_{N\nu_\mu}$ and $R(K^{(*)})$ with all relevant couplings below unity, while the $R(D^{(*)})$ can be accommodated with the relevant couplings $\sim \mathcal{O}(1)$.

Unfortunately, the vector leptoquark model requires a large amount of fine-tuning to avoid excessively large neutrino masses, as expected. With the top quark running in the loops, the loop contribution to the Dirac mass of the neutrinos is estimated to 1 MeV, requiring a Yukawa coupling tuned with an accuracy of 1 part in 10^7 . Without a mechanism reducing the loop mass contribution, the see-saw mechanism cannot solve the tuning issue without a singlet mass too large to explain the XENON1T excess. Therefore, going forward, finding a more elegant way of producing the correct neutrino masses in the vector leptoquark model would be desirable to make the model more appealing. One possible avenue, inspired by the SU(2) symmetry mechanism employed in the scalar leptoquark model, is to introduce a second vector leptoquark. One could explore the effects of imposing a symmetry, such as a simple exchange symmetry, between the leptoquarks to obtain cancellation of the 1-loop mass diagrams. The candidate leptoquark is a doublet vector, the only other vector leptoquark with couplings to both left- and right-chiral neutrinos.

In addition to the Voloshin symmetry, other mechanisms to obtain naturally large neutrino magnetic moments exist in the literature. For example, Barr, Freire and Zee proposed a spin-suppression mechanism, where the loop mass diagram is suppressed on the basis of spin conservation [72]. Babu and Mohapatra introduced a horizontal flavor gauge symmetry under which the electron and muon families form doublets [73], causing cancellation of the mass loop diagrams. For future work, it could be of interest to explore the implementation of these mechanisms to obtain a naturally large neutrino magnetic moment explaining the XENON1T data.

Appendix A

Feynman Rules

A.1 The Standard Electroweak Theory

Here we present the Feynman rules for the standard electroweak theory, including only the vertex factors relevant to this thesis. The unitary gauge is employed. We adopt the convention where $e = |e| > 0$ is the electric charge of the proton. q_f is the charge of a fermion f . The Feynman rules of this section are sourced from Refs. [3, 74].

Propagators

$$\text{Fermion propagator: } f \xrightarrow{p} f \implies \frac{i(\not{p} + m_f)}{p^2 - m_f^2 + i\epsilon} \quad (\text{A.1})$$

$$\text{Photon propagator: } A^\mu \xrightarrow{p} A^\nu \implies i \frac{-g^{\mu\nu}}{p^2 + i\epsilon} \quad (\text{A.2})$$

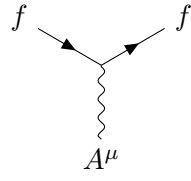
$$W \text{ propagator: } W^\mu \xrightarrow{p} W^\nu \implies i \frac{-g^{\mu\nu} + p^\mu p^\nu / m_W^2}{p^2 - m_W^2 + i\epsilon} \quad (\text{A.3})$$

$$Z \text{ propagator: } Z^\mu \xrightarrow{p} Z^\nu \implies i \frac{-g^{\mu\nu} + p^\mu p^\nu / m_Z^2}{p^2 - m_Z^2 + i\epsilon} \quad (\text{A.4})$$

$$\text{Higgs propagator: } H \xrightarrow{p} H \implies \frac{i}{p^2 - m_H^2 + i\epsilon} \quad (\text{A.5})$$

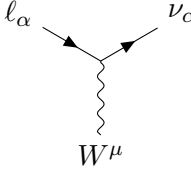
Vertices

Electromagnetic vertex:



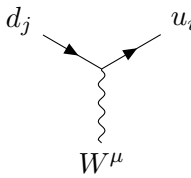
$$\Rightarrow -iq_f \gamma^\mu \quad (\text{A.6})$$

Charged current lepton vertex:



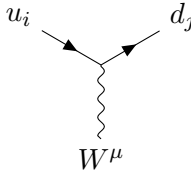
$$\Rightarrow -i \frac{g}{2\sqrt{2}} \gamma^\mu (1 - \gamma_5) \quad (\text{A.7})$$

Charged current quark vertex:



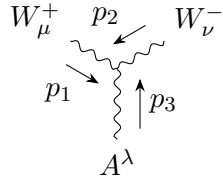
$$\Rightarrow -i \frac{g}{2\sqrt{2}} \gamma^\mu (1 - \gamma_5) V_{u_i d_j}^{\text{CKM}} \quad (\text{A.8})$$

Charged current quark vertex:



$$\Rightarrow -i \frac{g}{2\sqrt{2}} \gamma^\mu (1 - \gamma_5) \left(V_{u_j d_i}^{\text{CKM}} \right)^* \quad (\text{A.9})$$

W - W - γ vertex:



$$\Rightarrow ie \left[(p_1 - p_2)_\lambda g_{\mu\nu} + (p_2 - p_3)_\mu g_{\nu\lambda} + (p_3 - p_1)_\nu g_{\lambda\mu} \right] \quad (\text{A.10})$$

A.2 Leptoquarks

In this section, the Feynman rules for leptoquarks (LQs) used in this thesis are presented. The relevant leptoquarks and their quantum numbers under the Standard Model are shown in Table A.1.

Table A.1: Relevant leptoquark states and their quantum numbers under the Standard Model.

Leptoquark	$SU(3)_c$	$SU(2)_L$	$U(1)_Y$
S_1	$\bar{\mathbf{3}}$	$\mathbf{1}$	$1/3$
\tilde{R}_2	$\mathbf{3}$	$\mathbf{2}$	$1/6$
U_1	$\mathbf{3}$	$\mathbf{1}$	$2/3$

A thorough account of Feynman rules for scalar leptoquarks can be found in Ref. [75]. For a comprehensive review on leptoquarks, the reader is referred to Ref. [45].

The interaction vertices between leptoquarks, neutrinos and quarks come from the terms

$$\begin{aligned}
\mathcal{L} \supset & -y_L^{i\alpha} \overline{\nu_{\alpha L}^c} d_{iL} S_1 + (V_{u_i d_j}^{\text{CKM}})^* y_L^{j\alpha} \overline{\ell_{\alpha L}^c} u_{iL} S_1 + y_R^{iN} \overline{d_{iR}^c} N_R S_1 \\
& + \tilde{y}_L^{i\alpha} \overline{d_{iR}} \nu_{\alpha L} \tilde{R}_2^{-1/3} + \tilde{y}_R^{iN} \overline{d_{iL}} N_R \tilde{R}_2^{-1/3} \\
& - \tilde{y}_L^{i\alpha} \overline{d_{iR}} \ell_{\alpha L} \tilde{R}_2^{2/3} + V_{u_i d_j}^{\text{CKM}} \tilde{y}_R^{jN} \overline{u_{iL}} N_R \tilde{R}_2^{2/3} \\
& + V_{u_i d_j}^{\text{CKM}} x_L^{j\alpha} \overline{u_{iL}} \gamma_\mu \nu_{\alpha L} U_1^\mu + x_R^{iN} \overline{u_{iR}} \gamma_\mu N_R U_1^\mu \\
& + x_L^{i\alpha} \overline{d_{iL}} \gamma_\mu \ell_{\alpha L} U_1^\mu + x_R^{i\alpha} \overline{d_{iR}} \gamma_\mu \ell_{\alpha R} U_1^\mu + H.c.,
\end{aligned} \tag{A.11}$$

where the sums over quark generations i, j , and lepton flavor α are implied. Color conservation is implicitly enforced in each vertex. In the model of Ref. [32] which we discussed in Chapter 7, the couplings are $y_L^{3\mu} = \tilde{y}_R^{3N} \equiv y_2$, $y_R^{3N} = \tilde{y}_L^{3\mu} \equiv y_1$, with the rest of the couplings set to zero.

Propagators

$$\text{Scalar singlet LQ propagator: } S_1 \text{ ---}^p\text{---} S_1 \implies \frac{i}{p^2 - m_{S_1}^2 + i\varepsilon} \tag{A.12}$$

$$\text{Scalar doublet LQ propagator: } \tilde{R}_2 \text{ ---}^p\text{---} \tilde{R}_2 \implies \frac{i}{p^2 - m_{\tilde{R}_2}^2 + i\varepsilon} \tag{A.13}$$

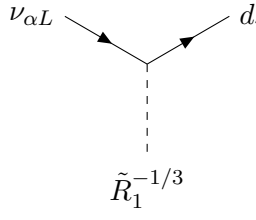
$$\text{Vector singlet LQ propagator: } U_1^\mu \text{ } \overset{p}{\sim} \text{ } U_1^\nu \implies i \frac{-g^{\mu\nu} + p^\mu p^\nu / m_{U_1}^2}{p^2 - m_{U_1}^2 + i\varepsilon} \tag{A.14}$$

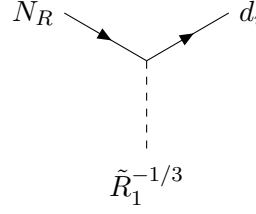
Vertices

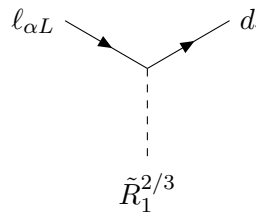
$$\begin{aligned}
S_1\text{-}\nu_L\text{-}d \text{ vertex: } & \begin{array}{c} \nu_{\alpha L} \swarrow \quad \searrow d_i \\ \quad \quad \quad \downarrow \\ \quad \quad \quad S_1 \end{array} \implies -iy_L^{i\alpha} P_L \tag{A.15}
\end{aligned}$$

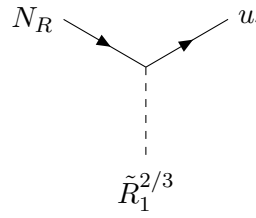
$$\begin{aligned}
S_1\text{-}\ell_L\text{-}u \text{ vertex: } & \begin{array}{c} \ell_{\alpha L} \swarrow \quad \searrow u_i \\ \quad \quad \quad \downarrow \\ \quad \quad \quad S_1 \end{array} \implies i(V_{u_i d_j}^{\text{CKM}})^* y_L^{j\alpha} P_L \tag{A.16}
\end{aligned}$$

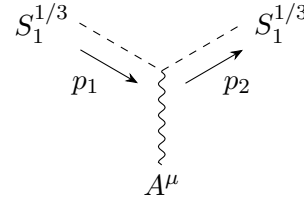
$$\begin{aligned}
S_1\text{-}N_R\text{-}d \text{ vertex: } & \begin{array}{c} N_R \swarrow \quad \searrow d_i \\ \quad \quad \quad \downarrow \\ \quad \quad \quad S_1 \end{array} \implies iy_R^{iN} P_R \tag{A.17}
\end{aligned}$$

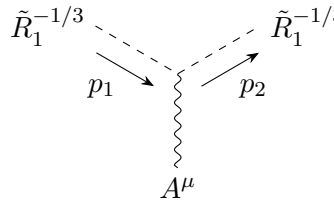
\tilde{R}_2 - ν_L - d vertex:  $\implies i\tilde{y}_L^{i\alpha} P_L$ (A.18)

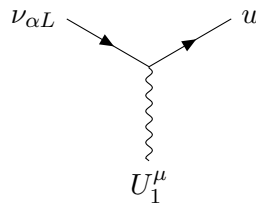
\tilde{R}_2 - N_R - d vertex:  $\implies i\tilde{y}_R^{iN} P_R$ (A.19)

\tilde{R}_2 - ℓ_L - d vertex:  $\implies -i\tilde{y}_L^{i\alpha} P_L$ (A.20)

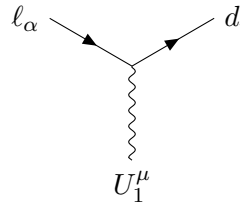
\tilde{R}_2 - N_R - u vertex:  $\implies iV_{u_i d_j}^{\text{CKM}} \tilde{y}_R^{jN} P_R$ (A.21)

S_1 - γ vertex:  $\implies -\frac{1}{3}ie (p_1^\mu + p_2^\mu)$ (A.22)

\tilde{R}_2 - γ vertex:  $\implies \frac{1}{3}ie (p_1^\mu + p_2^\mu)$ (A.23)

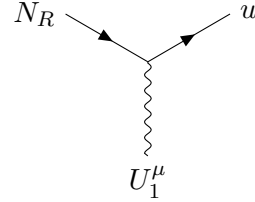
U_1 - ν_L - u vertex:  $\implies ix_L^{j\alpha} V_{u_i d_j}^{\text{CKM}} \gamma^\mu P_L$ (A.24)

U_1 - ℓ - d vertex:



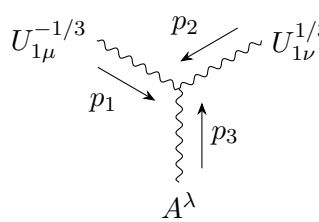
$$\Rightarrow i\gamma^\mu \left(x_L^{i\alpha} P_L + x_R^{i\alpha} P_R \right) \quad (\text{A.25})$$

U_1 - N_R - u vertex:



$$\Rightarrow ix_R^{iN} \gamma^\mu P_R \quad (\text{A.26})$$

U_1 - γ vertex:



$$\Rightarrow -\frac{2}{3}ie \left[(p_1 - p_2)_\lambda g_{\mu\nu} + (p_2 - p_3)_\mu g_{\nu\lambda} + (p_3 - p_1)_\nu g_{\lambda\mu} \right] \quad (\text{A.27})$$

A.3 Additional Feynman Rules for Majorana Fermions

When dealing with Majorana fermions, there are additional contributing diagrams to a given process due to the fact that ψ and $\bar{\psi}$ contain the same operators. To calculate these diagrams, special Feynman rules must be constructed. Dirac fermions carry fermion number flow, which is indicated by arrows on the external and internal fermion lines in diagrams. Majorana fermions do not carry fermion number flow, and are therefore drawn without arrows.

The procedure for dealing with Majorana fermions in Feynman diagrams is sourced from Ref. [40], and is as follows:

1. For a given process, draw all contributing diagrams.
2. For each fermion chain, assign an arbitrary direction of “fermion flow” (indicated by a gray arrow).
3. For each fermion chain, write the Dirac matrices in opposite order of the chosen fermion flow.
4. For each internal Dirac fermion, if the direction of fermion number flow is opposite to the chosen direction of fermion flow, substitute the propagator $S(p)$ for $S(-p)$.
5. For each vertex with Dirac fermions attached, if the direction of fermion number flow is opposite to the chosen direction of fermion flow, substitute the vertex Γ for $C\Gamma^T C^{-1}$.
6. For each external fermion, assign a spinor according to the chosen direction of fermion flow as follows:

$$\begin{array}{ccc} \bullet \xrightarrow{\quad} \xrightarrow{\quad} & \bullet \xleftarrow{\quad} \xrightarrow{\quad} & \bullet \xrightarrow{\quad} \xrightarrow{\quad} \end{array} \implies \bar{u}(p)$$

$$\begin{array}{ccc} \bullet \xrightarrow{\quad} \xrightarrow{\quad} & \bullet \xleftarrow{\quad} \xleftarrow{\quad} & \bullet \xleftarrow{\quad} \xleftarrow{\quad} \end{array} \implies v(p)$$

$$\begin{array}{ccc} \xrightarrow{\quad} \xrightarrow{\quad} \bullet & \xleftarrow{\quad} \xrightarrow{\quad} \bullet & \xrightarrow{\quad} \xrightarrow{\quad} \bullet \end{array} \implies u(p)$$

$$\begin{array}{ccc} \xleftarrow{\quad} \xrightarrow{\quad} \bullet & \xleftarrow{\quad} \xleftarrow{\quad} \bullet & \xleftarrow{\quad} \xleftarrow{\quad} \bullet \end{array} \implies \bar{v}(p)$$

Appendix B

Dirac Matrices

The Dirac matrices are 4×4 matrices defined by the anticommutator

$$\{\gamma^\mu, \gamma^\nu\} = g^{\mu\nu} \quad (\text{B.1})$$

and the Hermiticity condition

$$\gamma^{\mu\dagger} = \gamma^0 \gamma^\mu \gamma^0. \quad (\text{B.2})$$

The fifth gamma matrix is defined as

$$\gamma_5 = i\gamma^0\gamma^1\gamma^2\gamma^3, \quad (\text{B.3})$$

which satisfies the properties

$$\{\gamma_5, \gamma^\mu\} = 0, \quad (\gamma_5)^2 = 1, \quad \gamma_5^\dagger = \gamma_5. \quad (\text{B.4})$$

Traces of products of gamma matrices are

$$\begin{aligned} \text{tr}(\gamma^\mu\gamma^\nu) &= 4g^{\mu\nu}, \\ \text{tr}(\gamma^\mu\gamma^\nu\gamma^\lambda\gamma^\rho) &= 4(g^{\mu\nu}g^{\lambda\rho} - g^{\mu\lambda}g^{\nu\rho} + g^{\mu\rho}g^{\nu\lambda}), \\ \text{tr}(\text{odd \# of } \gamma) &= 0, \\ \text{tr } \gamma_5 &= \text{tr}(\gamma_5\gamma^\mu) = \text{tr}(\gamma_5\gamma^\mu\gamma^\nu) = \text{tr}(\gamma_5\gamma^\mu\gamma^\nu\gamma^\lambda) = 0, \\ \text{tr}(\gamma_5\gamma^\mu\gamma^\nu\gamma^\lambda\gamma^\rho) &= -4i\epsilon^{\mu\nu\lambda\rho}, \end{aligned} \quad (\text{B.5})$$

where $\epsilon^{\mu\nu\lambda\rho}$ is the totally antisymmetric symbol, equal to 1 for an even permutation of $(0, 1, 2, 3)$.

The constant spinors $u_s(p)$ and $v_s(p)$, describing particles and antiparticles of spin s and 4-momentum p , satisfy the momentum space Dirac equations

$$(\not{p} - m)u_s(p) = 0, \quad (\not{p} + m)v_s(p) = 0, \quad (\text{B.6})$$

and their adjoints are

$$\bar{u}_s(p) = u_s^\dagger(p)\gamma^0, \quad \bar{v}_s(p) = v_s^\dagger(p)\gamma^0. \quad (\text{B.7})$$

They satisfy the completeness relation

$$\sum_{s=1}^2 [u_{s\alpha}(p)\bar{u}_{s\beta}(p) - v_{s\alpha}(p)\bar{v}_{s\beta}(p)] = \delta_{\alpha\beta}, \quad (\text{B.8})$$

where the Greek indices refer to spinor space components.

The energy projection operators are defined by

$$\Lambda^{\pm} = \frac{\pm\not{p} + m}{2m}, \quad (\text{B.9})$$

in order to satisfy

$$\begin{aligned} \Lambda^+(p)u_s(p) &= u_s(p), & \Lambda^-(p)v_s(p) &= v_s(p), \\ \bar{u}_s(p)\Lambda^+(p) &= \bar{u}_s(p), & \bar{v}_s(p)\Lambda^-(p) &= \bar{v}_s(p), \end{aligned} \quad (\text{B.10})$$

and

$$\Lambda^+(p)v_s(p) = \Lambda^-(p)u_s(p) = \bar{v}_s(p)\Lambda^+(p) = \bar{u}_s(p)\Lambda^-(p) = 0. \quad (\text{B.11})$$

From the completeness relation Eq. (B.8), one finds that the energy projection operators can be written as

$$\Lambda_{\alpha\beta}^+(p) = \sum_{s=1}^2 u_{s\alpha}(p)\bar{u}_{s\beta}(p), \quad \Lambda_{\alpha\beta}^-(p) = -\sum_{s=1}^2 v_{s\alpha}(p)\bar{v}_{s\beta}(p). \quad (\text{B.12})$$

These relations are used to eliminate spin sums when evaluating unpolarized squared amplitudes.

Appendix C

Translating the Voloshin Lagrangian to 4-spinor Notation

In this section the flavor subscript on the electron neutrino is dropped, i.e. $\nu = \nu_e$, in order to avoid overly cluttered notation. Lower case Latin indices refer to two-spinor indices, and Greek indices refer to four-component spinor indices. The chiral basis for the gamma matrices is used in this section.

The Lagrangian in Eq. (6.1) is written in two-component spinor notation,

$$\mathcal{L} = f(\chi_\tau \chi_\nu) \eta - f'(\chi_\tau^c \chi_\nu^c) \eta^* + H.c. \quad (6.1)$$

In order to obtain the same Lagrangian in four-component notation, we first note that the neutrino Dirac mass term in [43] is written as

$$\mathcal{L}_{\text{Mass}} = m_\nu \epsilon^{ab} \chi_{\nu a}^c \chi_{\nu b} + H.c., \quad (C.1)$$

Where $a, b = (1, 2)$ and ϵ is the antisymmetric symbol. We let the four-component spinors be

$$\psi = \begin{pmatrix} \chi_a \\ \chi^{c\dagger\dot{a}} \end{pmatrix}, \quad \bar{\psi} = \left(\chi_a^\dagger \quad \chi^{ca} \right) \gamma^0 = \left(\chi^{ca} \quad \chi_a^\dagger \right), \quad (C.2)$$

where the two-component spinors with undotted indices transform under the left-chiral representation of the Lorentz group, and the spinors with dotted indices transform under the right-chiral representation. The indices are distinct since one cannot contract spinors of different representation to obtain a Lorentz scalar. Applying the rules for translating between four-component

and two-component notation provided in [8], we have for the neutrino mass term

$$\begin{aligned}
\mathcal{L}_{\text{Mass}} &= m_\nu \epsilon^{ab} \chi_{\nu a}^c \chi_{\nu b} + H.c. \\
&= m_\nu \chi_\nu^{ca} \chi_{\nu a} + H.c. \\
&= m_\nu \bar{\psi}_\nu^\beta \bar{L}_\beta^a L_a^\delta \psi_{\nu\delta} + H.c. \\
&= m_\nu \bar{\psi}_\nu^\beta (P_L)_\beta^\delta \psi_{\nu\delta} + H.c. \\
&= m_\nu \bar{\psi}_\nu^\beta (P_L)_\beta^\gamma (P_L)_\gamma^\delta \psi_{\nu\delta} + H.c. \\
&= m_\nu \bar{\psi}_{\nu R} \psi_{\nu L} + H.c. ,
\end{aligned} \tag{C.3}$$

where

$$\bar{L} = \begin{pmatrix} \mathbb{1} \\ \mathbb{0} \end{pmatrix}, \quad L = \begin{pmatrix} \mathbb{1} & 0 \\ 0 & \mathbb{1} \end{pmatrix}, \tag{C.4}$$

are 4×2 and 2×4 matrices respectively, with $\mathbb{0}$ the 2×2 matrix of zeros and $\mathbb{1}$ the 2×2 identity matrix. In the above calculation we used the properties $\bar{L}_\beta^a L_a^\delta = (P_L)_\beta^\delta$ and $P_L = (P_L)^2$. Eq. (C.3) is the familiar Dirac mass term, which justifies the construction of the 4-spinors in Eq. (C.2). In the interaction Lagrangian Eq. (6.1), we thus want to couple the upper components of ψ_ν and ψ_τ , and the scalar field η , with the coupling constant f , and the lower components of $\bar{\psi}_\nu^T$ and $\bar{\psi}_\tau^T$, and η^* , with the coupling constant f' . To pick out upper and lower components we use the chirality projectors

$$P_L = \begin{pmatrix} \mathbb{1} & 0 \\ 0 & 0 \end{pmatrix}, \quad P_R = \begin{pmatrix} 0 & 0 \\ 0 & \mathbb{1} \end{pmatrix}. \tag{C.5}$$

Thus, we have

$$\begin{aligned}
\mathcal{L} &= f \psi_{\tau L}^T \psi_{\nu L} \eta + f' \overline{\psi_{\tau R}} \overline{\psi_{\nu R}}^T \eta^* + H.c. \\
&= f \psi_\tau^T P_L \psi_\nu \eta + f' \overline{\psi}_\tau P_L \overline{\psi}_\nu^T \eta^* + H.c. \\
&= f \begin{pmatrix} \chi_\tau^a & \chi_{\tau\dot{a}}^{c\dagger} \end{pmatrix} \begin{pmatrix} \mathbb{1} & 0 \\ 0 & 0 \end{pmatrix} \begin{pmatrix} \chi_{\nu a} \\ \chi_\nu^{c\dagger\dot{a}} \end{pmatrix} \eta + f' \begin{pmatrix} \chi_\tau^{ca} & \chi_{\tau\dot{a}}^\dagger \end{pmatrix} \begin{pmatrix} \mathbb{1} & 0 \\ 0 & 0 \end{pmatrix} \begin{pmatrix} \chi_{\nu a}^c \\ \chi_\nu^{\dagger\dot{a}} \end{pmatrix} \eta^* + H.c. \\
&= f \tau^a \nu_a \eta + f' \tau^{ca} \nu_a^c \eta^* + H.c. \\
&= f(\tau\nu)\eta + f'(\tau^c\nu^c)\eta^* + H.c. ,
\end{aligned} \tag{6.2}$$

i.e. the Lagrangian in Eq. (6.2), using four-component notation, agrees with Eq. (6.1).

Appendix D

Rewriting the Numerator N^μ

In the evaluation of the one-loop diagram for the magnetic moment of a charged lepton, the numerator of the amplitude is

$$-\frac{1}{2}N^\mu = \bar{u}(q_f) \left[m^2\gamma^\mu + (\not{k} - y\not{p} + z\not{q}_i)\gamma^\mu\not{p} + (\not{k} - y\not{p} + z\not{q}_i)\gamma^\mu(\not{k} - y\not{p} + z\not{q}_i) - 2m(2k^\mu - 2yp^\mu + 2zq_i^\mu + p^\mu) \right] u(q_i), \quad (3.44)$$

from which we want to extract the term proportional to $p_\nu\bar{u}(q_f)\sigma^{\mu\nu}u(q_i)$. Our first goal will be to deal with the terms containing Feynman slashes. In the following we will make use of the momentum space Dirac equation, the anticommutation relation $\not{a}\not{b} = -\not{b}\not{a} - a \cdot b$ and the relation $\bar{u}(q_f)\not{p}u(q_i) = 0$. Terms with k will not contribute to the term we are ultimately interested in, so we will not consider them.

$$\begin{aligned} -\frac{1}{2}N^\nu &\supset \bar{u}(q_f) \left[(-y\not{p} + z\not{q}_i)\gamma^\mu\not{p} + (-y\not{p} + z\not{q}_i)\gamma^\mu(-y\not{p} + z\not{q}_i) \right] u(q_i) \\ &= \bar{u}(q_f) \left[\not{p}\gamma^\mu(-y\not{p} + y^2\not{p} - yz\not{q}_i) + \not{q}_i\gamma^\mu(z\not{p} - yz\not{p} + z^2\not{q}_i) \right] u(q_i) \\ &= \bar{u}(q_f) \left[(2p^\mu - \gamma^\mu\not{p})(-y\not{p} + y^2\not{p} - yz\not{q}_i) + (2q_i^\mu - \gamma^\mu\not{q}_i)(z\not{p} - yz\not{p} + z^2\not{q}_i) \right] u(q_i) \\ &= \bar{u}(q_f) \left\{ \gamma^\mu \left[-\not{p} \left((y^2 - y)\not{p} - yz\not{q}_i \right) - \not{q}_i \left(z(1 - y)\not{p} + z^2\not{q}_i \right) \right] \right. \\ &\quad \left. + 2p^\mu \left((y^2 - y)\not{p} - yz\not{q}_i \right) + 2q_i^\mu \left(z(1 - y)\not{p} + z^2\not{q}_i \right) \right\} u(q_i) \\ &= \bar{u}(q_f) \left\{ \gamma^\mu \left[-(y^2 - y)\not{p}\not{p} + yz\not{p}\not{q}_i - z(1 - y)\not{q}_i\not{p} - z^2\not{q}_i\not{q}_i \right] \right. \\ &\quad \left. + 2p^\mu(y^2 - y)\not{p} - 2yzp^\mu\not{q}_i + 2z(1 - y)q_i^\mu\not{p} + 2z^2q_i^\mu\not{q}_i \right\} u(q_i) \\ &= \bar{u}(q_f) \left\{ \gamma^\mu \left[(y - y^2)p^2 + yz\not{q}_i\not{q}_i - z\not{q}_i\not{q}_i - z(1 - y)(2q_i\not{p} - \not{p}\not{q}_i) - z^2\not{q}_i\not{q}_i \right] \right. \\ &\quad \left. - 2yzp^\mu m + 2z^2q_i^\mu m \right\} u(q_i) \end{aligned}$$

$$\begin{aligned}
&= \bar{u}(q_f) \left\{ \gamma^\mu \left[(y - y^2)p^2 + yz\not{q}_f m - z(1 - y)(2q_i q_f - 2q_i q_i + \not{q}_i \not{q}_i) - 2z^2 m^2 \right] \right. \\
&\quad \left. - z(1 - y)(-\gamma^\mu \not{q}_f \not{q}_i) - 2yzp^\mu m + 2z^2 q_i^\mu m \right\} u(q_i) \\
&= \bar{u}(q_f) \left\{ \gamma^\mu \left[(y - y^2)p^2 - z(1 - y)(2q_i q_f - 2m^2 + m^2) - 2z^2 m^2 \right] \right. \\
&\quad \left. + yz\gamma^\mu \not{q}_f m - z(1 - y)(\not{q}_f \gamma^\mu m - 2q_f^\mu m) - 2yzp^\mu m + 2z^2 q_i^\mu m \right\} u(q_i) \\
&= \bar{u}(q_f) \left\{ \gamma^\mu \left[(y - y^2)p^2 - z(1 - y)(-p^2 + m^2) - 2z^2 m^2 \right] \right. \\
&\quad \left. - yzm\not{q}_f \gamma^\mu + 2yzmq_f^\mu - z(1 - y)(m^2 \gamma^\mu - 2q_f^\mu m) - 2yzp^\mu m + 2z^2 q_i^\mu m \right\} u(q_i) \\
&= \bar{u}(q_f) \left\{ \gamma^\mu \left[(y - y^2 + z - yz)p^2 - zm^2 + yzm^2 - 2z^2 m^2 - yzm^2 - zm^2 + yzm^2 \right] \right. \\
&\quad \left. + 2yzmq_f^\mu + 2zmq_f^\mu - 2yzmq_f^\mu - 2yzmp^\mu + 2z^2 mq_i^\mu \right\} u(q_i) \\
&= \bar{u}(q_f) \left\{ \gamma^\mu \left[(y - y^2 + z - yz)p^2 + (-2z - 2z^2 + yz)m^2 \right] \right. \\
&\quad \left. - 2yzmp^\mu + 2z^2 mq_i^\mu + 2zmq_f^\mu \right\} u(q_i). \tag{D.1}
\end{aligned}$$

In addition, in Eq. (3.44) we have the terms

$$\bar{u}(q_f) [-2m(-2yp^\mu + 2zq_i^\mu + p^\mu)] u(q_i) = \bar{u}(q_f) [(4my - 2m)p^\mu - 4zmq_i^\mu] u(q_i). \tag{D.2}$$

Adding these terms to the ones above we obtain

$$\begin{aligned}
&-\frac{1}{2}N^\nu \supset \bar{u}(q_f) \left\{ \gamma^\mu \left[(y - y^2 + z - yz)p^2 + (-2z - 2z^2 + yz)m^2 \right] \right. \\
&\quad \left. - 2yzmp^\mu + (4my - 2m)p^\mu + 2z^2 mq_i^\mu + 2zmq_f^\mu - 4zmq_i^\mu \right\} u(q_i) \\
&= \bar{u}(q_f) \left\{ \gamma^\mu \left[(y - y^2 + z - yz)p^2 + (-2z - 2z^2 + yz)m^2 \right] + (-2yz + 4y - 2 + 2z)mp^\mu \right. \\
&\quad \left. - 2mz(1 - z)q_i^\mu \right\} u(q_i) \\
&= \bar{u}(q_f) \left\{ \gamma^\mu \left[(y - y^2 + z - yz)p^2 + (-2z - 2z^2 + yz)m^2 \right] + (-2yz + 4y - 2 + 2z)mp^\mu \right. \\
&\quad \left. - 2mz(1 - z)q_i^\mu + mz(1 - z)p^\mu - mz(1 - z)p^\mu \right\} u(q_i) \\
&= \bar{u}(q_f) \left\{ \gamma^\mu \left[(y - y^2 + z - yz)p^2 + (-2z - 2z^2 + yz)m^2 \right] \right. \\
&\quad \left. + (-2yz + 4y - 2 + 3z - z^2)mp^\mu - mz(1 - z)(q_i^\mu + q_f^\mu) \right\} u(q_i), \tag{D.3}
\end{aligned}$$

where we have used the fact that $2q_i + p = q_i + q_f$. We can now use the Gordon identity to rewrite

$$-mz(1 - z)\bar{u}(q_f)(q_i^\mu + q_f^\mu)u(q_i) = -2m^2 z(1 - z)\bar{u}(q_f)\gamma^\mu u(q_i) + imz(1 - z)\bar{u}(q_f)p_\nu \sigma^{\mu\nu} u(q_i) \tag{D.4}$$

The terms we have not included from Eq. (3.44) are terms proportional to k , and one term $m^2\gamma^\mu$. These do not contribute to the $\sigma^{\mu\nu}$ piece, and thus the term relevant to the magnetic moment is

$$N^\mu \supset -2imz(1-z)p_\nu\bar{u}(q_f)\sigma^{\mu\nu}u(q_i). \quad (3.45)$$

Bibliography

- [1] ATLAS, G. Aad et al. “Observation of a new particle in the search for the Standard Model Higgs boson with the ATLAS detector at the LHC”. In: *Phys. Lett. B* 716 (2012), pp. 1–29. DOI: 10.1016/j.physletb.2012.08.020. arXiv: 1207.7214 [hep-ex].
- [2] CMS, S. Chatrchyan et al. “Observation of a New Boson at a Mass of 125 GeV with the CMS Experiment at the LHC”. In: *Phys. Lett. B* 716 (2012), pp. 30–61. DOI: 10.1016/j.physletb.2012.08.021. arXiv: 1207.7235 [hep-ex].
- [3] C. Giunti and K. C. Wook. *Fundamentals of Neutrino Physics and Astrophysics*. Oxford: Oxford Univ., 2007. DOI: 10.1093/acprof:oso/9780198508717.001.0001.
- [4] J. K. Rowley, B. T. Cleveland, and R. Davis. “The chlorine solar neutrino experiment”. In: *AIP Conference Proceedings* 126.1 (1985), pp. 1–21. DOI: 10.1063/1.35149.
- [5] M. Voloshin and M. Vysotskij. “Neutrino magnetic moment and time variation of solar neutrino flux”. In: *Yad. Fiz.* 44 (1986), p. 845.
- [6] XENON, E. Aprile et al. “Excess electronic recoil events in XENON1T”. In: *Phys. Rev. D* 102.7 (2020), p. 072004. DOI: 10.1103/PhysRevD.102.072004. arXiv: 2006.09721 [hep-ex].
- [7] M. D. Schwartz. *Quantum Field Theory and the Standard Model*. Cambridge University Press, 2014.
- [8] H. K. Dreiner, H. E. Haber, and S. P. Martin. “Two-component spinor techniques and Feynman rules for quantum field theory and supersymmetry”. In: *Phys. Rept.* 494 (2010), pp. 1–196. DOI: 10.1016/j.physrep.2010.05.002. arXiv: 0812.1594 [hep-ph].
- [9] Super-Kamiokande, Y. Fukuda et al. “Evidence for oscillation of atmospheric neutrinos”. In: *Phys. Rev. Lett.* 81 (1998), pp. 1562–1567. DOI: 10.1103/PhysRevLett.81.1562. arXiv: hep-ex/9807003.
- [10] Particle Data Group, P. Zyla et al. “Review of Particle Physics”. In: *PTEP* 2020.8 (2020), p. 083C01. DOI: 10.1093/ptep/ptaa104.
- [11] CMS, *Probing Majorana neutrinos and the Weinberg operator in the same-charge dimuon channel through vector boson fusion processes in proton-proton collisions at $\sqrt{s} = 13$ TeV*. Tech. rep. Geneva: CERN, 2022. URL: <https://cds.cern.ch/record/2803671>.
- [12] A. Bellerive. “Review of solar neutrino experiments”. In: *Int. J. Mod. Phys. A* 19 (2004). Ed. by H. W. K. Cheung and T. S. Pratt, pp. 1167–1179. DOI: 10.1142/S0217751X04019093. arXiv: hep-ex/0312045.

- [13] C. Giunti and A. Studenikin. “Neutrino electromagnetic interactions: a window to new physics”. In: *Rev. Mod. Phys.* 87 (2015), p. 531. DOI: 10.1103/RevModPhys.87.531. arXiv: 1403.6344 [hep-ph].
- [14] M. Sajjad Athar et al. “Status and perspectives of neutrino physics”. In: *Prog. Part. Nucl. Phys.* 124 (2022), p. 103947. DOI: 10.1016/j.ppnp.2022.103947. arXiv: 2111.07586 [hep-ph].
- [15] H. Goldstein, C. Poole, and J. Safko. *Classical Mechanics*. Pearson, 2013.
- [16] J. Schwinger. “On Quantum-Electrodynamics and the Magnetic Moment of the Electron”. In: *Physical Review* 73.4 (1948), pp. 416–417. DOI: 10.1103/PhysRev.73.416.
- [17] T. Aoyama, T. Kinoshita, and M. Nio. “Theory of the Anomalous Magnetic Moment of the Electron”. In: *Atoms* 7.1 (2019), p. 28. DOI: 10.3390/atoms7010028.
- [18] L. Morel et al. “Determination of the fine-structure constant with an accuracy of 81 parts per trillion”. In: *Nature* 588.7836 (2020), pp. 61–65. DOI: 10.1038/s41586-020-2964-7.
- [19] D. Hanneke, S. F. Hoogerheide, and G. Gabrielse. “Cavity Control of a Single-Electron Quantum Cyclotron: Measuring the Electron Magnetic Moment”. In: *Phys. Rev. A* 83 (2011), p. 052122. DOI: 10.1103/PhysRevA.83.052122. arXiv: 1009.4831 [physics.atom-ph].
- [20] R. H. Parker et al. “Measurement of the fine-structure constant as a test of the Standard Model”. In: *Science* 360 (2018), p. 191. DOI: 10.1126/science.aap7706. arXiv: 1812.04130 [physics.atom-ph].
- [21] Muon g-2, B. Abi et al. “Measurement of the Positive Muon Anomalous Magnetic Moment to 0.46 ppm”. In: *Phys. Rev. Lett.* 126.14 (2021), p. 141801. DOI: 10.1103/PhysRevLett.126.141801. arXiv: 2104.03281 [hep-ex].
- [22] A. de Gouvea and J. Jenkins. “What can we learn from neutrino electron scattering?”. In: *Phys. Rev. D* 74 (2006), p. 033004. DOI: 10.1103/PhysRevD.74.033004. arXiv: hep-ph/0603036.
- [23] M. E. Peskin and D. V. Schroeder. *An introduction to quantum field theory*. Boulder, CO: Westview, 1995.
- [24] M. Nowakowski, E. A. Paschos, and J. M. Rodriguez. “All electromagnetic form-factors”. In: *Eur. J. Phys.* 26 (2005), pp. 545–560. DOI: 10.1088/0143-0807/26/4/001. arXiv: physics/0402058.
- [25] H. H. Patel. “Package-X: A Mathematica package for the analytic calculation of one-loop integrals”. In: *Comput. Phys. Commun.* 197 (2015), pp. 276–290. DOI: 10.1016/j.cpc.2015.08.017. arXiv: 1503.01469 [hep-ph].
- [26] Wolfram Research, Inc. *Mathematica, Version 12.3*. Champaign, IL, 2021. URL: <https://www.wolfram.com/mathematica>.
- [27] P. Vogel and J. Engel. “Neutrino electromagnetic form factors”. In: *Phys. Rev. D* 39 (11 1989), pp. 3378–3383. DOI: 10.1103/PhysRevD.39.3378.
- [28] W. Grimus and P. Stockinger. “Effects of neutrino oscillations and neutrino magnetic moments on elastic neutrino - electron scattering”. In: *Phys. Rev. D* 57 (1998), pp. 1762–1768. DOI: 10.1103/PhysRevD.57.1762. arXiv: hep-ph/9708279.

- [29] LSND, L. B. Auerbach et al. “Measurement of electron - neutrino - electron elastic scattering”. In: *Phys. Rev. D* 63 (2001), p. 112001. DOI: 10.1103/PhysRevD.63.112001. arXiv: hep-ex/0101039.
- [30] A. G. Beda et al. “The Results of Search for the Neutrino Magnetic Moment in GEMMA Experiment”. In: *Advances in High Energy Physics* 2012 (2012), p. 350150. DOI: 10.1155/2012/350150.
- [31] Borexino, M. Agostini et al. “Limiting neutrino magnetic moments with Borexino Phase-II solar neutrino data”. In: *Phys. Rev. D* 96.9 (2017), p. 091103. DOI: 10.1103/PhysRevD.96.091103. arXiv: 1707.09355 [hep-ex].
- [32] V. Brdar et al. “The Neutrino Magnetic Moment Portal: Cosmology, Astrophysics, and Direct Detection”. In: *JCAP* 01 (2021), p. 039. DOI: 10.1088/1475-7516/2021/01/039. arXiv: 2007.15563 [hep-ph].
- [33] COHERENT, D. Akimov et al. “Observation of Coherent Elastic Neutrino-Nucleus Scattering”. In: *Science* 357.6356 (2017), pp. 1123–1126. DOI: 10.1126/science.aao0990. arXiv: 1708.01294 [nucl-ex].
- [34] J. Colaresi et al. “Suggestive evidence for Coherent Elastic Neutrino-Nucleus Scattering from reactor antineutrinos”. In: (2022). arXiv: 2202.09672 [hep-ex].
- [35] M. Atzori Corona et al. *Impact of the Dresden-II and COHERENT neutrino scattering data on neutrino electromagnetic properties and electroweak physics*. 2022. arXiv: 2205.09484 [hep-ph].
- [36] N. Viaux et al. “Neutrino and axion bounds from the globular cluster M5 (NGC 5904)”. In: *Phys. Rev. Lett.* 111 (2013), p. 231301. DOI: 10.1103/PhysRevLett.111.231301. arXiv: 1311.1669 [astro-ph.SR].
- [37] K. S. Babu, S. Jana, and M. Lindner. “Large Neutrino Magnetic Moments in the Light of Recent Experiments”. In: *JHEP* 10 (2020), p. 040. DOI: 10.1007/JHEP10(2020)040. arXiv: 2007.04291 [hep-ph].
- [38] N. Vassh et al. “Majorana Neutrino Magnetic Moment and Neutrino Decoupling in Big Bang Nucleosynthesis”. In: *Phys. Rev. D* 92.12 (2015), p. 125020. DOI: 10.1103/PhysRevD.92.125020. arXiv: 1510.00428 [astro-ph.CO].
- [39] K. Fujikawa and R. E. Shrock. “Magnetic Moment of a Massive Neutrino and Neutrino-Spin Rotation”. In: *Phys. Rev. Lett.* 45 (12 1980), pp. 963–966. DOI: 10.1103/PhysRevLett.45.963.
- [40] A. Denner et al. “Feynman rules for fermion-number-violating interactions”. In: *Nuclear Physics B* 387.2 (1992), pp. 467–481. DOI: [https://doi.org/10.1016/0550-3213\(92\)90169-C](https://doi.org/10.1016/0550-3213(92)90169-C).
- [41] G. Gelmini and M. Roncadelli. “Left-handed neutrino mass scale and spontaneously broken lepton number”. In: *Physics Letters B* 99.5 (1981), pp. 411–415. DOI: [https://doi.org/10.1016/0370-2693\(81\)90559-1](https://doi.org/10.1016/0370-2693(81)90559-1).
- [42] R. N. Mohapatra and G. Senjanovi ć. “Neutrino Mass and Spontaneous Parity Nonconservation”. In: *Phys. Rev. Lett.* 44 (14 1980), pp. 912–915. DOI: 10.1103/PhysRevLett.44.912.

- [43] M. B. Voloshin. “On Compatibility of Small Mass with Large Magnetic Moment of Neutrino”. In: *Sov. J. Nucl. Phys.* 48 (1988), p. 512.
- [44] N. F. Bell et al. “Model independent bounds on magnetic moments of Majorana neutrinos”. In: *Phys. Lett. B* 642 (2006), pp. 377–383. DOI: 10.1016/j.physletb.2006.09.055. arXiv: hep-ph/0606248.
- [45] I. Doršner et al. “Physics of leptoquarks in precision experiments and at particle colliders”. In: *Phys. Rept.* 641 (2016), pp. 1–68. DOI: 10.1016/j.physrep.2016.06.001. arXiv: 1603.04993 [hep-ph].
- [46] V. Brdar and A. Greljo. personal communication. 2022.
- [47] L. Lavoura. “General formulae for $f(1) \rightarrow f(2) \gamma$ ”. In: *Eur. Phys. J. C* 29 (2003), pp. 191–195. DOI: 10.1140/epjc/s2003-01212-7. arXiv: hep-ph/0302221.
- [48] H. Hettmansperger, M. Lindner, and W. Rodejohann. “Phenomenological Consequences of sub-leading Terms in See-Saw Formulas”. In: *JHEP* 04 (2011), p. 123. DOI: 10.1007/JHEP04(2011)123. arXiv: 1102.3432 [hep-ph].
- [49] G. Hooft. “Naturalness, Chiral Symmetry, and Spontaneous Chiral Symmetry Breaking”. In: *Recent Developments in Gauge Theories*. Ed. by G. Hooft et al. Boston, MA: Springer US, 1980, pp. 135–157. DOI: 10.1007/978-1-4684-7571-5_9.
- [50] P. D. Bolton, F. F. Deppisch, and P. S. Bhupal Dev. “Neutrinoless double beta decay versus other probes of heavy sterile neutrinos”. In: *JHEP* 03 (2020), p. 170. DOI: 10.1007/JHEP03(2020)170. arXiv: 1912.03058 [hep-ph].
- [51] S. Friedrich et al. “Limits on the Existence of sub-MeV Sterile Neutrinos from the Decay of ${}^7\text{Be}$ in Superconducting Quantum Sensors”. In: *Phys. Rev. Lett.* 126.2 (2021), p. 021803. DOI: 10.1103/PhysRevLett.126.021803. arXiv: 2010.09603 [nucl-ex].
- [52] C. Cornella, J. Fuentes-Martin, and G. Isidori. “Revisiting the vector leptoquark explanation of the B-physics anomalies”. In: *JHEP* 07 (2019), p. 168. DOI: 10.1007/JHEP07(2019)168. arXiv: 1903.11517 [hep-ph].
- [53] K. Ban et al. *A comprehensive study of vector leptoquark with $U(1)_{B_3-L_2}$ on the B-meson and Muon $g-2$ anomalies*. 2021. arXiv: 2104.06656 [hep-ph].
- [54] D. J. Robinson, B. Shakya, and J. Zupan. “Right-handed neutrinos and $R(D^{(*)})$ ”. In: *JHEP* 02 (2019), p. 119. DOI: 10.1007/JHEP02(2019)119. arXiv: 1807.04753 [hep-ph].
- [55] A. Azatov et al. “Combined explanations of B-physics anomalies: the sterile neutrino solution”. In: *JHEP* 10 (2018), p. 092. DOI: 10.1007/JHEP10(2018)092. arXiv: 1807.10745 [hep-ph].
- [56] CMS, A. M. Sirunyan et al. “Constraints on models of scalar and vector leptoquarks decaying to a quark and a neutrino at $\sqrt{s} = 13$ TeV”. In: *Phys. Rev. D* 98 (3 2018), p. 032005. DOI: 10.1103/PhysRevD.98.032005.
- [57] Belle, M. Huschle et al. “Measurement of the branching ratio of $\bar{B} \rightarrow D^{(*)} \tau^- \bar{\nu}_\tau$ relative to $\bar{B} \rightarrow D^{(*)} \ell^- \bar{\nu}_\ell$ decays with hadronic tagging at Belle”. In: *Phys. Rev. D* 92.7 (2015), p. 072014. DOI: 10.1103/PhysRevD.92.072014. arXiv: 1507.03233 [hep-ex].

- [58] Belle, S. Hirose et al. “Measurement of the τ lepton polarization and $R(D^*)$ in the decay $\bar{B} \rightarrow D^* \tau^- \bar{\nu}_\tau$ ”. In: *Phys. Rev. Lett.* 118.21 (2017), p. 211801. DOI: 10.1103/PhysRevLett.118.211801. arXiv: 1612.00529 [hep-ex].
- [59] Belle, S. Hirose et al. “Measurement of the τ lepton polarization and $R(D^*)$ in the decay $\bar{B} \rightarrow D^* \tau^- \bar{\nu}_\tau$ with one-prong hadronic τ decays at Belle”. In: *Phys. Rev. D* 97.1 (2018), p. 012004. DOI: 10.1103/PhysRevD.97.012004. arXiv: 1709.00129 [hep-ex].
- [60] Belle, G. Caria et al. “Measurement of $\mathcal{R}(D)$ and $\mathcal{R}(D^*)$ with a semileptonic tagging method”. In: *Phys. Rev. Lett.* 124.16 (2020), p. 161803. DOI: 10.1103/PhysRevLett.124.161803. arXiv: 1910.05864 [hep-ex].
- [61] BaBar, J. P. Lees et al. “Evidence for an excess of $\bar{B} \rightarrow D^{(*)} \tau^- \bar{\nu}_\tau$ decays”. In: *Phys. Rev. Lett.* 109 (2012), p. 101802. DOI: 10.1103/PhysRevLett.109.101802. arXiv: 1205.5442 [hep-ex].
- [62] BaBar, J. P. Lees et al. “Measurement of an Excess of $\bar{B} \rightarrow D^{(*)} \tau^- \bar{\nu}_\tau$ Decays and Implications for Charged Higgs Bosons”. In: *Phys. Rev. D* 88.7 (2013), p. 072012. DOI: 10.1103/PhysRevD.88.072012. arXiv: 1303.0571 [hep-ex].
- [63] LHCb, R. Aaij et al. “Measurement of the ratio of branching fractions $\mathcal{B}(\bar{B}^0 \rightarrow D^{*+} \tau^- \bar{\nu}_\tau) / \mathcal{B}(\bar{B}^0 \rightarrow D^{*+} \mu^- \bar{\nu}_\mu)$ ”. In: *Phys. Rev. Lett.* 115.11 (2015). [Erratum: *Phys. Rev. Lett.* 115, 159901 (2015)], p. 111803. DOI: 10.1103/PhysRevLett.115.111803. arXiv: 1506.08614 [hep-ex].
- [64] LHCb, R. Aaij et al. “Measurement of the ratio of the $B^0 \rightarrow D^{*-} \tau^+ \nu_\tau$ and $B^0 \rightarrow D^{*-} \mu^+ \nu_\mu$ branching fractions using three-prong τ -lepton decays”. In: *Phys. Rev. Lett.* 120.17 (2018), p. 171802. DOI: 10.1103/PhysRevLett.120.171802. arXiv: 1708.08856 [hep-ex].
- [65] LHCb, R. Aaij et al. “Test of Lepton Flavor Universality by the measurement of the $B^0 \rightarrow D^{*-} \tau^+ \nu_\tau$ branching fraction using three-prong τ decays”. In: *Phys. Rev. D* 97.7 (2018), p. 072013. DOI: 10.1103/PhysRevD.97.072013. arXiv: 1711.02505 [hep-ex].
- [66] HFLAV, Y. S. Amhis et al. “Averages of b-hadron, c-hadron, and τ -lepton properties as of 2018”. In: *Eur. Phys. J. C* 81.3 (2021), p. 226. DOI: 10.1140/epjc/s10052-020-8156-7. arXiv: 1909.12524 [hep-ex].
- [67] HFLAV. *Spring 2021 Update*. 2021. URL: <https://hflav-eos.web.cern.ch/hflav-eos/semi/spring21/html/RDsDsstar/RDRDs.html> (visited on 04/08/2022).
- [68] G. Hiller and F. Kruger. “More model-independent analysis of $b \rightarrow s$ processes”. In: *Phys. Rev. D* 69 (2004), p. 074020. DOI: 10.1103/PhysRevD.69.074020. arXiv: hep-ph/0310219.
- [69] LHCb, R. Aaij et al. “Test of lepton universality in beauty-quark decays”. In: *Nature Phys.* 18.3 (2022), pp. 277–282. DOI: 10.1038/s41567-021-01478-8. arXiv: 2103.11769 [hep-ex].
- [70] LHCb, R. Aaij et al. “Test of lepton universality with $B^0 \rightarrow K^{*0} \ell^+ \ell^-$ decays”. In: *JHEP* 08 (2017), p. 055. DOI: 10.1007/JHEP08(2017)055. arXiv: 1705.05802 [hep-ex].
- [71] W. Altmannshofer and P. Stangl. “New physics in rare B decays after Moriond 2021”. In: *Eur. Phys. J. C* 81.10 (2021), p. 952. DOI: 10.1140/epjc/s10052-021-09725-1. arXiv: 2103.13370 [hep-ph].

- [72] S. M. Barr, E. M. Freire, and A. Zee. “Mechanism for large neutrino magnetic moments”. In: *Phys. Rev. Lett.* 65 (21 1990), pp. 2626–2629. DOI: 10.1103/PhysRevLett.65.2626.
- [73] K. S. Babu and R. N. Mohapatra. “Model for large transition magnetic moment of the electron neutrino”. In: *Phys. Rev. Lett.* 63 (3 1989), pp. 228–231. DOI: 10.1103/PhysRevLett.63.228.
- [74] F. Mandl and G. Shaw. *Quantum Field Theory*. Wiley, 2010.
- [75] A. Crivellin and L. Schnell. “Complete Lagrangian and set of Feynman rules for scalar leptoquarks”. In: *Comput. Phys. Commun.* 271 (2022), p. 108188. DOI: 10.1016/j.cpc.2021.108188. arXiv: 2105.04844 [hep-ph].